2015

Cognitive Analysis of Multi-Sensor Information

Elizabeth Lynn Fox
Wright State University

COGNTIIVE ANALYSIS OF MULTI-SENSOR INFORMATION

A thesis submitted in partial fulfillment of the
requirements for the degree of
Masters of Science

By

Elizabeth Lynn Fox
B.S., Wright State University, 2013

2015
Wright State University

WRIGHT STATE UNIVERSITY

GRADUATE SCHOOL

JUNE 4, 2015

I HEREBY RECOMMEND THAT THE THESIS PREPARED UNDER MY SUPERVISION BY Elizabeth Fox ENTITLED Cognitive Analysis of Multisensor Information BE ACCEPTED IN PARTIAL FULFILLMENT OF THE REQUIREMENTS FOR THE DEGREE OF Master of Science.

Joseph Houpt, Ph.D.
Thesis Director

Scott Watamaniuk, Ph.D.
Graduate Program Director

Debra Steele-Johnson, Ph.D.
Chair, Department of Psychology

Committee on
Final Examination

Leslie Blaha, Ph.D.

Ion Juvina, Ph.D.

Robert E.W. Fyffe, Ph.D.
Vice President for Research and
Dean, Graduate School

ABSTRACT

Fox, Elizabeth Lynn. M.S. Department of Psychology, Wright State University, 2015. Cognitive Analysis of Multi-sensor Information.

Multispectral imagery can supply an observer with different components of information to, in combination, lead to critical decisions. Human observers can be presented with two fusion techniques: 1) cognitive fusion presents the two sensor images within 5 degrees of visual angle and 2) algorithmic fusion aims to enhance image quality by combining relevant information from two individual sensor images into one composite image. Researchers have used methods such as comparing performance across different algorithms or comparing algorithmic fusion to a single-sensor image. However, cognitive fusion is a technique that provides all of the sensor information and, if utilized efficiently, may yield better performance than algorithmic fusion. I used a cognitive framework, systems factorial technology (Townsend & Nowaza, 1995) to test specific underlying mechanisms of information processing across both fusion techniques in two discrimination tasks. The results of my Experiments demonstrate that the efficiency of processing sensor information is just as good for cognitive fusion as algorithmic fusion across both discrimination tasks. Future research with multi-sensor displays should not disregard the potential benefits that displaying all of the available information may have over the algorithmic interpretations of important information.

TABLE OF CONTENTS

LIST OF FIGURES

LIST OF TABLES

ACKNOWLEDGEMENTS

Foremost, I would like to sincerely thank my advisor, Dr. Joseph Houpt for continuously supporting me through not only my thesis study and research but also for inspiring me and whole-heartedly guiding me through my undergraduate studies. His patience, encouragement, passion for research and immense amount of knowledge has challenged me to always hunger to know more and to willfully step outside my comfort zone. I cannot express my gratitude enough for both the academic and personal growth he has helped me achieve. As I work toward my Ph.D. in the upcoming years, I look forward to absorbing even more of his everlasting supply of knowledge and wisdom.

I would also like to thank the rest of my thesis committee: Dr. Leslie Blaha and Dr. Ion Juvina for their encouragement and insightful comments throughout the thesis preparation and writing process.

I gratefully thank Dr. Leslie Blaha for offering me the internship opportunities in my undergraduate and graduate studies. I appreciate the engagement and contributions I could make in larger research projects and the ability to work in diverse teams in the laboratory.

I would like to thank Jennifer Bittner for her vast knowledge in working with multi-sensor imagery and sorting through and organizing thousands of images to make finalizing a set of stimuli a much smoother process. Also, I greatly appreciate Alan Pinkus allowing me to use the multi-sensor imagery collected in the Netherlands on the TNO project and Dave Dommett for making sure the images were correctly registered for image fusion.

Many friends and colleagues have given their motivating and calming words to help me overcome obstacles and to stay focused on my goals. They ensured my head was clear of narrow focused thoughts and spent countless hours debating into the night. I greatly value their friendships and aspire to provide them with the same support and encouragement they have given to me.

This work was supported by AFOSR Grant FA9550-13-1-0087 awarded to JWH.

1. INTRODUCTION

Information from various parts of the electromagnetic spectrum is beneficial for determining different types of environmental information. For example, visible imagery (Figure 1A) is best for detecting edges and fine details, long-wave infrared (LWIR) imagery (Figure 1B) is useful for detecting heat information (e.g., occluded heat producing objects such as a person behind a bush), and near infrared (night vision) can pick up detail in conditions with low illumination. Together, the LWIR and visible sensors can supply the operator with complementary information and aid in a task such as determining a target (e.g., person) location relative to an object in the scene (Toet, IJspeert, Waxman, & Aguilar, 1997).

Algorithmic image fusion aims to enhance image quality by combining relevant information from two individual sensor images into one composite image. It offers two substantial benefits: 1) it restricts the amount of visual information the operator must attend to; and 2) the resultant image may possess emergent features not found in either single image alone (Krebs & Sinai, 2002; Leckie, 1990). However, when an observer is presented with algorithmically fused imagery, he or she must rely on the algorithm to correctly identify important features because the total available information is condensed into one image. This caveat of limiting the information given to the observer suggests another way to display multi-sensor information: cognitive fusion. Cognitive fusion gives the operator the responsibility of extracting and combining relevant sensor information rather than relying on the image fusion algorithm. To allow for cognitive fusion, two sensor images can be presented next to one another, giving the observer all of the information from each sensor. I use cognitive fusion to describe performance with separate images, not necessarily a cognitive or perceptual process. Any redundancy across the sensors could yield performance improvement compared to

individual or algorithmic sensor presentation (Duncan, 1980; Kahneman, 1973). Alternatively, cognitive fusion could hinder performance because the participant may be unable to attend to both sensor images.

Algorithms can use transforms such as Laplacian pyramid or wavelet. A pyramid transform (e.g. Laplacian) utilizes several band-pass filters to down sample each sensor image resulting in a series of images at different resolution qualities. Then each component image is interpolated (expand in size) and combined into a composite image using a linear transform (Blum, 2006). Figure 1C is an example of Laplacian pyramid fusion of the individual LWIR and visible images. Alternatively, the discrete wavelet transform (DWT) passes a series of wavelets (oscillating functions) across the image and combines them to get a composite fused image. Variations of the DWT can provide additional edge and line contour information (Blum, 2006; Smeelen, Schwering, Toet, & Loog, 2014).

A. B. C.

Figure 1. An example of a visible (A), long-wave infrared (B), and the combination of 1A and 1B using the Laplacian fusion algorithm (C). I used these images for the discrimination task in Experiment 1 (discussed in later sections).

To date, research has focused on ranking various fusion algorithms and identifying the specific tasks for which a particular algorithm or set of sensors yields best image quality

statistics. Researchers have used methods such as comparing performance across different algorithms or comparing algorithmic fusion to a single-sensor image. Previous research has lead to inconclusive evidence across experiments assessing algorithmic fusion using both objective computer vision metrics and basic human performance measures (Essock, Sinai, DeFord, Hansen, & Srinivasan, 2010; Krebs & Sinai, 2002; Krebs, Xing, & Ahumada, 2002; McCarley & Krebs, 2000). On the other hand, cognitive fusion has received no attention relative to image fusion research. Discussion of whether data fusion is appropriate as opposed to presenting an observer with all of the available information is discussed with display design (Klein, Moon, & Hoffman, 2006A, Klein, Moon, & Hoffman, 2006B). But, this has not been explored with multisensor information and is a necessary step forward.

Additionally, in order for me to make any hypotheses about why humans may perform better or worse with a specific fusion type or set of sensors I must establish an understanding of how humans process multi-sensor information. Using a cognitive framework based on specific model assumptions I can indicate properties such as: changes in an individual's cognitive processing speed across single and multi-sensor information, whether multi-sensor information is processing simultaneously or sequentially, how much information is needed to make a decision and if an interaction between sensor processes occur. I can make specific hypotheses about how humans are processing multi-sensor information and suggest remedies to correct for inefficient processing by identifying these cognitive properties.

In the experiments reported here, I used a mathematical approach to analyze the underlying cognitive processes of the two types of multi-sensor displays. I completed a full analysis of two display types, one using a single image comprised of multiple sensors (algorithmic fusion) and one using two single-sensor images next to one another (cognitive

fusion). I also completed the analyses across two task types, discrimination and a more difficult task, visual search with discrimination.

1.1 Previous Research

Computer vision research has demonstrated the benefits of algorithmic fusion above single-sensor displays in domains such as concealed weapon detection (Üner, Ramac, Varshney, & Alford, 1997), remote sensing (Wald, Ranchin & Mangolini, 1997), medical diagnosis, and military surveillance. However, no consistent evidence has supported the use of one particular algorithm or set of sensors across all domains (Blum, 2006; Dong & Zhuang, 2009). Computer vision techniques require no equipment or complex organization and therefore are thought of as easier to collect and control than human evaluation. Such techniques measure preservation of edge information in a fused image at the individual pixel level (Xydeas & Petrović, 2000), the local 8 x 8 pixel grid level (Piella & Heijmans, 2003), or the global image level (Petrović & Xydeas, 2004; Qu, Zhang, Yan, 2002). In final evaluation stages, these metrics must be validated against a "ground truth," or human testing, before they can be applied the field. Therefore, human evaluation is critical for image assessment even though it is deemed as "heavy in organizational and equipment requirements with strict test conditions" (Petrović, 2007).

No optimal fusion image is available to compare various methods of algorithmic fusion and metrics do not provide information of perceptual quality of the image. Rather metrics only provide a quantitative assessment of the amount of information from each single-sensor image that is represented in the final composite image (Smeelen et al., 2014). Subjective user experience metrics like overall preference or comfort along with perceptual exploration can lead to a more comprehensive evaluation of image displays (Petrović, 2007). But such analyses demand human assessment and are usually an afterthought evaluation (Toet, Hogervorst,

Nikolov, Lewis, Dixon, Bull, & Canagarajah, 2010).

Researchers stress the need for human operators in the interface design process because machines alone cannot account for unexpected situations (Blasch & Plano, 2005). For example, pilots reported they primarily used the algorithmically fused display but were more confident in their decisions by having the ability to switch between the individual sensors using flight tasks (Ryan & Tinker, 1995). Subjective and basic human performance measures (speed, accuracy) are the primary human evaluation techniques for image quality assessment (Sims & Phillips, 1997).

Subjective measures included asking participants to rank multi-sensor images from several fusion algorithms based upon their impression and comfort (Krishnamoorthy & Soman, 2010; Petrović, 2007; Ryan & Tinker, 1995; Steele & Perconti, 1997). Performance measures involved visual tasks focused on evaluating algorithmic fusion advantages in target detection, orientation, and recognition for domains like aviation (Steele & Perconti, 1997; Ryan & Tinker, 1995) and scene surveillance (Toet & Franken, 2003; Toet et al., 1997).

To date, human performance based research has shown both improvements and decrements with algorithmically fused imagery relative to a single individual sensor. Several researchers suggest these differences in performance may result from methodological changes (Ahumada & Krebs, 2000; Essock, Sinai, McCarley, Krebs, & DeFord, 1999; Steele & Perconti, 1997), various task descriptions (Essock, Sinai, DeFord, Hansen, & Srinivasan, 2010; Krebs & Sinai, 2002; Krebs, Xing, & Ahumada, 2002; McCarley & Krebs, 2000) and alternative fusion algorithms or sensor combinations (McCarley & Krebs, 2000). Therefore, researchers have invested efforts to determine what factors of algorithmic image fusion may facilitate better performance. Additionally, several researchers have looked into the use and benefits of color

fusion (e.g., Toet, de Jong, Hogervorst, & Hooge, 2014; McCarley & Krebs, 2006; Sinai, McCarley, Krebs, & Essock, 1999; Toet et al., 1997; Steele & Perconti, 1997) but for the scope of this thesis, I will focus only on gray scale fusion.

A unique method using human identified important information was developed to assess transfer of information from the individual sensor images to the composite image (Toet et al., 2010) The participants were given several images and instructed to draw detailed contours of important features within each image. The drawings were used as a reference to measure the extent that the algorithmically fused image included the meaningful information from each single-sensor image, as indicated by the participants. This technique allowed the human to define important features rather than merely using rate of information transfer to the composite image from each single-sensor image (i.e., computer vision metrics). Nonetheless, this puts the weight of important information on the items in the image that have clear edges to outline rather than the information that may allow the participant to complete a more real-world task. By asking participants to identify important features relative to a real-world task can yield conclusions about what types of information the observer uses for a specific task and the transfer of the defined important features to the composite image.

Another method of assessment is to force observers to use specific features of each single-sensor image to make a correct response choice. Then, compare human performance with the composite image to performance of single-sensor images. In a well-designed study, Toet et al. (1997) instructed participants to report the position of a person relative to a naturally occurring object or bound such as a fence, tree, and pathway. Participants indicated whether the person was in front of or behind the object. The algorithmically fused image gave additional information about the spatial layout of the scene by supplying complementary information of

edge and heat information from individual sensor images. However, the study was designed to demand processing of both the LWIR and visible image in order to make a correct response. The visible image was used to determine where the path, tree or fence was located and the LWIR image gave additional heat information to accurately locate the target. Steele and Perconti (1997) suggested that LWIR images alone (compared to visible alone or a composite LWIR and visible image) are best for target detection tasks. A single LWIR image often allows for rapid, accurate detection of heat-emitting objects (e.g., people). In several investigations of detection tasks, LWIR images outperform visible or algorithmically fused images (Steele & Perconti, 1997; Toet et al., 1997; Krebs & Sinai, 2002). For all variations of the relative position task, participants achieved accuracy improvements with algorithmically fused images (Toet at al., 1997). Furthermore, simply comparing single sensor to multi-sensor information when both sources are needed to achieve high accuracy does not allow for an alternative outcome. Such a study would benefit from comparing multi-sensor information presented with algorithmic fusion compared to presentation of all the available information simultaneously (i.e., cognitive fusion).

In a similar study, Krebs and Sinai (2002) used three types of tasks to examine the change of multisensor fusion benefits as task difficulty increased. In the "easier" person and vehicle detection tasks, participants performed no better with multi-sensor images than single-sensor images. As predicted the benefits of algorithmic fusion increased as difficulty increased in a global scene orientation and a scene recognition task. As the task difficulty increased across these studies, the amount and quality of useful information from each sensor also may have changed. In the detection tasks, information from the LWIR image was sufficient to make a decision given that heat information is shown to benefit in detection tasks. The task manipulations may not necessarily be an increase in cognitive or physical difficulty rather a

change in what information is important from each individual sensor to make a decision. For the detection tasks unique heat information is important, but with global image orientation and scene recognition tasks the holistic image detail and consistency of illumination may be more informative. A more systematic approach is necessary to make comparisons in human performance across difficulty levels or tasks. Again, this study would benefit in comparing multi-sensor algorithmic fusion to cognitive fusion rather than solely to single-sensor images.

Another application of multi-sensor fusion was investigated to aid in driver detection of nighttime road hazards under various levels of difficulty. McCarley and Krebs (2000) combined LWIR and visible sensors and asked participants to detect pedestrians in the visual field at various visibility levels (i.e., low, moderate, and high). In contrast to Krebs and Sinai (2002) the manipulation of difficulty was more systematic with oncoming traffic headlights either turned off (low illumination), on low beam (moderate illumination), or high beam (high illumination). The task remained the same and all other environmental information was not manipulated. They found algorithmic fusion benefits at a moderate level of visibility while maintaining performance equal to visible sensors alone with high visibility. However, with low illumination fusion, reaction times with algorithmic fusion were slower than with visible-only imagery. The benefits of image fusion vary with the quality of the input images (McCarley et at., 2000). Again, algorithmic performance was compared solely to individual sensor performance and even more specific to this study, only to visible sensor performance.

In a later follow-up study, McCarley and Krebs (2006) used a multidimensional signal detection approach, General Recognition Theory (GRT; Ashby & Townsend, 1986), to understand how the perception quality of each input image affect one another. They found the contrast manipulation in one sensor changed the perception of contrast in the alternative.

Therefore, algorithmic image fusion may demonstrate a tradeoff of perceptibility of single-band information (McCarley & Krebs, 2006). For example, given a single fused image, the quality of information in a visible image will alter the perception of information from the LWIR image. The use of GRT allows for understanding of some cognitive properties involved in algorithmically fused imagery. However, there are benefits to understanding more underlying cognitive properties about both cognitive and algorithmic fusion techniques of multi-sensor information rather than solely algorithmic fusion.

1.2 Present Study

Previous conclusions about the use of image fusion were inconsistent with no clear understanding for what experimental manipulations caused performance changes and why changes occurred. I will use a cognitive framework to test specific underlying mechanisms. This is a valuable step forward because I can determine how and why performance changes across systematic experimental manipulations. Fast and accurate responses are desired in multi-sensor tasks. Therefore, if decreases in performance are found with multi-sensor information, I can diagnose what processes are inefficient and suggest how to improve or alter processing to yield better performance. I can only suggest remedies by first understanding the properties of basic multi-sensor information processing across a few closely related experimental manipulations.

In the current study, I used two fusion techniques and two task difficulty levels. I examine algorithmic and cognitive fusion in left/right discrimination and left/right discrimination with spatial uncertainty tasks. My hypotheses were based on previous research and a brief pilot study.

1.3 Hypotheses

In pilot studies I investigated cognitive processing of a Landolt C (Figure 2). I found less efficient processing (decrease in performance) of LWIR and visible information with multi-sensor imagery. Also I found information was processed simultaneously and responses were made based on whichever sensor finished processing first. In the current studies, I expect to see improvements in processing mechanisms due to more difficulty imagery (Krebs et al., 2002). Based on the findings of perceptual nonseperability of single-sensor information (McCarley and Krebs, 2006), I also predict that information from each sensor is processed simultaneously with high interdependence in algorithmically fused images. Here I give a general outline of my hypotheses. I provide hypotheses for specific properties of information processing of multi-sensor information in the Analyses subsection of the General Method. Below is a general understanding for what I expect. Later, I explain the mathematical approach I use and indicate what specific cognitive properties relate back to the hypotheses stated below.

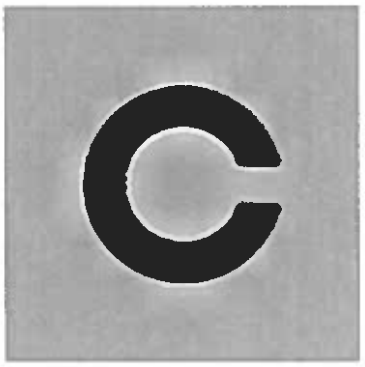

Figure 2. Multi-sensor Landolt C comprised of both visible and LWIR information. These stimuli were used in pilot studies. Distribution A: Approved for public release; distribution unlimited. 88ABW Cleared 01/21/2014; 88ABW-2014-0191.

1. With a discrimination task I predict efficiency decrements with multi-sensor information for both algorithmic and cognitive fusion with algorithmic fusion significantly worse than cognitive fusion.

1A. I also predict that cognitive and algorithmically fused image information is processed simultaneously; however, I predict a highly interactive structure (coactive; discussed further in later sections) for algorithmically fused information processing.

2. In a second experiment with a discrimination task with target location uncertainty, I predict more efficient cognitive mechanisms with both multi-sensor fusion techniques.

2A. I also predict the structure of information processing to be consistent with the discrimination task (Hypothesis 1A).

2. GENERAL METHOD

2.1 Overview

In the experiments reported here, I used the double factorial paradigm (Townsend & Nowaza, 1995; Houpt, Blaha, McIntire, Havig & Townsend, 2014), a paradigm developed to capture the underlying cognitive processes of multiple sources of information. I describe the statistical framework and corresponding paradigm in following subsections. I investigated processes of two sensors across two fusion techniques and two task difficulty levels, a 2x2x2 mixed design. The two fusion techniques, algorithmic and cognitive, were explained previously. The tasks are explained in the respective Experiment method section.

2.2 Participants

I recruited 10 students (6 male, 4 female) attending Wright State University for this study. Participants' ages ranged from 20 to 37 years ($M = 25$ years). All participants self reported right-handedness, normal or corrected to normal vision, normal color vision, and no difficulties reading English. All 10 participants completed 5 sessions for each experiment: Experiment 1 and Experiment 2. Participants were compensated \$8 per session with a \$2 per session completion bonus: \$8 + \$2 bonus x 10 days = \$100 in total.

2.3 Materials

Stimuli were presented using PsychoPy (Peirce, 2009) on a 20-inch Sony Trinitron monitor. Similar to the procedures in Bittner, Schill, Blaha, and Houpt (2014), stimuli were randomly selected within sensor type and target type from a set of 20 to avoid additional cues from artifacts of sensor noise. Therefore, I selected 10 sensor images that slight varied from one another for each response option (left or right) within the 2AFC task in both Experiment 1 and Experiment 2. For example, in Experiment 1 I selected 5 images of a man pointing left and a 5

pointing right for both LWIR (Figure 3A) and visible (Figure 3B) imagery. In addition, I selected 5 images of another man pointing left and 5 pointing right that varied in appearance from the previous man for both LWIR (Figure 3C) and visible (Figure 3D) imagery. The stimuli varied across Experiment 1 and Experiment 2 so various examples of each are shown in the respective Experiment method sections later in the document. The sensors and fusion techniques are described below.

2.3.1 Image Collection. TNO Defense located in Soesterberg, Netherlands constructed the TRICLOBS 3-band night vision system consisting of two digital image intensifiers (Photonis ICU's) and an uncooled long-wave infrared microbolometer (XenICS Gobi 384). The night vision sensor suite registers visual (400-700 nm), near infrared (700 – 1000 nm) and long-wave infrared (8-14 μm) bands of the electromagnetic spectrum. The optical axes of the three cameras were aligned using two dichroic beam splitters (ITO filter to reflect the LWIR part of the incoming radiation into the thermal camera, and a B43-958 hot mirror to split the transmitted radiation into a visual and NIR part). The registration of the individual images therefore requires only a minimal amount of computational effort. Software has been developed to register the signals from all 3 cameras simultaneously, display the images, and write them to a hard disk (Toet, 2013; Toet & Hogervorst, 2009). The raw imagery was handed over to Dr. Alan Pinkus (WPAFB, Dayton, Ohio). Additional simple image registration was conducted at AFRL.

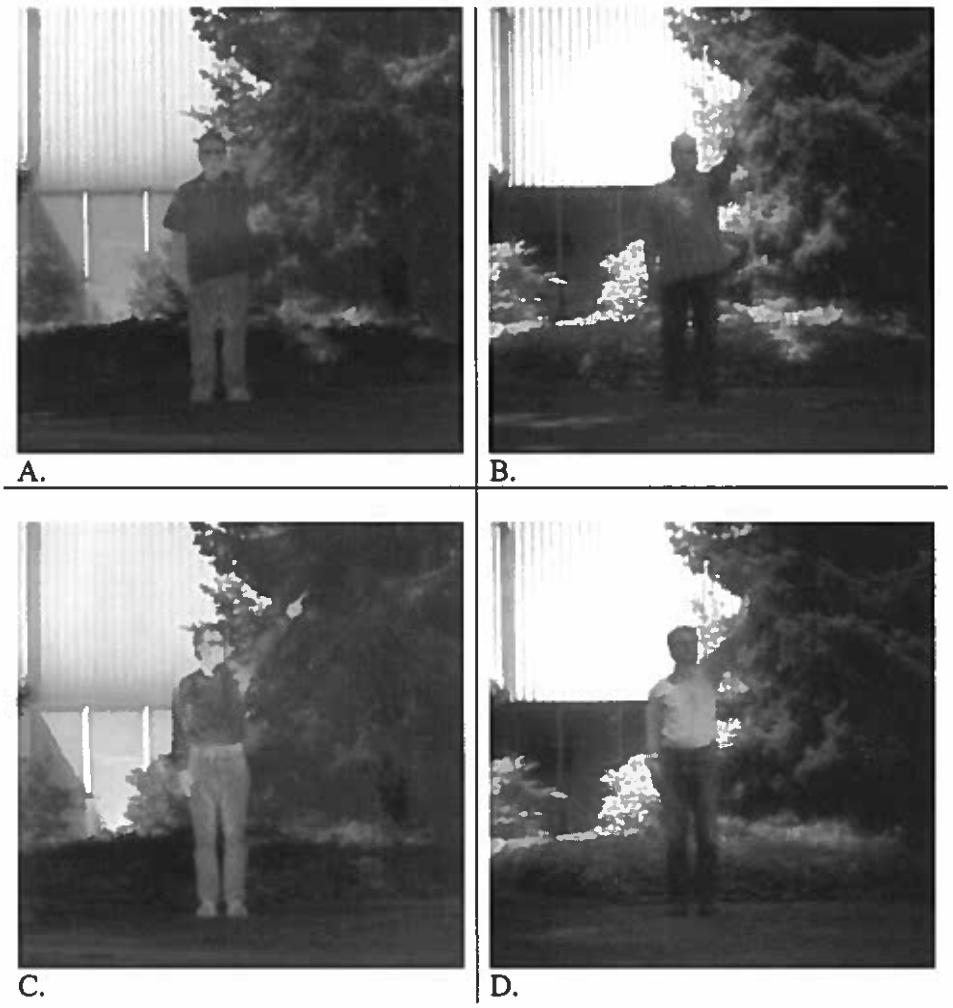

Figure 3. Examples of the two individuals pointing right used for stimuli in Experiment 1. Images consist of each individual point right with LWIR imagery (3A and 3C) and visible imagery (3B and 3D).

2.3.2 Sensors. I used imagery from two sensors, visible and long-wave infrared (LWIR). There are numerous sensors to investigate but I will focus only on two for my study. I chose visible and LWIR because of the contrast in the type of information each one holds. As I mentioned in the introduction, visible images display detail of features while LWIR highlight heat information. When presented together the sensors can potentially improve performance in detection and discrimination tasks (Krebs & Sinai, 2002; Toet et al., 1997).

2.3.3 Fusion. I used two types of fusion techniques, algorithmic and cognitive. Algorithmic fusion attempts to combine important features from each sensor into a single image. I used the Laplacian Pyramid Transform (LPT) to combine visible and LWIR information into one composite image. The LPT is a pixel-level, pyramid based algorithm. Subjective and image quality assessments support the use of LPT (Petrović, 2007). The algorithmic images were always presented in the center of the screen. Cognitive fusion presents both single-sensor images within 5 degrees of visual angle. The images are presented directly to the left and right of center screen.

2.3.4 Stimulus Manipulation. One manipulation requirement of the cognitive framework I used is to speed up and slow down the processing of sensors' information. I further explain these details in the proposed Analyses subsection below. I used the QUEST psychometric method (Watson & Pelli, 1983) at the start of each session, excluding Day 1 of each experiment, to slow down the processing of each single-sensor image. This method systematically manipulated the amount of random noise added to the stimulus for 120 trials. Upon completion, the block returned an estimate of the amount of noise necessary to obtain 90% accuracy. This procedure was conducted for each sensor in independent, randomly ordered blocks. Next, I copied the original stimulus set and added an amount of random Gaussian noise equivalent to the psychometric estimation value. An example of a LWIR image (Figure 4A) with noise is shown in Figure 4B and a visible image (Figure 4C) with noise is shown in Figure 4D. These images (Figure 4B and 4D) represented stimuli intended to slow down the cognitive processing of the sensor information. I accounted for daily individual variability by estimating noise values for each person at the start of each session.

Each combination of original stimuli (high salience or H) and stimuli with noise (low salience or L) were used in the following block of trials to systematically speed up and slow down processing of each single-sensor: $H_{LWIR} + H_{visible}$, $H_{LWIR} + L_{visible}$, $L_{LWIR} + H_{visible}$, and $L_{LWIR} + L_{visible}$. This procedure was done every session after the two psychometric blocks. For algorithmically fused trials, the stimulus noise was added before fusing the two images together.

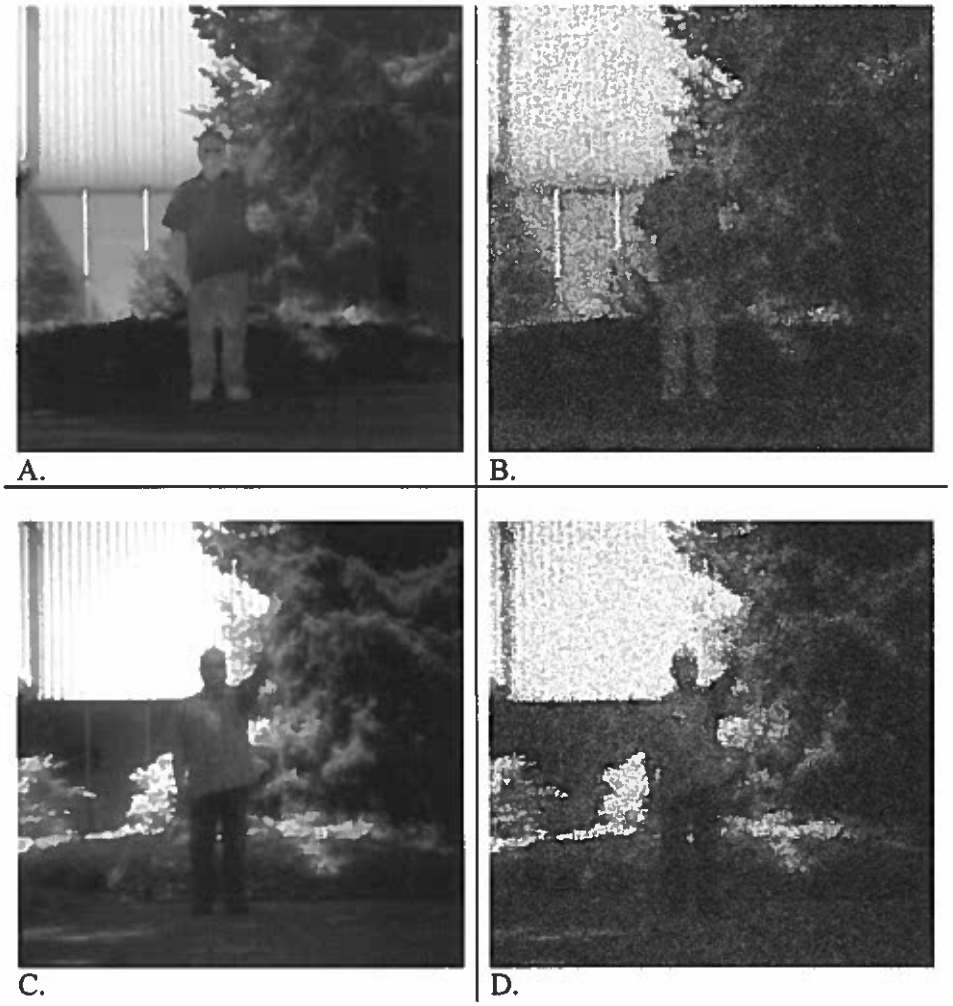

Figure 4. An example of a LWIR image (A) with Gaussian noise (B) and a visible image (C) with Gaussian noise (D) used in Experiment 1.

2.4 Procedures

Participants had 10 days of 1-hour experimental session. Five sessions were dedicated to each experiment: Experiment 1 and Experiment 2. Session 1 and 6 had 6 blocks of trials to test Hypotheses 1 and 2, each session was 50 minutes in total (Figure 5). The remaining sessions (2-5, 7-10) consisted of two psychophysical blocks (10 minutes) and a third 45-minute block testing Hypotheses 1A and 2A (Figure 6). The blocks within the first session were pseudo-randomized and the remaining sessions alternated between algorithmic (A) or cognition (C) fusion. Specific numbers of trials are tailored for my planned analyses and discussed in further detail in following subsections.

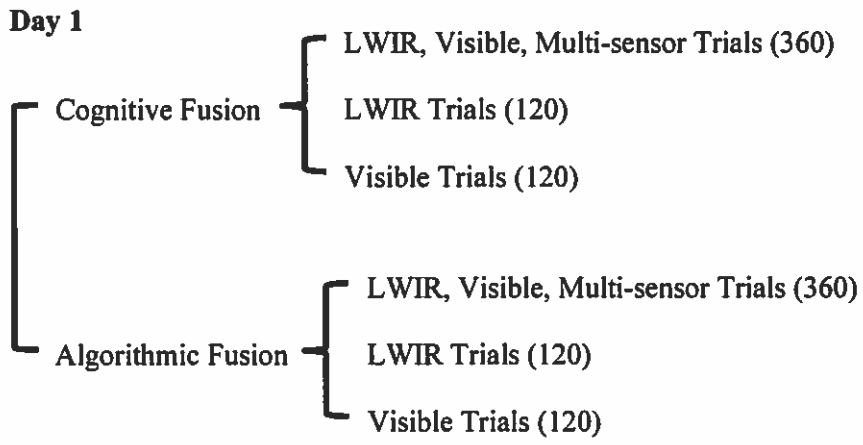

Figure 5. On Day 1 of each Experiment participants complete all 6 experimental blocks with order of cognitive and algorithmic fusion randomized and the 3 blocks within each in a randomized order. Beside the name of each is the number of trials for the respective experimental block.

Day 2-4, 6-10

Cognitive Fusion: QUEST - Visible (120) + QUEST - LWIR (120) → High and Low Salience Trials (1080)

OR

Algorithmic Fusion: QUEST - Visible (120) + QUEST - LWIR (120 → High and Low Salience Trials (1080)

Figure 6. On experimental session 2-4 and 6-10 the fusion techniques alternated and the one that came first was randomly chosen. Two QUEST blocks were randomly ordered and upon completion of both, a block of trials with all possible combinations of high and low salience stimuli was completed. More detailed explanation of trials is in subsequent sections.

2.4.1 Stimulus Presentation. On every trial a localization box (Figure 7 & Figure 8) was presented for a random interval of time between 400 and 500ms followed by the stimulus. The stimulus was displayed for 250 msec. In an algorithmic fusion block one image was randomly selected and always presented in the middle of the screen (Figure 7). In cognitive fusion blocks LWIR-only and visible-only trials displayed one image randomly placed to the left or right of the center (Figure 8). Figure 8 illustrates a cognitive fusion trial when both sensors were presented. Sensor presentation was also randomly placed to the left or right of the center for multi-sensor presentation. The stimuli for cognitive fusion trials were displayed within 5 degrees visual angle to ensure no saccade was necessary for perceptual processing of the information. A blank screen was presented for 1750msec to leave a sufficient amount of time for response (2 seconds in total). No trial feedback was given.

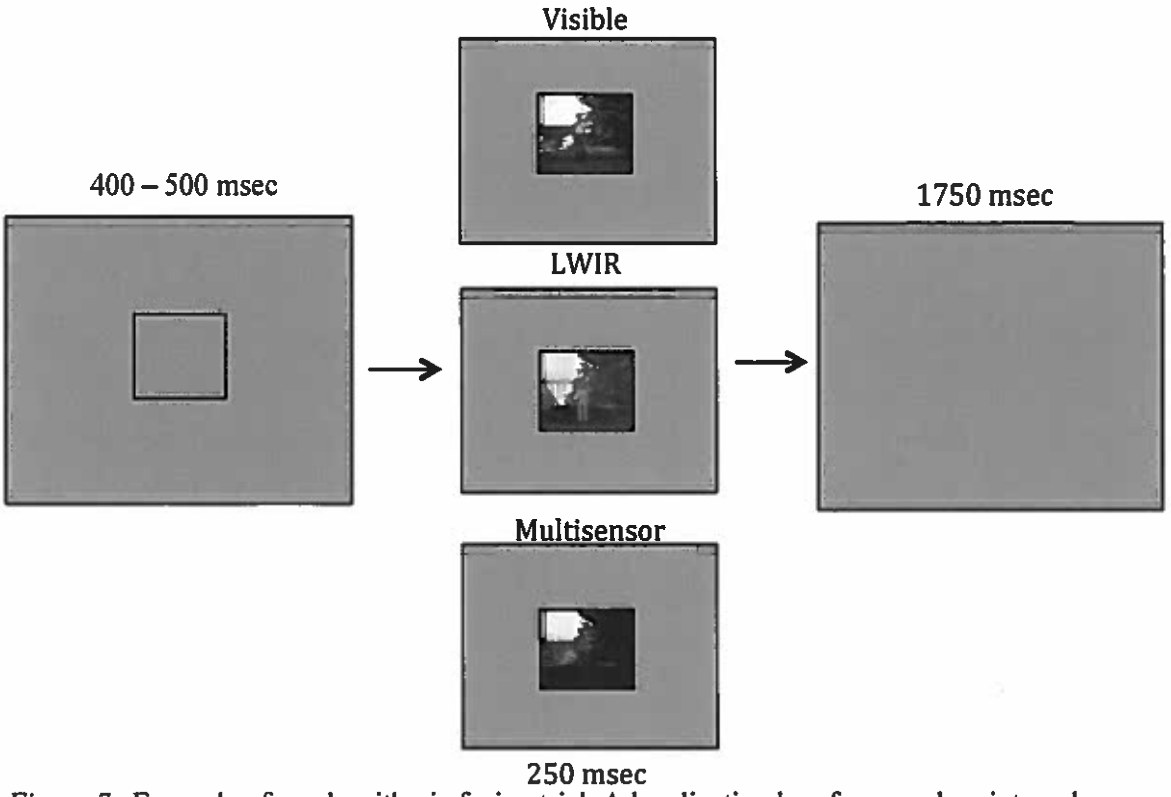

Figure 7. Example of an algorithmic fusion trial. A localization box for a random interval between 400-500msec was followed by the presentation of a visible-only (top-middle image), LWIR-only image (center-middle), or multi-sensor image (bottom-middle) for 250msec. All images were presented in the center of the screen.

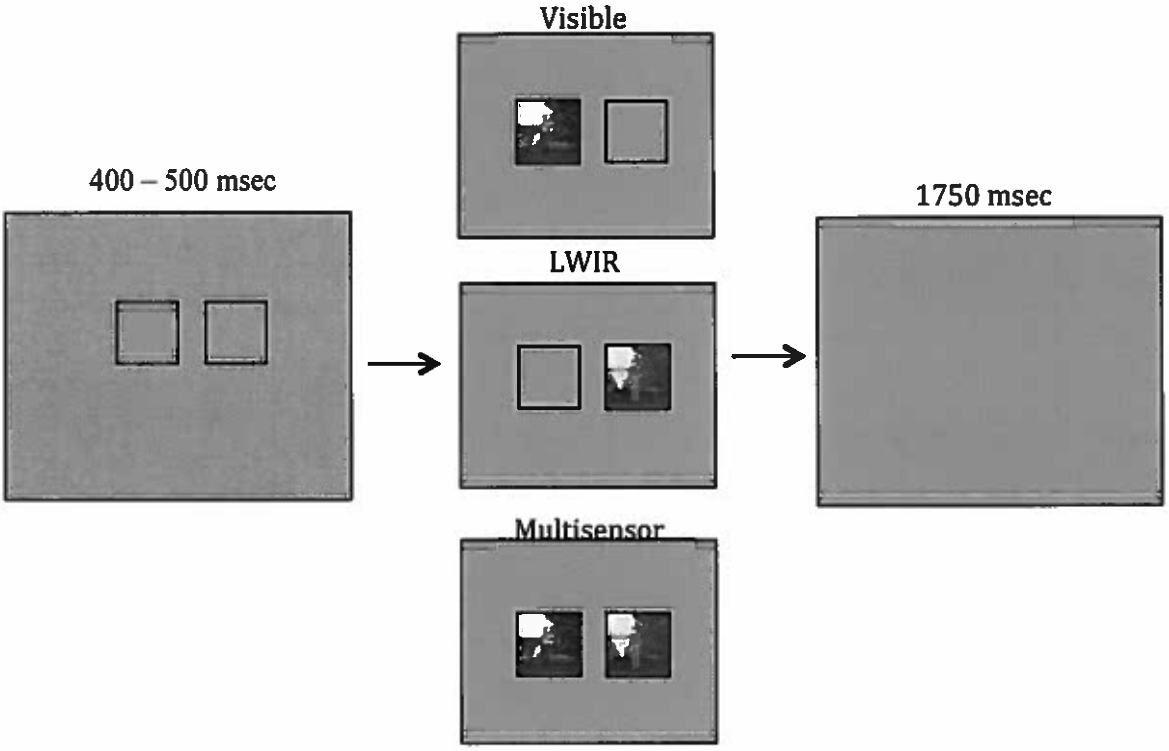

Figure 8. Example of a cognitive fusion trial. Two localization boxes were presented for a random interval between 400-500msec and followed by the presentation of a visible-only (top-middle image), LWIR-only image (center-middle), or multi-sensor image (bottom-middle) for 250msec. All images were presented within 5 degrees of visual angle with each randomly placed to the left and right of center screen.

2.5 Analyses

I used measures of Systems Factorial Technology (Townsend & Nowaza, 1995) to investigate cognitive mechanisms of multi-sensor information. This framework supplies information about important cognitive properties including workload capacity, independence, architecture, and stopping-rule. Workload capacity refers to the change in processing rate of each sensor going from single to multi-sensor presentation. Independence is the degree to which the sensor information interacts. Architecture is the spatio-temporal organization of sensor processing, whether processing is simultaneous or sequential. Stopping-rule refers to whether

one or both sensors are finished processing when a response is made. One statistical measure of SFT, the capacity coefficient, is used to examine workload capacity and independence. Two additional measures, the survivor interaction contrast (SIC) and mean interaction contrast (MIC), are used to observe unique architecture and stopping-rule response time signatures. The double factorial paradigm (DFP) is methodology developed to ensure appropriate manipulations for computing measures of SFT. I describe each measure of SFT and the DFP below.

2.5.1 Capacity Coefficient. The capacity coefficient is the ratio of observed performance with multi-sensor information to the predicted, model-based performance (Equation 1). The model prediction is the sum of performance with each single-sensor image. The model prediction is an individual level baseline and assumes unlimited capacity, independent, and parallel processing (UCIP). Unlimited capacity is evidence of no change in processing rate of the individual sensors for multi-sensor presentation. Independent processing indicates no cross talk or facilitation between sensor information. Parallel model predictions support simultaneous processing of all sensor information.

A cumulative hazard function represents overall performance for a given trial type (visible-only, LWIR-only, and multi-sensor). A cumulative hazard function, $H(t)$, indicates the amount of processing completed at a given time (t). The capacity coefficient ratio is a function of the amount of processing completed for multi-sensor trials to the amount of processing a UCIP model would predict at any time, t. The capacity coefficient assuming only one source of information must be finished processing (i.e., OR processing) is defined as:

$$C_{\mathrm{OR}}(t)\frac{H_{\text{multi-sensor}}(t)}{H_{\text{visible}}(t)+H_{\mathrm{LWIR}}(t)}. \quad (1)$$

The numerator is the cumulative hazard function of multi-sensor trials and the denominator is the summation of the integrated hazard functions of visible-only and LWIR-only trials. If all

assumptions are satisfied, the ratio equals 1, C(t) = 1. If one or more assumptions are violated, the ratio is greater than 1 (super capacity) or less than 1 (limited capacity).

Based on my general hypotheses, I outline the corresponding capacity coefficient results I expect to find:

1. A limited workload capacity for both fusion types in a simple discrimination task.
2. In a more complex, visual search with discrimination task, I predict improvements in capacity from the simple task. Therefore, I predict unlimited or super workload capacity for both cognitive and algorithmic fusion.

2.5.2 Survivor Interaction Contrast. The SIC examines the interaction between two sources of information when slowing down and speeding up cognitive processing (Equation 2). I add random noise to each sensor to effectively slow down and speed up processing rates. The salience manipulation must satisfy the assumptions of selective influence to affect only the speed of processing for the respective sensor information. Assumptions are tested using Kolmogorov-Smirnov (K-S) test and the following statistical tests must indicate significance with alpha = .05: $S_{HH} < S_{HL}$, $S_{HL} < S_{LL}$, $S_{HH} < S_{LH}$, $S_{LH} < S_{LL}$ (Figure 9).

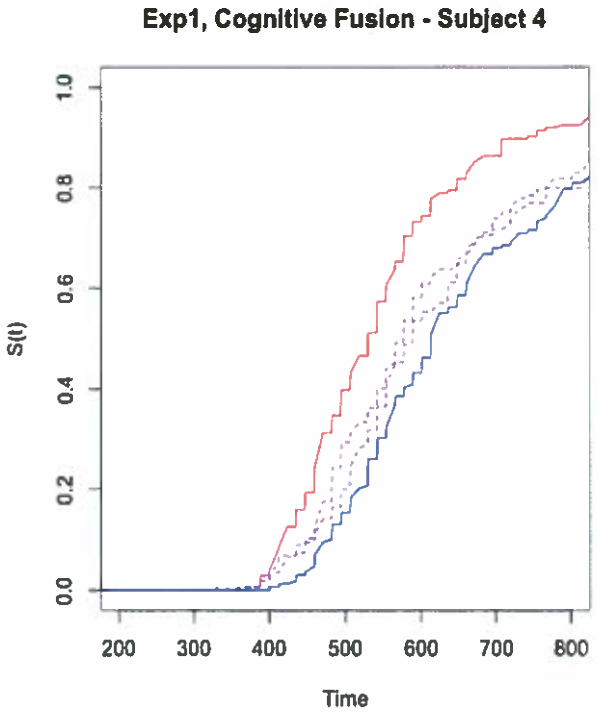

Figure 9. Ordering of survivor functions that satisfy all assumptions of selective influence. The red line represents the fastest distribution when both sources have high salience (S_{HH}) and the blue line represent the slowest distribution when both sources have low salience (S_{LL}). The purple dashed lines represent the two variations of high and low salience in each source (S_{HL} and S_{LH}).

If selective influence holds, the SIC will indicate one of five classes of models. Positive and negative SIC deviations from zero are tested using the Houpt-Townsend statistic (Houpt & Townsend; 2010) and are used to classify the unique processing model (see Figure 10). The Houpt-Townsend statistic is not computed for those violating assumptions of selective influence. Parallel-AND indicates both visible and LWIR information is processed simultaneously and to completion before a response is made. With a Parallel-OR model all information is processed simultaneously but only the information from the fastest sensor channel is used to make a

decision. Serial-AND models process visible and LWIR information sequentially and all processing is completed before a response is made. Serial-OR models process information sequentially but only one type of sensor information is used to make a decision. A coactive model does not have a particular stopping rule. Rather both of the sensors are processed simultaneously and information pools together to reach one decision threshold.

Each structural model demonstrates a distinct distributional signature after computing the SIC. The SIC is defined as:

$$\mathrm{SIC}(t) = [S_{\mathrm{LL}}(t) - S_{\mathrm{LH}}(t)] - [S_{\mathrm{HL}}(t) - S_{\mathrm{HH}}(t)]. \quad (2)$$

If underlying processes are serial then the mean area under the curve is zero. If processing is parallel then the mean area under the curve is different from zero (positive or negative). The distinction between parallel and serial models is tested using the mean interaction contrast (MIC). This measures is comparable to the SIC but returns a mean contrast value rather than a function. It is defined as:

$$\mathrm{MIC}(t) = [M_{\mathrm{LL}} - M_{\mathrm{LH}}] - [M_{\mathrm{HL}} - M_{\mathrm{HH}}]. \quad (3)$$

The MIC alone is not sufficient to detect variations of parallel and serial models. Therefore, I used the Houpt-Townsend statistic to detect significantly positive (D+) or negative (D-) deviations from zero in the SIC function. Our alpha level is .33 because the null hypothesis is zero and could otherwise favor a serial-OR signature (Houpt, 2014). If cognitive mechanisms utilize a parallel-AND model then the SIC is all negative (significant D-, MIC < 0), parallel-OR results in an all positive SIC (significant D+, MIC > 0), and serial-OR models result in a flat SIC (MIC = 0). Both a serial-AND and coactive model result in an SIC that is first negative then positive (significant D+ and D-). MIC is useful to further distinguish between serial-AND and

coactive processes. For the coactive model is a variation of parallel processing (MIC > 0) while a serial-AND model indicates MIC = 0.

A hierarchical Bayesian analysis can estimate a full posterior distribution for both group and individual level inferences of parallel and serial models (Houpt & Fifić, 2013). The model allows for analysis with a fewer number of trials/participants than required for SIC statistics to draw meaningful conclusions of underlying processing mechanisms. I ensure a sufficient burn in period for Markov-Chain Monte Carlo sampling to obtain convergence across all chains and adequate measures of effect size and adjustment for autocorrelation across all participants. An adequate measure of effect size is a Gelman-Rubin statistic of 1.10 or smaller (Gelman & Rubin, 1992). The model assumes inverse-Gaussian response time distributions. Prior distributions are defined as MIC = 0 as the most likely model (50%) while MIC > 0 and MIC < 0 are less likely with equal probability (25%). This prior was used based on the possible classes of models, serial-OR or serial-AND is MIC = 0, parallel-OR is MIC > 0, and parallel-AND is MIC < 0.

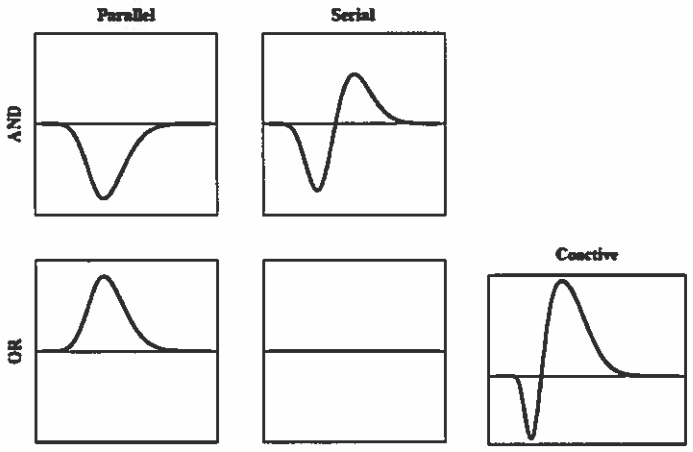

Figure 10. Five distinct model distribution signatures including parallel-AND (top left), parallel-OR (bottom left), serial-AND (top right), serial-OR (bottom middle), and coactive (bottom right).

To further elaborate on the predictions discussed in the Hypotheses section I describe how each relates to specific SIC signatures:

1A. For the simple discrimination task I predict simultaneous processing of sensor information with a cognitive fusion display. I hypothesize only one sensor will finish processing before a decision is made, parallel-OR processing. For algorithmically fused imagery, I predict to find a coactive cognitive architecture.

2A. For the more complex visual search with discrimination task, I hypothesize to find the same cognitive architecture described in Hypothesis 1A (above).

2.5.3 Double Factorial Paradigm. My experimental paradigm must manipulate workload for the capacity coefficient and salience for the SIC. Two condition types are required for estimating the UCIP model prediction and computing a ratio of the baseline model to multi-sensor performance comparison: a condition with all sensor information present (HH or multi-sensor trials) and individual sensor trials (ØH or visible-only and HØ or LWIR-only). The salience manipulations change processing speed of the different sensors to infer about temporal arrangement. The salience manipulations must satisfy the assumptions of selective influence to only affect the speed of processing for the respective sensor information. Therefore, the survivor function of multi-sensor information with no noise (S_{HH}) must be the fastest and the survivor function of multi-sensor information with noise added to both sensors (S_{LL}) must be the slowest, $S_{HH} < \{S_{HL}, S_{LH}\} < S_{LL}$. The processing speed of each sensor was factorially manipulated according to DFP guidelines outlined in a recent article (Houpt, Blaha, McIntire, Havig, Townsend, 2014). Each trial type is shown in Table 1. Table 2 indicates the specific trials presented on the first day of each Experiment to test Hypotheses 1 and 2. Table 3 indicates the full double factorial paradigm to make conclusions about Hypotheses 1A and 2A. The numbers

within each box represent the number of trials for each combination of sensor images. In the full factorial paradigm trials are balanced using methods that suggest presenting multi-sensor, visible-only, and LWIR-only images for the same number of trials (Houpt et al., 2014).

Table 1. Double factorial paradigm. Each element identifies the salience level for LWIR and visible sensors (i.e. H_1L_2 = high salience LWIR and low salience visible). In this design, at least one signal was present for each trial so there were no Absent-Absent trials.

		Visible (2)		
	Salience	High	Low	Absent(Ø)
LWIR (1)	High	H_1H_2	H_1L_2	$H_1Ø_2$
	Low	L_1H_2	L_1L_2	$L_1Ø_2$
	Absent(Ø)	$Ø_1H_2$	$Ø_1L_2$	X

Table 2. Specific trials presented on the first day of each experiment to test Hypotheses 1 and 2. 120 trials of visible-only, LWIR-only, and multi-sensor images were completed.

		Visible (2)	
		High	Ø
LWIR (1)	High	120	120
	Ø	120	X

Table 3. The full double factorial paradigm to make conclusions about Hypotheses 1A and 2A. All multisensor combinations of high and low salience were each presented 180 times and while each single-sensor high and low salience stimuli were presented on 360 trials.

		Visible (2)		
	Salience	High	Low	Absent(Ø)
LWIR (1)	High	180	180	360
	Low	180	180	360
	Absent(Ø)	360	360	X

3. EXPERIMENT 1

3.1 Methods

Experiment 1 was always the first 5 days of participation. All 5 sessions involved a left/right discrimination task.

3.1.1 Procedures. Participants were asked to discriminate whether a person's arm was pointing left or right (Figure 3A-3D). If the participant determined left, they pressed the left mouse button, if right, they pressed the right mouse button. The participants were told to perform the task as quickly and accurately as possible and were informed they must achieve at least 90% accuracy to order for me to conduct any further analyses.

3.2 Results

A summary of capacity coefficient and SIC results across both algorithmic and cognitive fusion for the discrimination task in Experiment 1 for each participant is listed in Table 19. The following sections address the results of several measures that test my hypotheses.

3.2.1 General Analyses. Participant 1 did not achieve 80% accuracy in all conditions are therefore was not included in the capacity analyses of cognitive fusion multi-sensor information. Summary statistics of response time and accuracy are outlined for each participant for visible-only (Table 4), LWIR-only (Table 5) and multi-sensor (Table 6) in the algorithmic fusion block and for each participant in the cognitive fusion block (Table 7-9). Group response time statistics are provided in Table 10 and Figure 11. Using a Bayesian linear model there is barely mentionable evidence for a main effect of fusion type (algorithmic, cognitive) and subject over a model with main effects of sensor (visible-only, LWIR-only, multisensor) and subject, $BF = 1.15$.

A one-way ANOVA was conducted for each sensor and fusion type to test response time variability within each set of 10 images across all participants. Analysis of variance showed that the effect of individual image was not significant across visible-only $F(19,1180) = 1.19$, $p = 0.26$, or LWIR-only images, $F(19,1180) = 1.49$, $p = 0.08$ when presented in the center of the screen (algorithmic fusion condition). With cognitive fusion presentation (left or right of center screen) analysis of variance showed significant effect of image across LWIR-only, $F(19,1180) = 3.52$, $p < .05$, but not with visible-only images, $F(19,1180) = 1.39$, $p = 0.12$. Significant effects of image were shown for images chosen for algorithmic fusion, $F(19,1180) = 3.42$, $p < .05$.

Table 4. Individual mean and standard deviation of response time and accuracy for the visible-only trials within the cognitive fusion-capacity block in Experiment 1.

	Response Time		Accuracy	
Participant	*M*	*SD*	*M*	*SD*
1	476.59	263.21	89.17	31.21
2	540.47	192.74	90.00	30.13
3	450.81	78.15	90.00	30.13
4	579.28	281.76	95.00	21.89
5	455.83	138.21	85.00	35.86
6	551.45	163.50	95.83	20.07
7	664.72	329.78	80.83	39.53
8	547.49	184.33	98.33	12.86
9	575.49	89.50	98.33	12.86
10	567.94	121.89	97.50	15.68

Table 5. Individual mean and standard deviation of response time and accuracy for the LWIR-only trials within the cognitive fusion-capacity block in Experiment 1.

	Response Time		Accuracy	
Participant	*M*	*SD*	*M*	*SD*
1	854.86	712.83	62.50	48.62
2	572.43	253.91	83.33	37.42
3	462.30	91.93	90.00	30.13
4	593.33	282.41	94.17	23.54
5	486.52	174.19	90.00	30.13
6	579.62	151.28	96.67	18.03
7	674.35	316.87	84.17	36.66
8	564.00	184.40	97.50	15.68
9	611.69	108.40	95.83	20.07
10	578.25	122.65	95.83	20.07

Table 6. Individual mean and standard deviation of response time and accuracy for the multisensor trials within the cognitive fusion-capacity block in Experiment 1.

	Response Time		Accuracy	
Participant	*M*	*SD*	*M*	*SD*
1	599.03	448.00	89.17	31.21
2	483.77	110.40	98.33	12.86
3	421.89	61.67	97.50	15.68
4	533.59	179.55	98.33	12.86
5	415.13	70.73	98.33	12.86
6	520.45	139.19	97.50	15.68
7	650.40	333.45	93.50	26.45
8	512.92	130.20	100.00	0.00
9	555.77	96.25	100.00	0.00
10	515.64	12.73	99.17	9.13

Table 7. Individual mean and standard deviation of response time and accuracy for the visible-only trials within the algorithmic fusion-capacity block in Experiment 1.

	Response Time		Accuracy	
Participant	*M*	*SD*	*M*	*SD*
1	369.14	166.17	92.50	26.45
2	427.51	146.85	96.67	18.03
3	374.26	58.01	96.67	18.03
4	468.80	23136	94.17	23.54
5	377.29	170.88	95.83	20.07
6	411.21	91.92	98.33	12.86
7	469.10	178.51	95.00	21.89
8	351.98	52.98	97.50	12.68
9	612.01	113.09	99.17	0.09
10	463.99	107.61	100.00	0.00

Table 8. Individual mean and standard deviation of response time and accuracy for the LWIR-only trials within the algorithmic fusion-capacity block in Experiment 1.

	Response Time		Accuracy	
Participant	*M*	*SD*	*M*	*SD*
1	363.07	64.74	94.17	23.54
2	441.35	153.25	95.83	20.07
3	390.04	61.59	96.67	18.03
4	502.71	290.83	96.67	18.03
5	379.65	94.24	92.50	26.45
6	415.29	174.18	97.50	15.68
7	527.46	248.52	92.50	26.50
8	354.82	63.24	97.50	15.68
9	651.72	170.28	99.17	0.09
10	458.60	87.16	100.00	0.00

Table 9. Individual mean and standard deviation of response time and accuracy for the multisensor trials within the algorithmic fusion-capacity block in Experiment 1.

	Response Time		Accuracy	
Participant	*M*	*SD*	*M*	*SD*
1	395.64	219.96	86.67	34.14
2	432.32	96.36	96.67	18.02
3	406.80	168.53	94.17	23.54
4	499.01	193.83	98.33	12.86
5	402.29	206.82	93.33	25.05
6	447.91	108.62	99.17	9.13
7	545.60	304.75	94.17	23.54
8	368.66	87.19	96.67	18.03
9	654.78	169.29	97.50	15.68
10	507.05	169.96	99.17	9.13

Table 10. Mean and standard deviation of response time at the group level across each trial type (visible-only, LWIR-only, multisensor) of both the algorithmic and cognitive fusion capacity blocks in Experiment 1.

	Condition	*M*	*SD*
Algorithmic	Visible	422.63	26.53
	LWIR	441.46	26.57
	Multisensor	442.59	26.45
Cognitive	Visible	506.78	26.66
	LWIR	539.31	26.65
	Multisensor	523.95	26.44

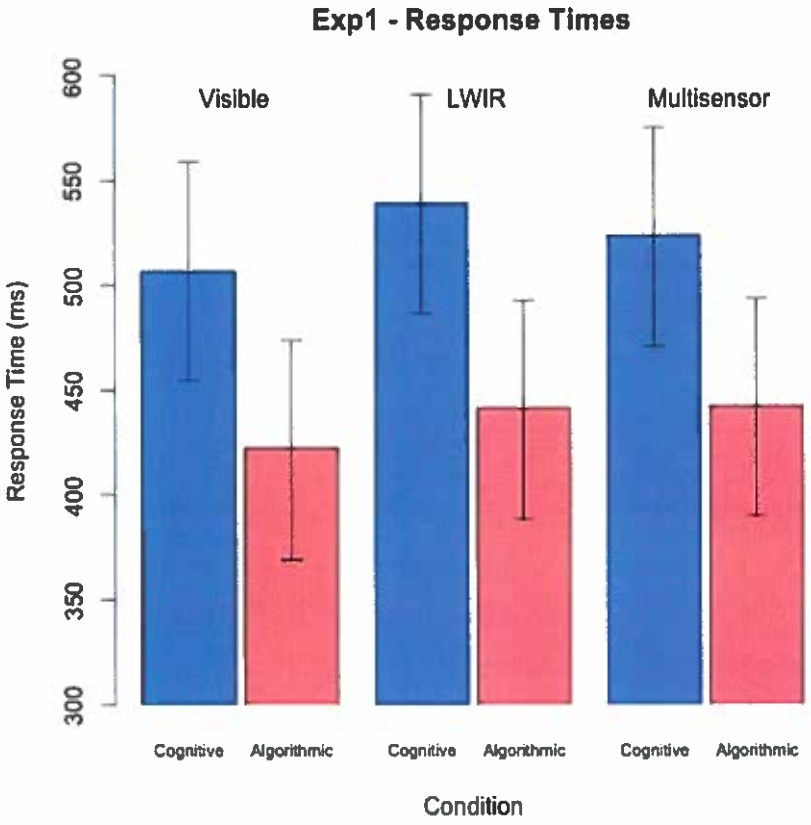

Figure 11. Group level Bayesian estimated mean and 95% highest density interval for both algorithmic and cognitive fusion with visible-only, LWIR-only, and multi-sensor trials. The salmon colored bars represent the algorithmic fusion trials (center of screen) and the purple-blue bars represent the cognitive fusion trials (randomly placed to the left/right of center screen).

3.2.2 Capacity Coefficient. The capacity coefficient function was below 1 for some time for both cognitive and algorithmic fusion. Individual capacity z-scores in Experiment 1 ranged from -9.5 to -6.4 for algorithmic fusion (Table 11) and from -4.2 to 0.08 for cognitive fusion (Table 12). The performance hypotheses were supported; I found a limited workload capacity across both fusion techniques with algorithmic fusion decisively more limited than cognitive fusion, BF = 850 (Figure 12). However, looking at individual level analyses 4 participants

exhibited an unlimited workload capacity for cognitive fusion blocks (Participants 2, 3, 5, 10). At the group level, processing efficiency of multi-sensor information was worse than what was predicted by a UCIP model across both fusion techniques. However, individual analyses show some individuals process multi-sensor cognitive fusion information with equal efficiency as UCIP model predictions (unlimited capacity).

Table 11. Individual level capacity, z-score, and p-value for algorithmic multi-sensor images compared to each sensor alone (UCIP model).

Subject	Capacity	z-score	p-value
1	Limited	-8.174	$p < .05$
2	Limited	-6.367	$p < .05$
3	Limited	-8.182	$p < .05$
4	Limited	-7.694	$p < .05$
5	Limited	-7.780	$p < .05$
6	Limited	-9.155	$p < .05$
7	Limited	-7.436	$p < .05$
8	Limited	-7.547	$p < .05$
9	Limited	-7.660	$p < .05$
10	Limited	-9.500	$p < .05$

Table 12. Individual level capacity, z-score, and p-value for multi-sensor cognitive fusion compared to each sensor alone (UCIP model).

Subject	Capacity	z-score	p-value
1	N/A	N/A	N/A
2	Unlimited	-0.088	$p = 0.930$
3	Unlimited	-0.653	$p = 0.514$
4	Limited	-4.056	$p < .05$
5	Unlimited	0.088	$p = 0.930$
6	Limited	-3.322	$p < .05$
7	Limited	-4.219	$p < .05$
8	Limited	-4.066	$p < .05$
9	Limited	-2.362	$p < .05$
10	Unlimited	-0.826	$p = 0.409$

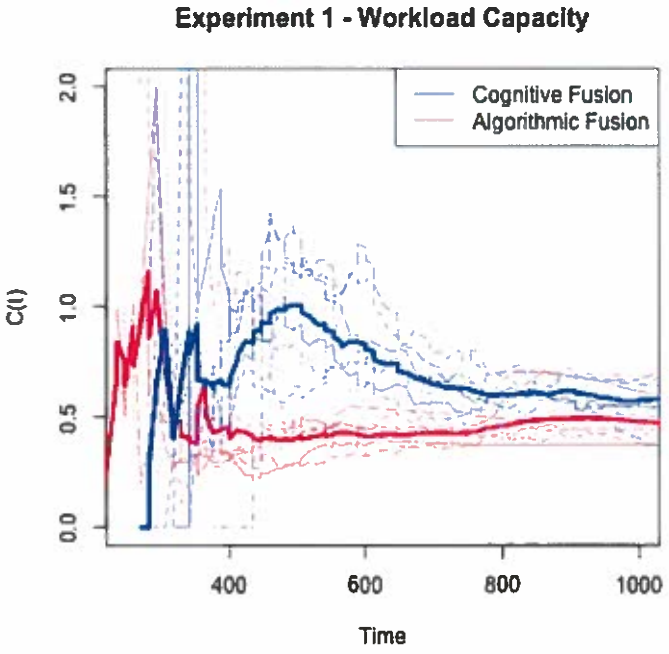

Figure 12. The capacity coefficient for both algorithmic and cognitive fusion in Experiment 1. The reference line is C(t) = 1 (unlimited capacity). The bold red line shows the group level for algorithmic fusion with red dashed lines showing each individual. The bold blue line shows the group level for cognitive fusion with the blue dashed lines showing each individual.

3.2.3 Blocking Effects. Most participants' performance exhibited no difference across sensor response time distributions when pulling each individual sensor trials into a separate block of trials using a Bayesian t-test. However, some participants did show evidence for an effect. Table 13 and 14 list visible effects with algorithmic and cognitive sensor presentation, respectively. Likewise, Table 15 and 16 lists LWIR effects with algorithmic and cognitive sensor presentation, respectively. The direction indicates whether the presence of additional sensors increased (positive) or decreased (negative) response times. The direction was only reported for those participants with BF > 3 in favor of an effect.

3.2.3.1 Visible Images. Participant 1 achieved low accuracy performance and was not used for analyses of sensor effect. For visible-only trials with algorithmic fusion presentation, there was decisive evidence of an effect for only one participant, Participant 9 ($M_{context}$ = 609.73ms, $M_{no\ context}$ = 520.79ms), while the block with just visible-only trials were faster than visible-only trials in a block randomized with other sensor types. There was a BF < .30 for 5 participants, which indicates evidence against a difference. The Bayes Factor for a visible effect with algorithmic fusion is listed for each participant in Table 13.

Table 13. Visible signal effect in presence and absence of LWIR and multi-sensor imagery for the algorithmically combined, single-image display.

Subject	Bayes Factor	Direction
1	N/A	N/A
2	BF = 0.29	N/A
3	BF = 0.26	N/A
4	BF = 0.44	N/A
5	BF = 0.15	N/A
6	BF = 0.19	N/A
7	BF = 0.20	N/A
8	BF = 0.56	N/A
9	BF = 9.09×10^9	Positive
10	BF = 0.49	N/A

For visible-only trials with cognitive fusion display, decisive evidence for an effect was found for participant 2, 8, and 10 (Table 14); all of which had faster mean response times when presented visible-only trials in isolation rather than randomly interleaved with multi-sensor and LWIR trials. There was evidence against an effect for 4 participants (3, 4, 6, and 9), BF < .30.

Table 14. Visible signal effect in presence and absence of LWIR and multi-sensor imagery for the cognitive fusion, single-image display.

Subject	Bayes Factor	Direction
1	N/A	N/A
2	BF = 9.69	Positive
3	BF = 0.15	N/A
4	BF = 0.15	N/A
5	BF = 0.40	N/A
6	BF = 0.20	N/A
7	BF = 0.31	N/A
8	BF = 6.13×10^{10}	Positive
9	BF =0.25	N/A
10	BF = 1.94×10^{6}	Positive

3.2.3.2 LWIR Images. For LWIR-only trials with algorithmic fusion presentation, there was decisive evidence of an effect for 3 participants. Participant 4 ($M_{context}$ = 451.08ms, $M_{no\ context}$ = 497.36ms) and Participant 6 ($M_{context}$ = 401.83ms, $M_{no\ context}$ = 477.01ms) had a negative effect of the presence of visible and multi-sensor images. Therefore LWIR-only trials in isolation were slower than those in context of visible and multi-sensor trials. Using a Bayesian t-test I found decisive evidence for positive effects for Participant 9 ($M_{context}$ = 642.07ms, $M_{no\ context}$ = 563.93ms). Therefore for this Participant LWIR-only trials in isolation were faster than in the presence of visible and multi-sensor trials. There was a BF < .30 for 3 participants, which indicated evidence against a difference in response times. The Bayes Factor for a LWIR effect with algorithmic fusion is listed for each participant in Table 15.

Table 15. LWIR signal effect in presence of absence of visible and multi-sensor imagery for the algorithmically combined, single-image display.

Subject	Bayes Factor	Direction
1	N/A	N/A
2	BF = 0.88	N/A
3	BF = 0.24	N/A
4	BF = 3.47×10^{-2}	Negative
5	BF = 0.55	N/A
6	BF = 217.75	Negative
7	BF = 0.50	N/A
8	BF = 0.14	N/A
9	BF = 1.30×10^{5}	Positive
10	BF = 0.17	N/A

I found evidence of an effect for 5 participants in LWIR-only trials with cognitive fusion presentation. Three participants exhibited a positive relationship (faster RT with LWIR-only isolation) and 2 had a negative relationship (slower RT with LWIR-only trial isolation). There was a BF < .3 for 3 participants (Participant 3, 6 and 7), which was evidence against any effect. Table 16 lists each subject along with a corresponding Bayes Factor for evidence of an effect of LWIR with cognitive fusion and the direction of the effect (where necessary).

Table 16. LWIR signal effect in presence of absence of visible and multi-sensor imagery for the algorithmically combined, single-image display.

Subject	Bayes Factor	Direction
1	N/A	N/A
2	BF = 3.22	Positive
3	BF = 0.15	N/A
4	BF = 3.16	Negative
5	BF = 0.34	N/A
6	BF = 0.15	N/A
7	BF = 0.21	N/A
8	BF = 1.69×10^{5}	Positive
9	BF = 7.70	Negative
10	BF = 2.39×10^{2}	Positive

3.2.4 Survivor Interaction Contrast. For algorithmically fused images, no participant's data satisfied the assumptions of selective influence thereby precluding the use of the SIC for model classification (Table 17). If selective influence held across the group, all assumptions listed in Table 17 would show significance at $p < .05$. Individual participant's ordering of survivor functions and corresponding SIC (uninterruptable) are shown in Figure 13 – 22.

Table 17. Distribution comparison K-S tests by participant for algorithmically fused images.

Subject	$D_{HH\text{-}HL}$	$D_{HL\text{-}LL}$	$D_{HH\text{-}LH}$	$D_{LH\text{-}LL}$
1	0.010	0.074	0.011	0.072
2	0.079	0.087	0.068	0.069
3	0.084	0.038	0.150*	0.038
4	0.112	0.051	0.135*	0.103
5	0.095	0.045	0.061	0.034
6	0.092	0.103	0.056	0.000
7	0.074	0.055	0.022	0.094
8	0.100	0.109	0.081	0.058
9	0.034	0.098	0.031	0.103
10	0.132~*	0.081	0.039	0.117~*

Note: ~* $p < .10$, * $p < .05$, ** $p < .01$, *** $p < .001$.

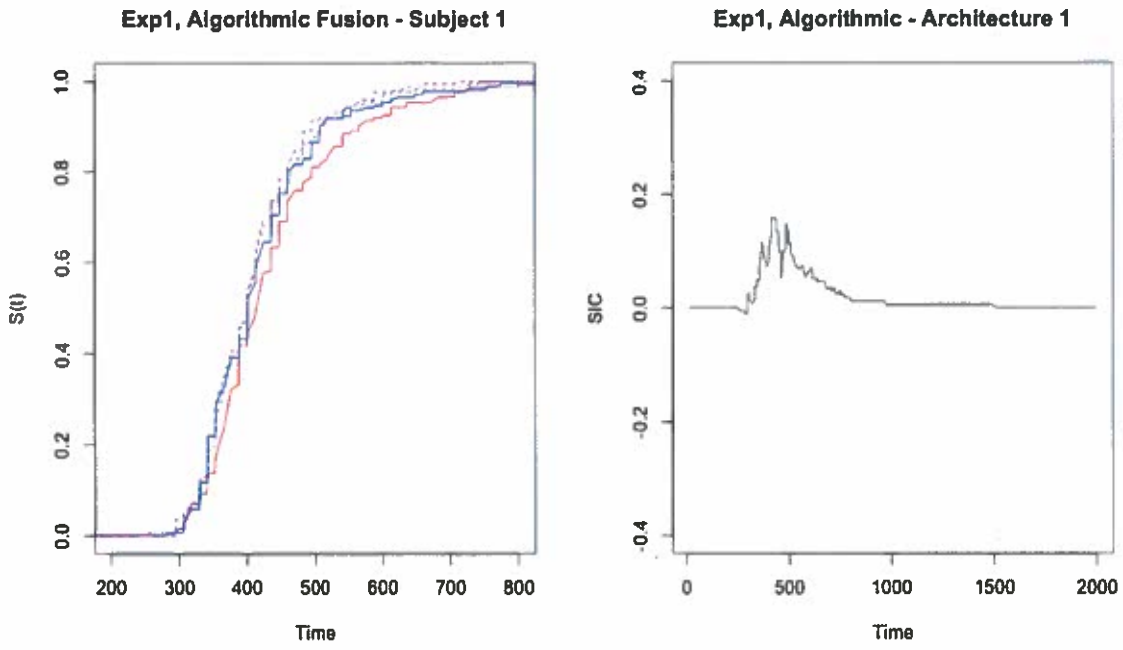

Figure 13. SIC analyses of selective influence and architecture for Participant 1 in the Experiment 1, algorithmic fusion block. The plot to the left shows the ordering of survivor functions. If the red line is fastest (furthest to the left) and the blue line is the slowest (furthest to the right), selective influence holds. If selective influence holds, the SIC function (plot to the right) is tested for positive and negative deviations from zero. If selective influence does not hold, SIC results are uninterruptable.

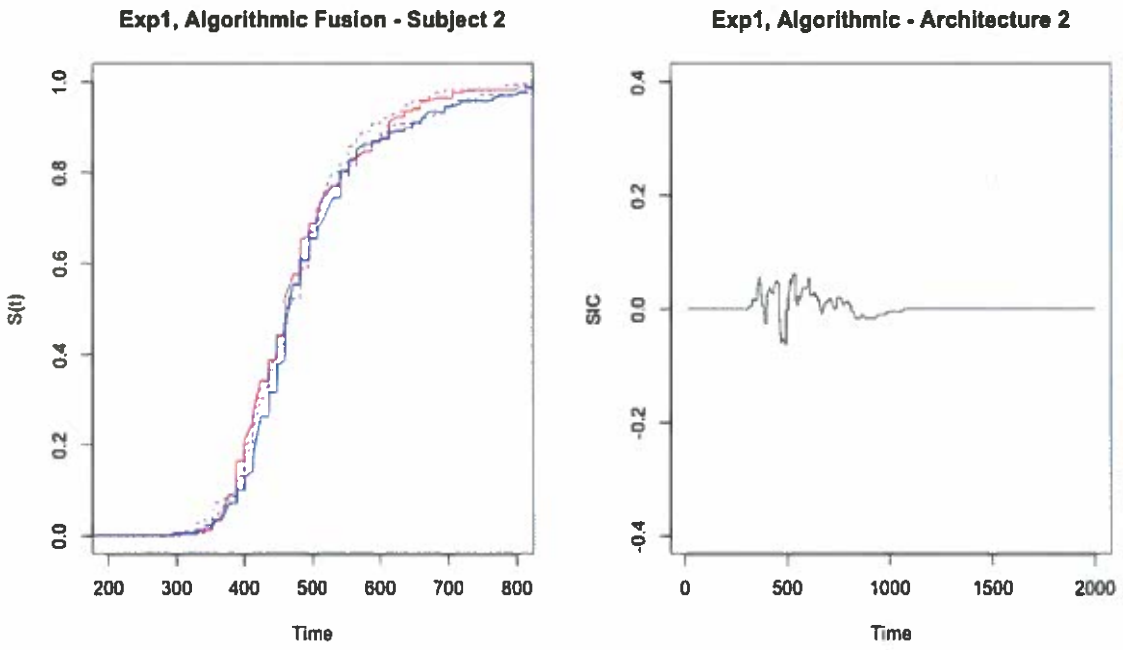

Figure 14. SIC analyses of selective influence and architecture for Participant 2 in the Experiment 1, algorithmic fusion block.

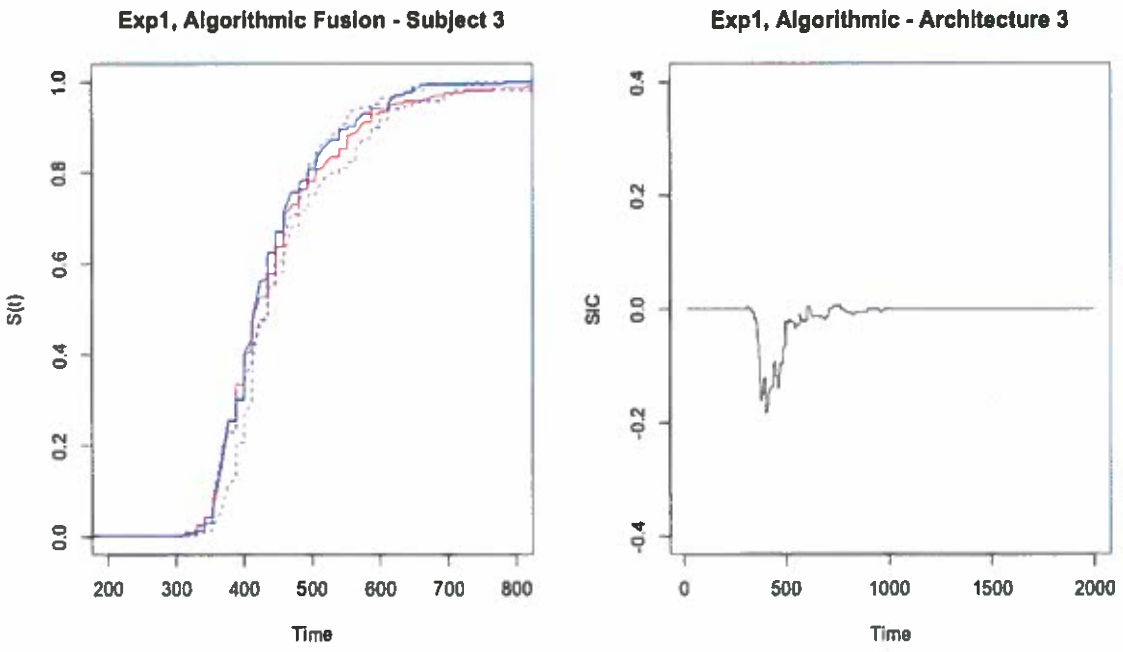

Figure 15. SIC analyses of selective influence and architecture for Participant 3 in the Experiment 1, algorithmic fusion block.

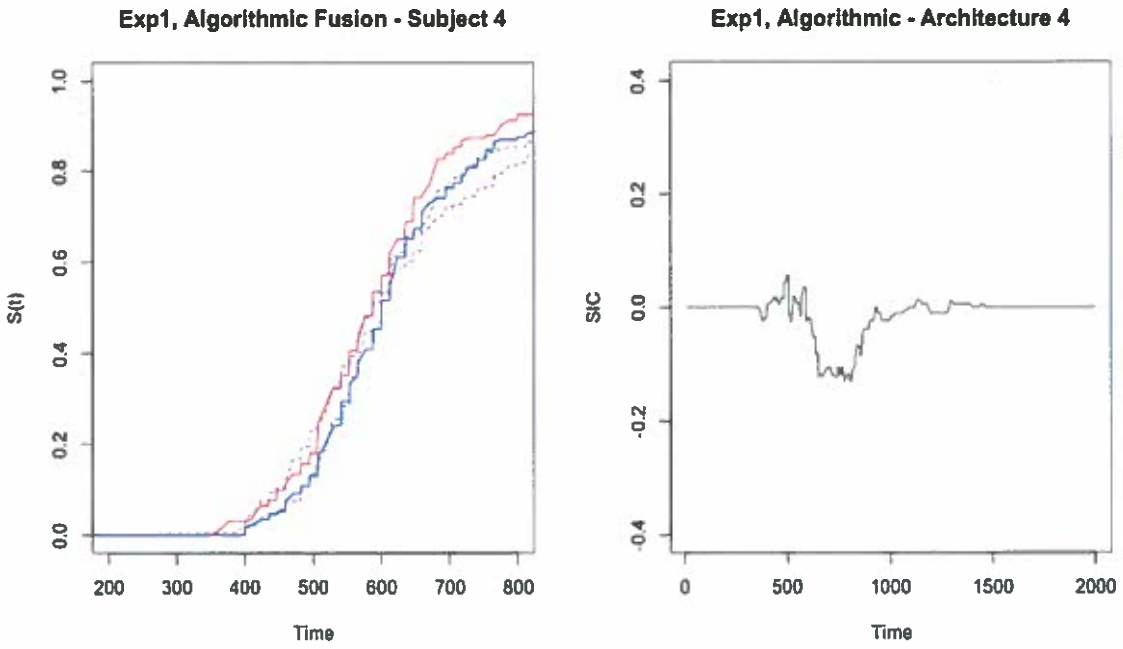

Figure 16. SIC analyses of selective influence and architecture for Participant 4 in the Experiment 1, algorithmic fusion block.

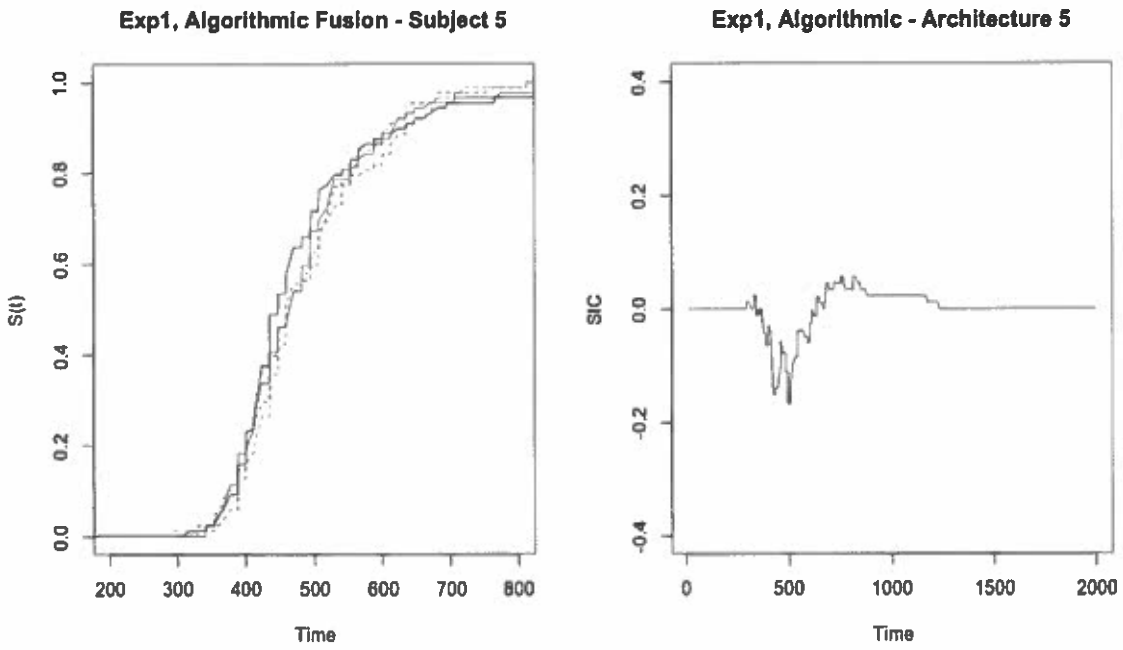

Figure 17. SIC analyses of selective influence and architecture for Participant 5 in the Experiment 1, algorithmic fusion block.

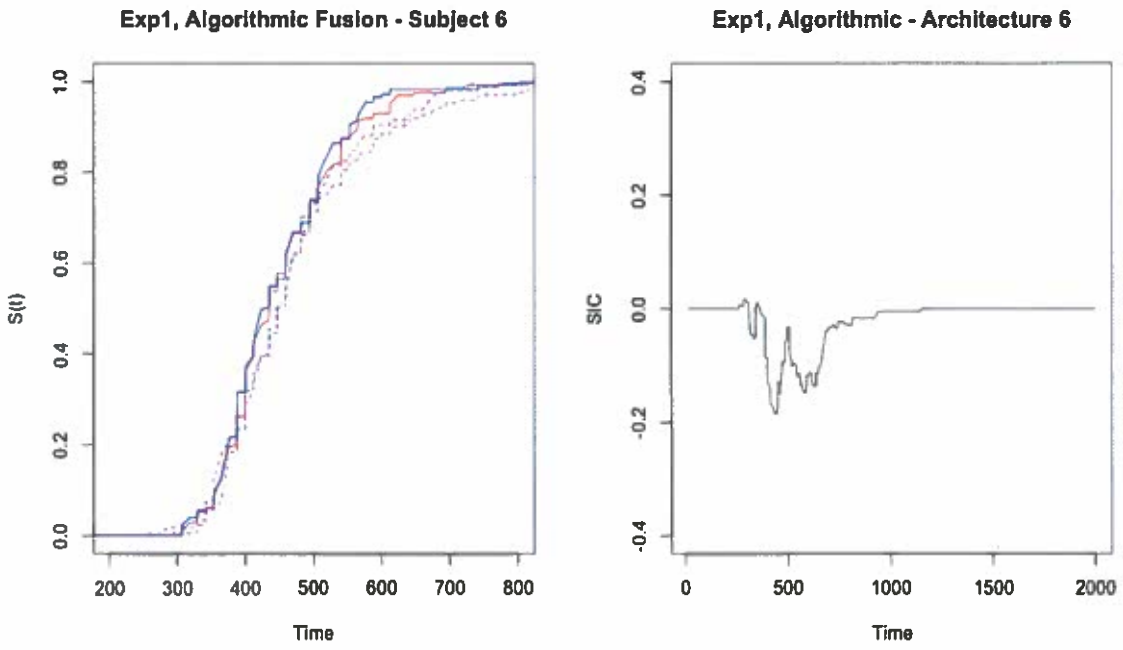

Figure 18. SIC analyses of selective influence and architecture for Participant 6 in the Experiment 1, algorithmic fusion block.

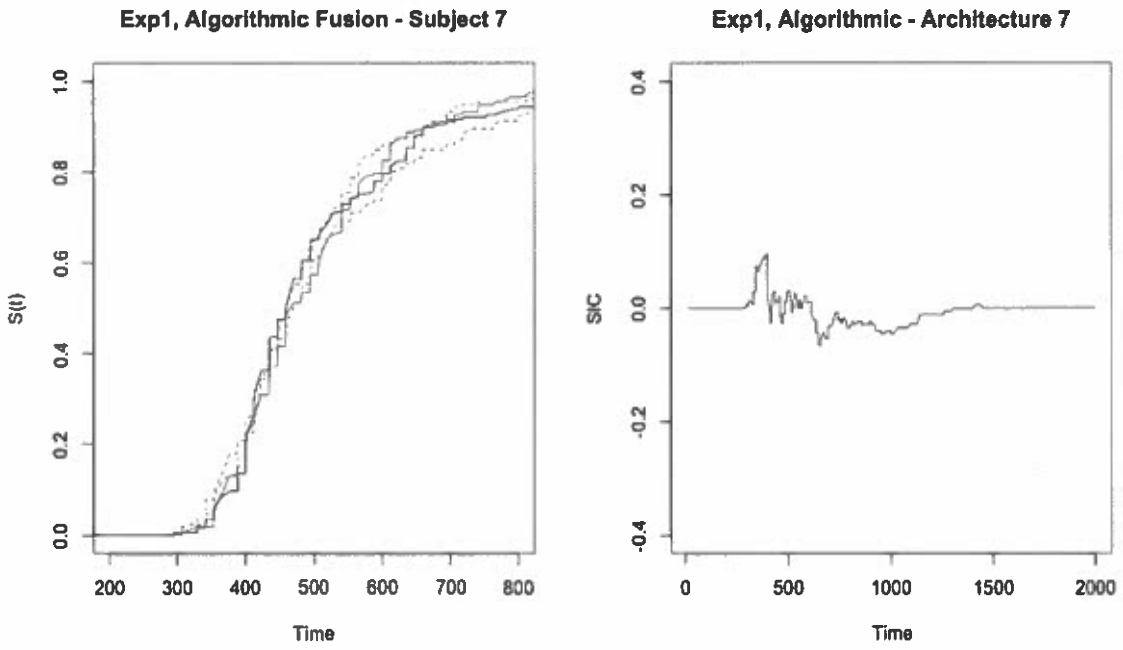

Figure 19. SIC analyses of selective influence and architecture for Participant 7 in the Experiment 1, algorithmic fusion block.

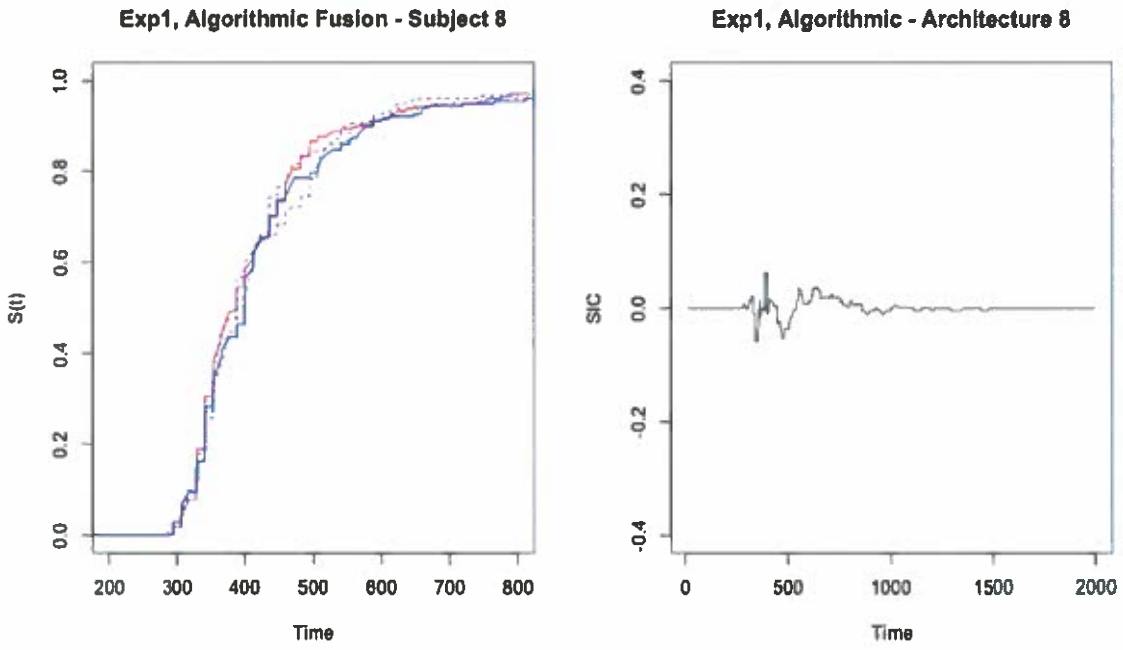

Figure 20. SIC analyses of selective influence and architecture for Participant 8 in the Experiment 1, algorithmic fusion block.

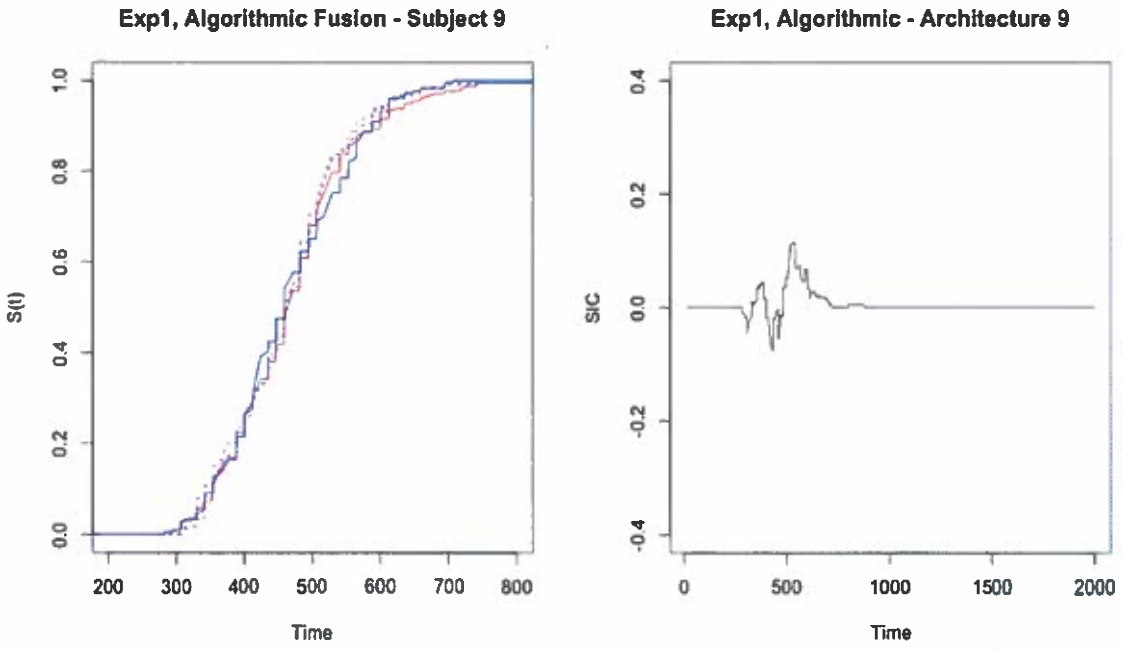

Figure 21. SIC analyses of selective influence and architecture for Participant 9 in the Experiment 1, algorithmic fusion block.

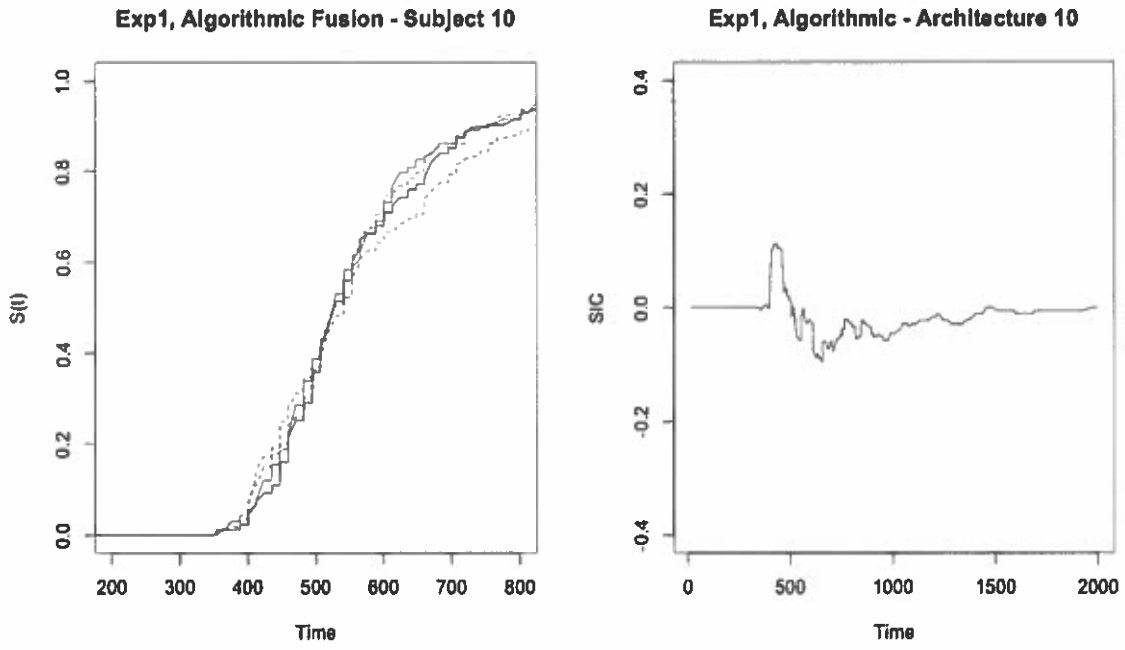

Figure 22. SIC analyses of selective influence and architecture for Participant 10 in the Experiment 1, algorithmic fusion block.

For cognitive fusion SIC analyses, selective influence was satisfied for 7 participants. The Houpt-Townsend SIC statistic (Houpt & Townsend, 2010) indicated 3 participants had a significant positive SIC (parallel-OR), 2 participants showed an all negative SIC (parallel–AND), and 2 participants showed no positive and negative deviations from zero (Serial–OR). For all tests alpha = .33, as explained previously in the Methods section. The remaining 3 participants failed tests of selective influence leading to ambiguous SIC interpretations. Table 18 lists each participant's Houpt-Townsend SIC statistic for both positive and negative deviations from zero and corresponding K-S statistics with level of significance. Individual figures of ordering of survivor functions and corresponding SIC are listed below in Figure 23 – 32.

Table 18. Cognitive fusion results including: Houpt-Townsend statistic (D+, D-) and tests of selective influence for each participant in Experiment 1. Bold D+ and D- statistics indicate a significant Houpt-Townsend statistic at $p < 0.33$.

Subject	D+	D-	$D_{HH\text{-}HL}$	$D_{HL\text{-}LL}$	$D_{HH\text{-}LH}$	$D_{LH\text{-}LL}$
1	N/A	N/A	0.043	0.176**	0.112	0.057
2	N/A	N/A	0.220***	0.064	0.143*	0.146*
3	N/A	N/A	0.100	0.095	0.163**	0.068
4	0.018	**0.131**	0.231***	0.115~*	0.190**	0.157**
5	**0.136**	0.035	0.256***	0.225**	0.159***	0.349***
6	**0.179**	0.055	0.196**	0.203**	0.119~*	0.309***
7	0.062	**0.139**	0.201***	0.077	0.118~*	0.122~*
8	**0.159**	0.073	0.268***	0.275***	0.238***	0.252***
9	0.096	0.086	0.295***	0.293***	0.293***	0.284***
10	0.101	0.011	0.207***	0.233***	0.171**	0.269***

Note: **H-T statistic** = $p < 0.33$, ~* = $p < .10$, * = $p < .05$, ** = $p < .01$, *** = $p < .001$.

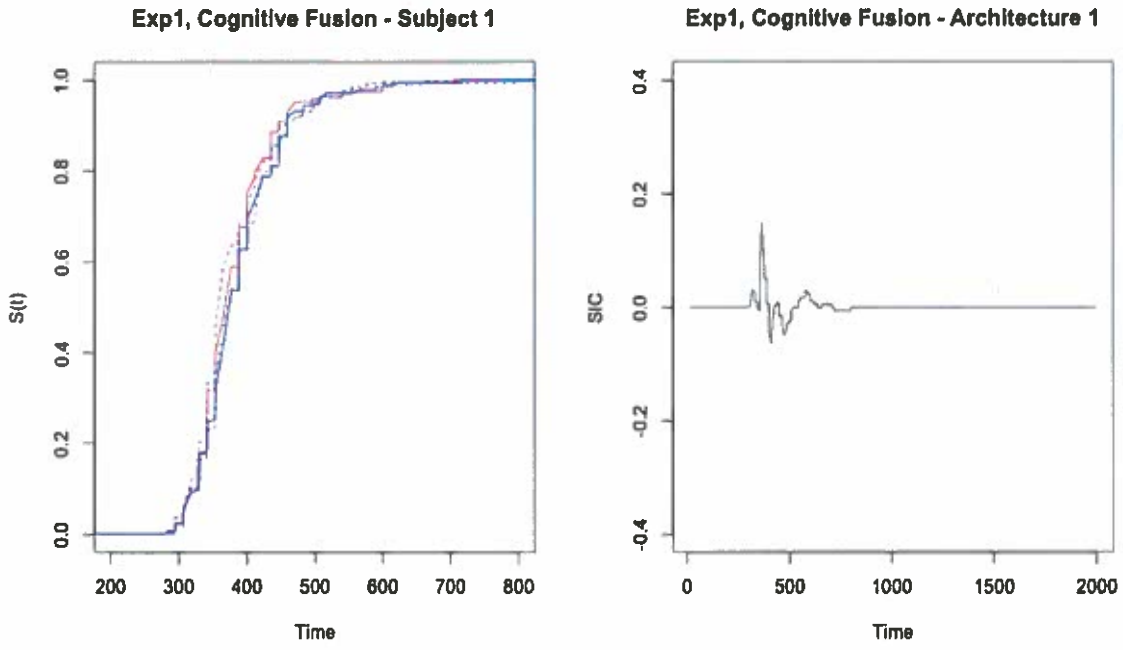

Figure 23. SIC analyses of selective influence and architecture for Participant 1 in the Experiment 1, cognitive fusion block. The plot to the left shows the ordering of survivor functions. If the red line is fastest (furthest to the left) and the blue line is the slowest (furthest to the right) then selective influence holds. If selective influence holds, the SIC function (plot to the right) is tested for positive and negative deviations from zero. If selective influence does not hold, SIC results are uninterruptable.

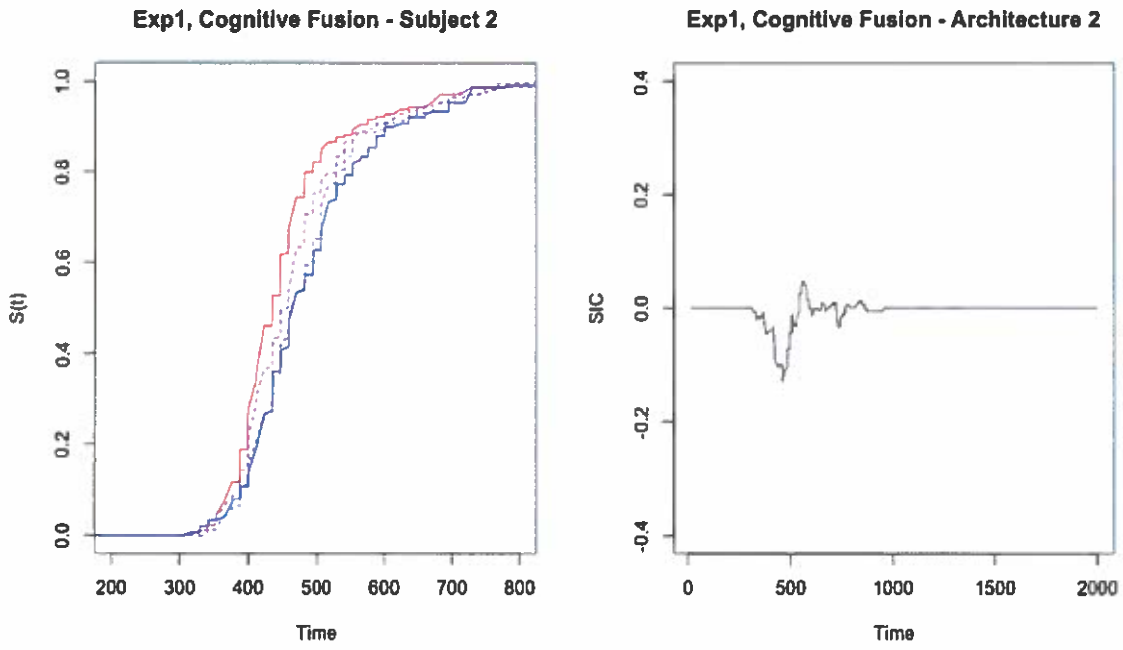

Figure 24. SIC analyses of selective influence and architecture for Participant 2 in the Experiment 1, cognitive fusion block.

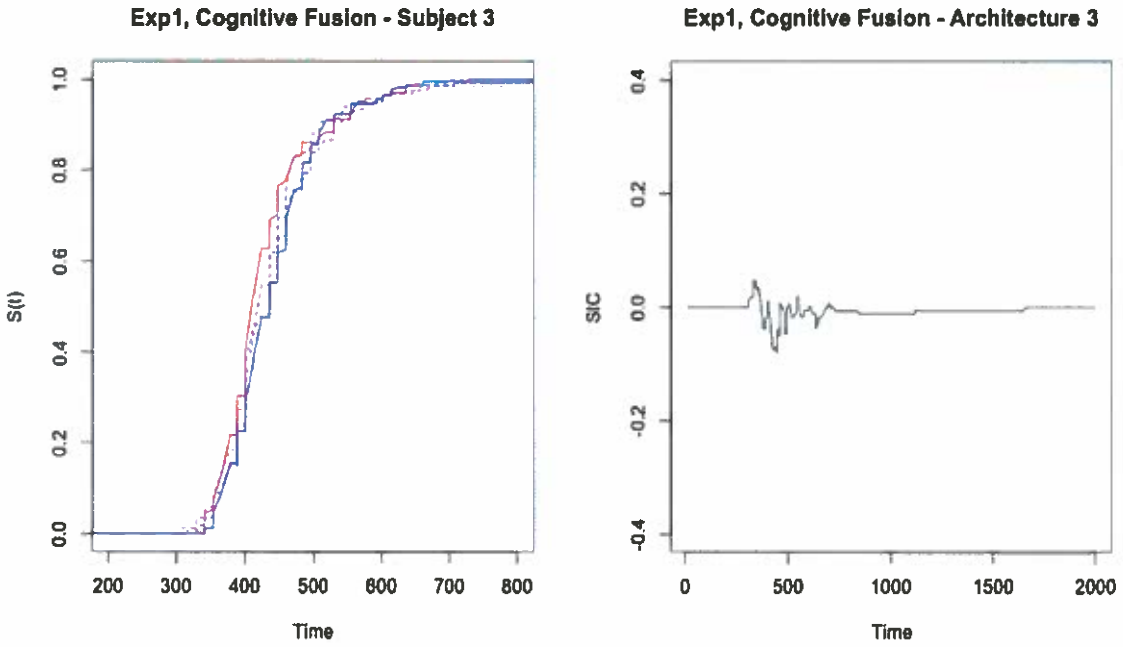

Figure 25. SIC analyses of selective influence and architecture for Participant 3 in the Experiment 1, cognitive fusion block.

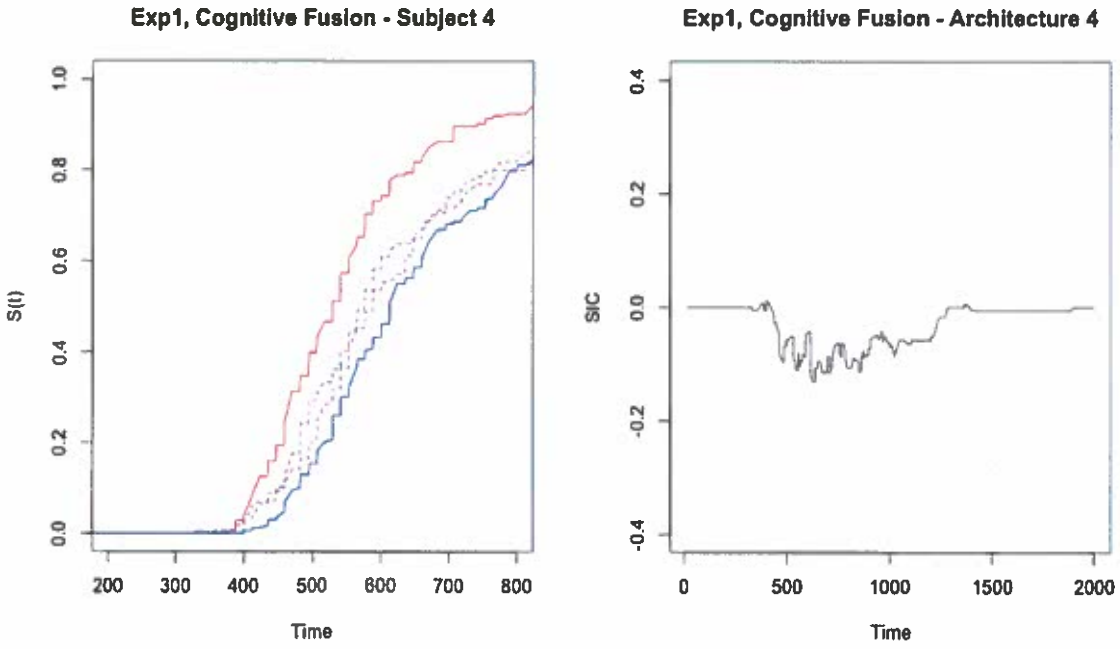

Figure 26. SIC analyses of selective influence and architecture for Participant 4 in the Experiment 1, cognitive fusion block.

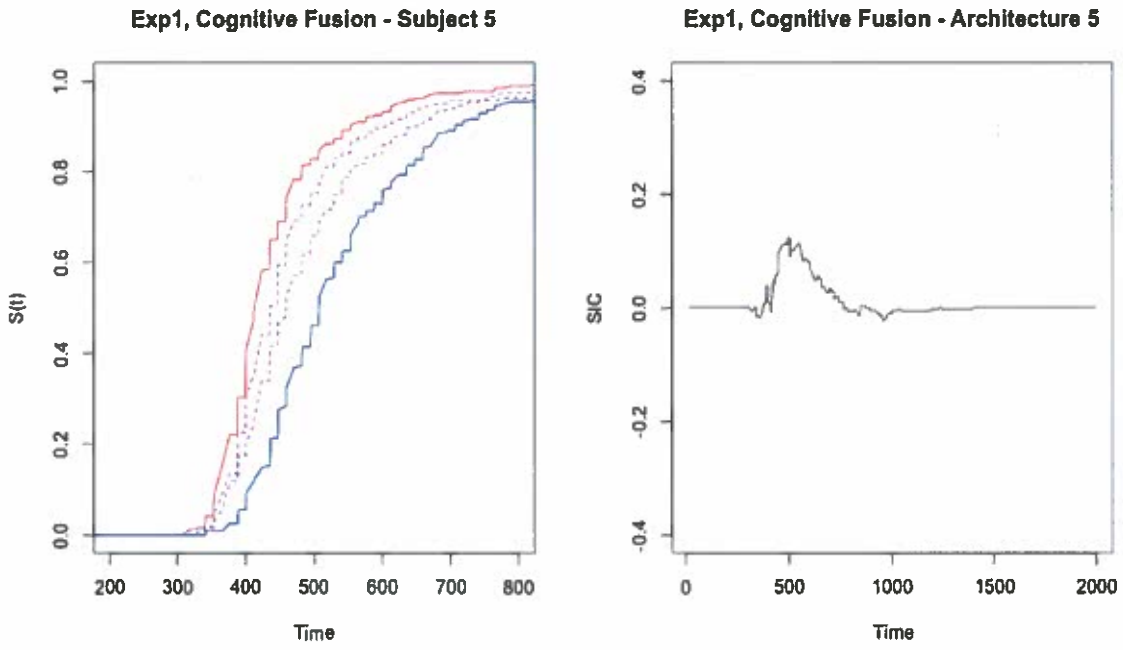

Figure 27. SIC analyses of selective influence and architecture for Participant 5 in the Experiment 1, cognitive fusion block.

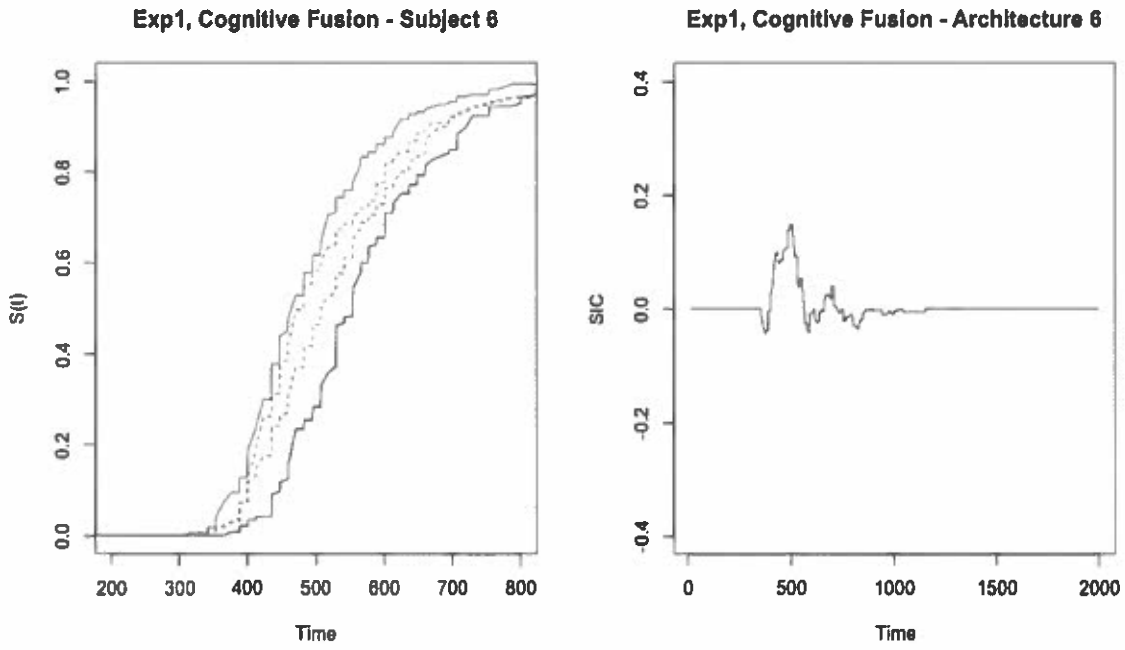

Figure 28. SIC analyses of selective influence and architecture for Participant 6 in the Experiment 1, cognitive fusion block.

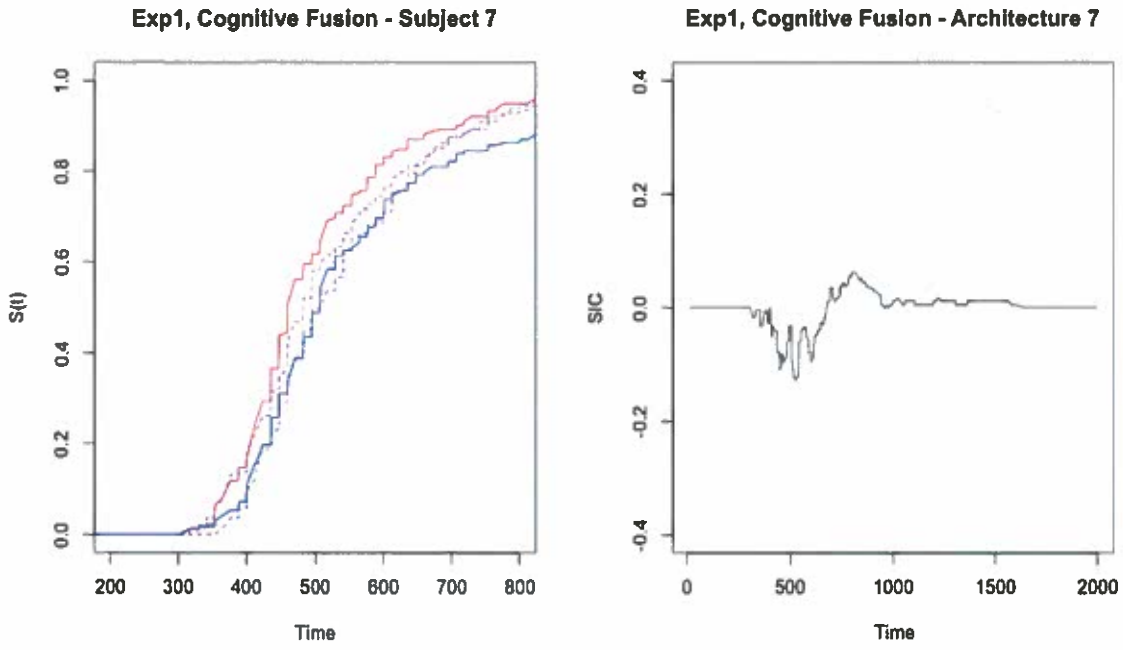

Figure 29. SIC analyses of selective influence and architecture for Participant 7 in the Experiment 1, cognitive fusion block.

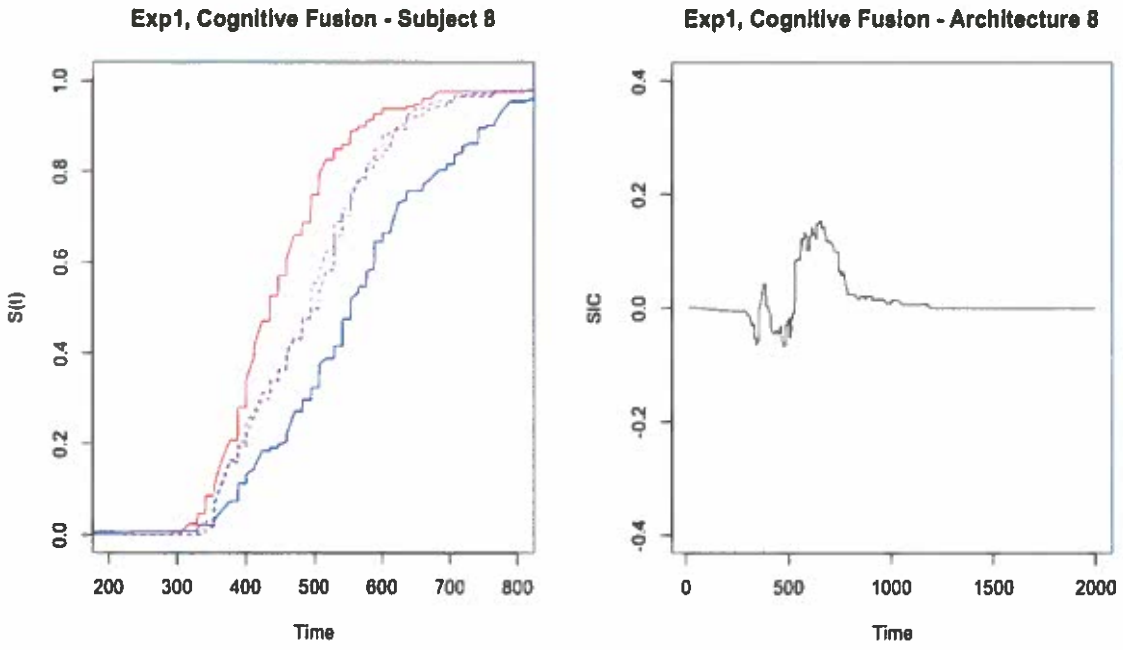

Figure 30. SIC analyses of selective influence and architecture for Participant 8 in the Experiment 1, cognitive fusion block.

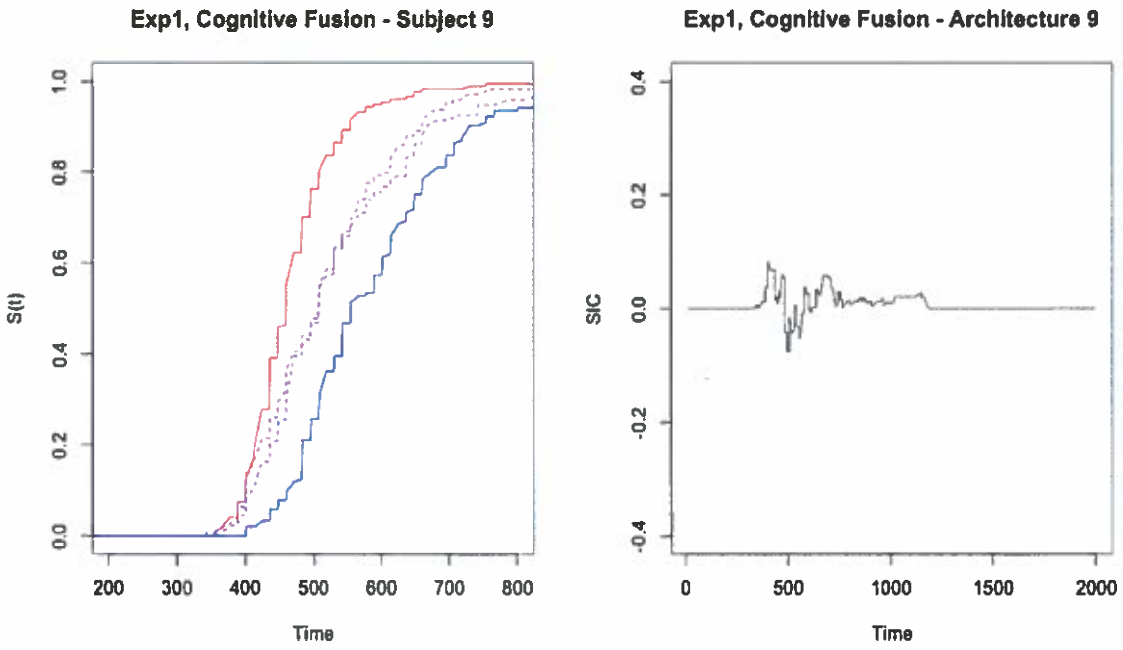

Figure 31. SIC analyses of selective influence and architecture for Participant 9 in the Experiment 1, cognitive fusion block.

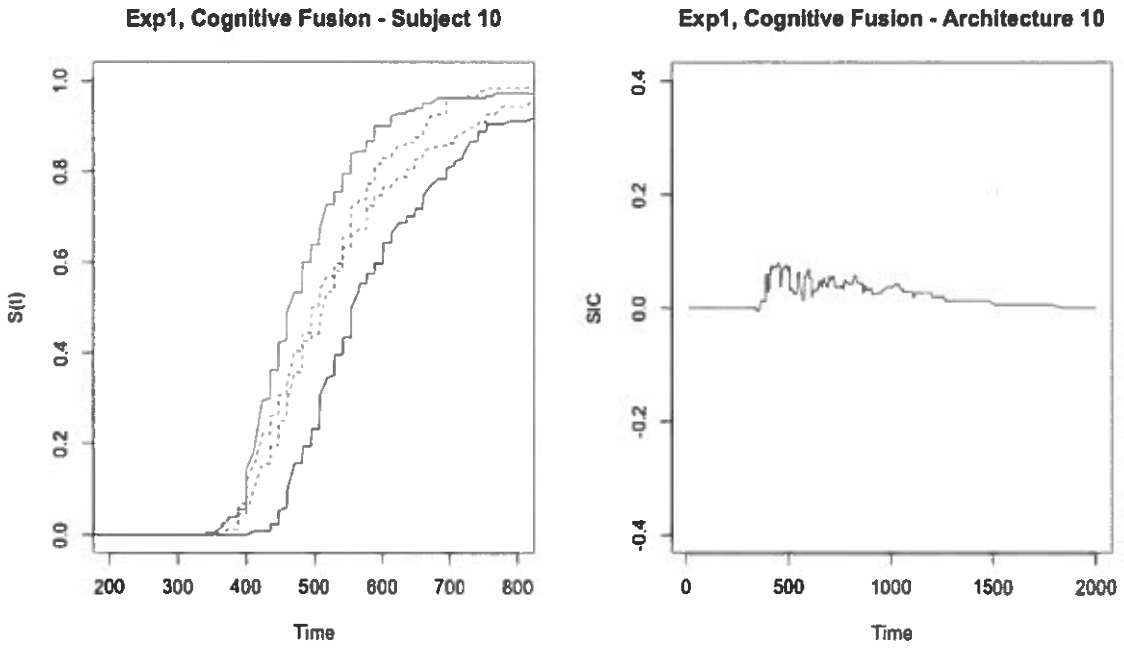

Figure 32. SIC analyses of selective influence and architecture for Participant 10 in the Experiment 1, cognitive fusion block.

Subsequent MIC analyses using a hierarchical Bayesian model indicate posterior probability distributions with MIC = 0 most likely (57.7%) while MIC < 0 (24.2%) and MIC > 0 (18.2%) are less likely models at the group level. However, the posterior distribution did not change much from the prior, MIC = 0 at 50%, MIC > 0 at 25%, and MIC < 0 at 25%. Therefore, more participants are needed to make stronger conclusions about the likelihood of the underlying structure of information processing at the group level. Using 4000 burn-in samples there was sufficient convergence of MCMC sampling chains was achieved with Gelman-Rubin statistic ranging from $\hat{r} = 1.01 - 1.12$. Further individual MIC analyses did not favor any one particular model for any participant; more individual trials are needed to make conclusions.

Table 19. Summary table of capacity and SIC analyses across algorithmic and cognitive fusion in Experiment 1 for each participant.

Experiment 1				
	Algorithmic		*Cognitive*	
Participant	**Capacity**	**SIC**	**Capacity**	**SIC**
1	Limited	N/A	Limited	N/A
2	Limited	N/A	Unlimited	N/A
3	Limited	N/A	Unlimited	N/A
4	Limited	N/A	Limited	Parallel-AND
5	Limited	N/A	Unlimited	Parallel-OR
6	Limited	N/A	Limited	Parallel-OR
7	Limited	N/A	Limited	Parallel-AND
8	Limited	N/A	Limited	Parallel-OR
9	Limited	N/A	Limited	Serial-OR
10	Limited	N/A	Unlimited	Serial-OR

3.3 Discussion

All participants' performance with algorithmically fused multi-sensor information resulted in limited workload capacity. Individual sensor performance for both LWIR and visible imagery was just as good if not better than multi-sensor performance. When this is the case, the capacity coefficient will always indicate limited workload capacity. The algorithmic fusion did not aid in performance above that of individual sensors for the left/right pointing discrimination task. However, with cognitive fusion of multi-sensor information almost half of the participants' performance (4 participants) exhibited unlimited workload capacity. Cognitive fusion presents all of the available information to the participant and allows him or her to decide what information is important from each. An unlimited workload capacity indicated that participants were efficiently using the available information from both sensor images when presented with both simultaneously to achieve performance equal to that predicted by a UCIP model.

Additional analyses of architecture indicated that multi-sensor cognitive fusion images were processed with several different strategies across participants. Some participant's imply parallel processing (Participant 4, 5, 6, 7, 8); however of this subset with cognitive fusion, all

performance except Participant 5 exhibited limited workload capacity (Table 19). Therefore, such participants may exhibit changes in capacity for each individual sensor with multi-sensor information and/or violations of independence between the sensor channels. With the cognitive fusion presentation technique, some participants' performance indicated better utilization of information than when presented with algorithmically fused images for the same image set and task, regardless of spatio-temporal strategy of information processing.

4. EXPERIMENT 2

Experiment 2 was conducted to further investigate the cognitive process of multisensor information across both algorithmic and cognitive fusion. However, the imagery and task will slightly vary from those used in Experiment 1. The results of Experiment 2 will indicate the generalizability of cognitive processes across a two systematic manipulations: the introduction of spatial uncertainty the target location and the discrimination task instructions.

4.1 Methods

Experiment 2 was always the last 5 days of participation. All 5 sessions involved a discrimination task with spatial uncertainty of the target.

4.1.1 Procedures. Participants were asked to find the target (a person); then, discriminate whether a person was facing left or right (Figure 33A-33F). The direction the man was facing was randomly chosen on each trial. Then contingent on the direction, 1 of 10 left/right facing images was randomly selected for presentation. Five of the available images to choose from were of one target man (Figure 33A-33C) and 5 were an alternative target man (Figure 33D-33F). If the participant determined left, they pressed the left mouse button, if right, they pressed the right mouse button. The participants were told to perform the task as quickly and accurately as possible and were informed they must achieve at least 90% accuracy to order for me to conduct any further analyses. For low salience imagery intended to slow down processing random Gaussian was systematically manipulated using the QUEST method previously explained; examples are shown in Figure 34A-34D.

Experiment 1 and 2 had equivalent stimulus presentation time: 250ms. Although the participant now must account for spatial uncertainty of the target, pilot studies have shown 250ms is enough to invoke fast response times while obtaining a high accuracy (~90%).

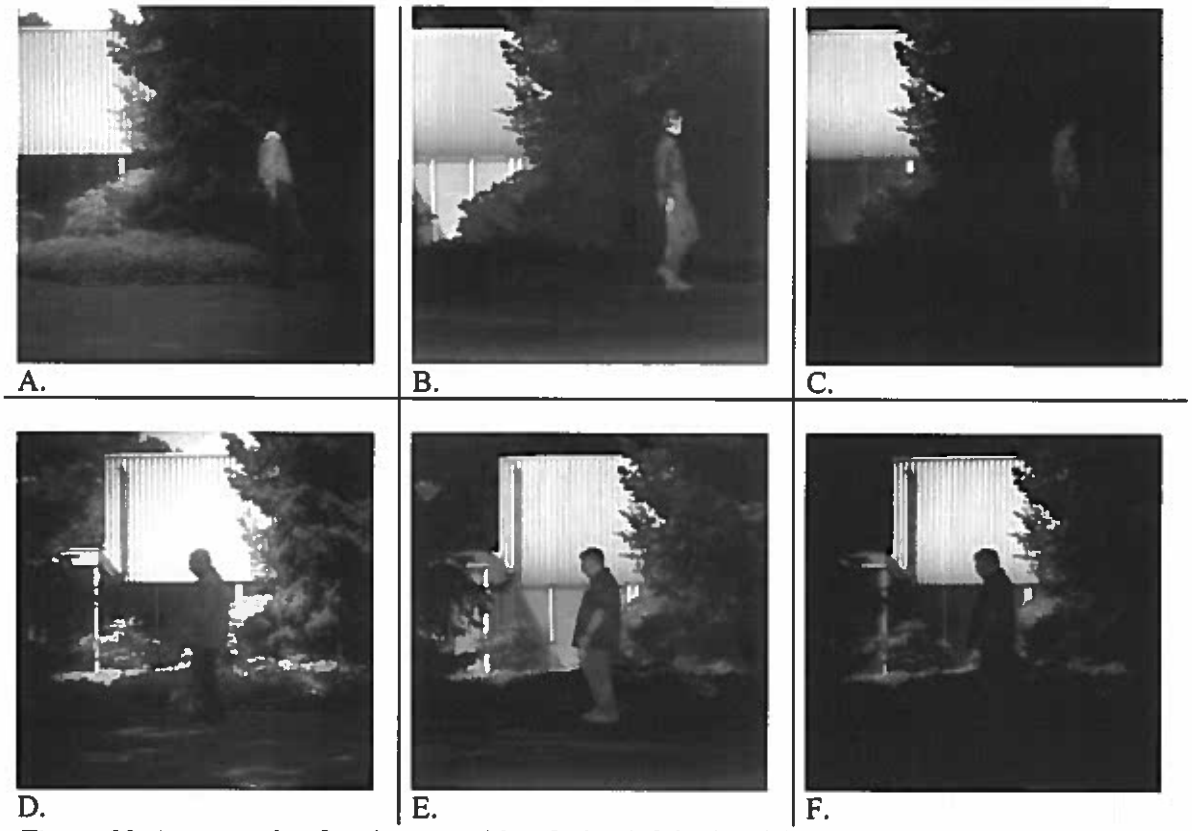

Figure 33. An example of each target either facing left in the visible-only (A), LWIR-only (B), and Laplacian algorithmically fused (C) image or facing right in the visible-only (D), LWIR-only (E), and Laplacian algorithmically fused (F) used in Experiment 2.

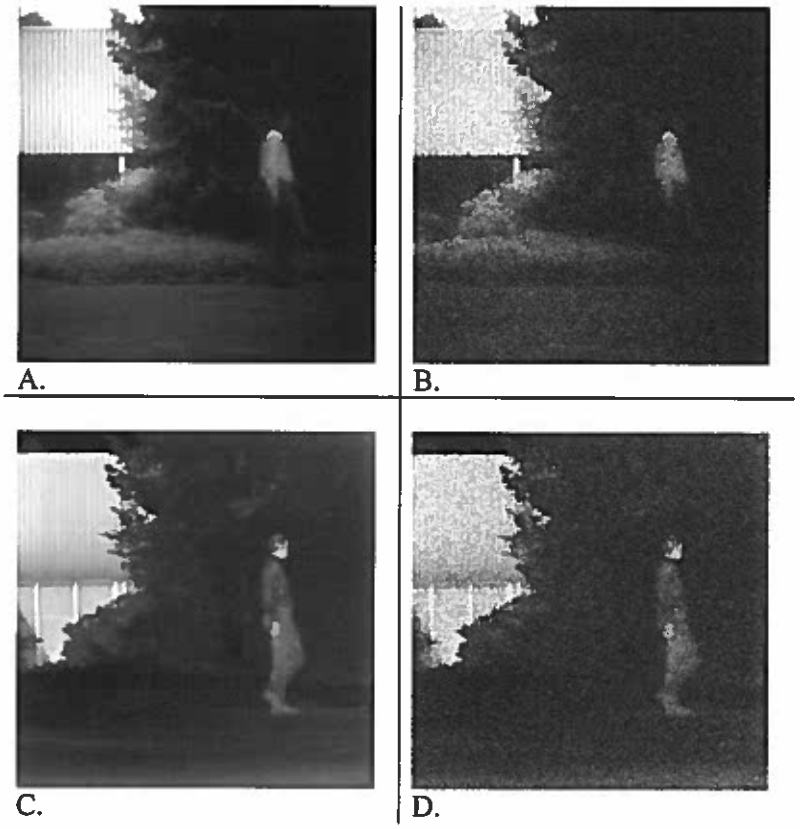

Figure 34. An example of visible-only image (A) with random Gaussian noise (B) and a LWIR-only image (C) with random Gaussian noise (D). The noise added to the stimuli was individualized each day of participation and to each sensor image to target 90% accuracy.

4.2 Results

A summary of capacity coefficient and SIC results across both algorithmic and cognitive fusion for the discrimination task in Experiment 2 for each participant is listed in Table 34. The following sections address the results of several measures that test my hypotheses.

4.2.1 General Analyses. Summary statistics of response time and accuracy are outlined for each participant for visible-only (Table 20), LWIR-only (Table 21) and multi-sensor (Table 22) in the algorithmic fusion block and for each participant in the cognitive fusion block (Table 23-25). Group response time statistics are provided in Table 26 and Figure 35. Using a Bayesian

linear model there is decisive evidence for a main effect of fusion type (algorithmic, cognitive), sensor (visible-only, LWIR-only, multisensor) and subject with an interaction between fusion type and sensor over a model with just the main effects of fusion type, sensor and subject, BF = 286,428.6. I used a Bayesian linear model to test whether the change of task from Experiment 1 to Experiment 2 sufficiently manipulated human performance. There was decisive evidence for a model including main effects of all independent measures (task, fusion type, sensor, and subject) above a model without the main effect of task, $BF = 4.92 \times 10^{275}$.

A one-way ANOVA was conducted for each sensor and fusion type to test response time variability within each set of 10 images. Analysis of variance showed that the effect of individual image was significant across visible-only, $F(19,1180) = 14.04$, $p < .05$, LWIR-only $F(19,1180) = 1.61$, $p < .05$, and the images used for fusion, $F(19,1180) = 4.88$, $p < .05$ with algorithmic fusion presentation. Likewise, there were significant effects of image across visible-only, $F(19,1180) = 16.42$, $p < .05$, and LWIR-only, $F(19,1180) = 3.77$, $p < .05$ in the cognitive fusion conditions.

Table 20. Individual mean and standard deviation of response time and accuracy for the visible-only trials within the cognitive fusion-capacity block in Experiment 2.

	Response Time		Accuracy	
Participant	*M*	*SD*	*M*	*SD*
1	638.49	423.46	80.00	40.17
2	575.40	137.41	91.67	27.75
3	535.67	124.31	81.67	38.86
4	820.53	380.29	85.83	35.02
5	573.81	138.39	83.33	37.42
6	580.01	156.67	86.67	34.14
7	639.93	205.14	85.83	35.02
8	654.24	214.53	85.83	35.02
9	565.01	112.98	90.00	30.13
10	670.05	218.30	88.33	32.24

Table 21. Individual mean and standard deviation of response time and accuracy for the LWIR-only trials within the cognitive fusion-capacity block in Experiment 2.

	Response Time		Accuracy	
Participant	*M*	*SD*	*M*	*SD*
1	479.78	135.85	94.17	23.54
2	535.56	93.43	99.17	9.13
3	533.00	108.25	89.17	31.21
4	674.45	176.81	100.00	0.00
5	512.31	98.90	98.33	12.86
6	523.23	100.64	97.50	15.68
7	556.48	128.22	95.83	20.07
8	555.56	169.66	98.33	12.86
9	513.24	102.09	99.17	9.13
10	586.86	169.24	100.00	0.00

Table 22. Individual mean and standard deviation of response time and accuracy for the multi-sensor trials within the cognitive fusion-capacity block in Experiment 2.

	Response Time		Accuracy	
Participant	*M*	*SD*	*M*	*SD*
1	492.90	169.49	93.33	25.05
2	533.20	167.01	96.67	18.03
3	497.81	91.19	89.17	31.21
4	700.73	246.39	98.33	12.86
5	532.82	119.61	99.17	9.13
6	518.30	95.52	95.83	20.07
7	570.30	158.15	95.83	20.07
8	555.67	125.67	96.67	18.03
9	522.03	90.65	95.83	20.07
10	562.53	134.67	96.67	18.03

Table 23. Individual mean and standard deviation of response time and accuracy for the visible-only trials within the algorithmic fusion-capacity block in Experiment 2.

	Response Time		Accuracy	
Participant	*M*	*SD*	*M*	*SD*
1	473.36	199.81	80.83	39.53
2	544.82	116.94	98.33	12.86
3	456.65	81.21	87.50	33.21
4	627.09	273.22	88.33	32.24
5	541.67	150.62	88.33	32.24
6	492.08	112.57	90.83	28.98
7	583.47	162.41	90.00	30.13
8	664.96	252.05	80.83	39.53
9	505.61	105.45	89.17	31.21
10	666.95	231.22	88.33	32.24

Table 24. Individual mean and standard deviation of response time and accuracy for the LWIR-only trials within the algorithmic fusion-capacity block in Experiment 2.

	Response Time		Accuracy	
Participant	*M*	*SD*	*M*	*SD*
1	453.99	169.10	95.00	21.89
2	515.77	91.45	100.00	0.00
3	456.73	69.17	92.50	26.45
4	551.89	152.10	99.17	9.13
5	492.14	133.16	99.17	9.13
6	461.89	136.98	98.33	12.86
7	552.18	169.69	97.50	15.68
8	610.82	268.99	87.50	33.21
9	461.17	61.64	100.00	0.00
10	617.09	298.88	97.50	15.68

Table 25. Individual mean and standard deviation of response time and accuracy for the multisensor trials within the algorithmic fusion-capacity block in Experiment 2.

	Response Time		Accuracy	
Participant	*M*	*SD*	*M*	*SD*
1	498.50	261.49	69.17	46.37
2	577.18	123.74	85.83	35.02
3	485.38	100.14	75.00	43.49
4	653.18	251.21	85.83	35.02
5	589.04	159.34	85.00	35.86
6	551.79	121.83	72.50	44.84
7	664.69	218.93	87.50	33.21
8	732.73	129.67	73.33	44.41
9	573.87	322.61	84.17	36.66
10	760.58	322.61	76.67	42.47

Table 26. Mean and standard deviation of response time at the group level across each trial type (visible-only, LWIR-only, multisensor) of both the algorithmic and cognitive fusion capacity blocks in Experiment 2.

	Condition	*M*	*SD*
Algorithmic	Visible	538.05	25.02
	LWIR	511.21	24.87
	Multisensor	541.21	24.82
Cognitive	Visible	597.38	25.00
	LWIR	550.21	24.91
	Multisensor	558.52	24.72

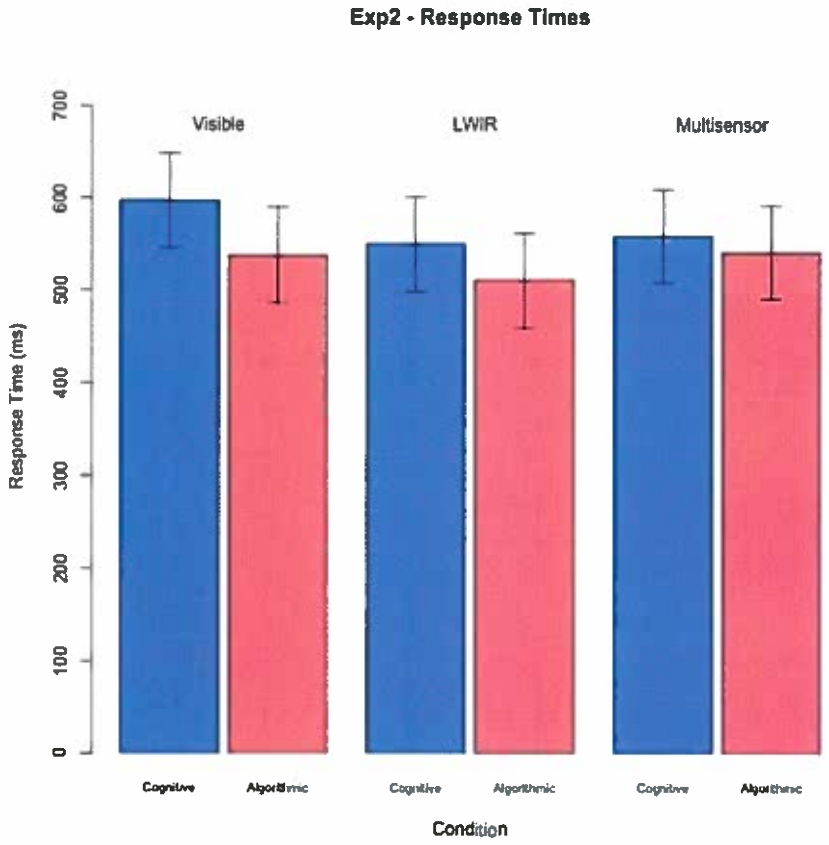

Figure 35. Group level Bayesian estimated mean and 95% highest density interval for both algorithmic and cognitive fusion with visible-only, LWIR-only, and multi-sensor trials. The salmon colored bars represent the algorithmic fusion trials (center of screen) and the purple-blue bars represent the cognitive fusion trials (randomly placed to the left/right of center screen).

4.2.2 Capacity Coefficient. Similar to Experiment 1, Participant 1 did not obtain at least 80% accuracy in all conditions for further analysis of workload capacity with multi-sensor information. The cumulative hazard function was less than one, $C(t) < 1$, for some time for both cognitive and algorithmic fusion. Capacity z-scores in Experiment 2 ranged from -10.7 to -8.5 for algorithmic fusion (Table 27) and from -4.9 to -2.2 for cognitive fusion (Table 28). I

hypothesized that individual's efficiency of both algorithmic and cognitive fusion was at least as high as respective UCIP predictions for the more difficult task in Experiment 2. The performance hypotheses were not supported; I found decisive evidence for limited workload capacity across both fusion techniques (algorithmic BF = 7.2×10^7, cognitive BF = 7.3×10^4) with algorithmic fusion decisively more limited than cognitive fusion, BF = 2.4×10^4 (Figure 36).

Table 27. Individual level capacity, z-score, and p-value for algorithmic multi-sensor images compared to each sensor alone (UCIP model).

Subject	Capacity	z-score	p-value
1	N/A	N/A	N/A
2	Limited	-9.586	$p < .05$
3	Limited	-9.137	$p < .05$
4	Limited	-8.597	$p < .05$
5	Limited	-9.702	$p < .05$
6	Limited	-10.748	$p < .05$
7	Limited	-9.517	$p < .05$
8	Limited	-8.980	$p < .05$
9	Limited	-10.036	$p < .05$
10	Limited	-9.750	$p < .05$

Table 28. Individual level capacity, z-score, and p-value for cognitive fusion of multi-sensor images compared to each sensor alone (UCIP model).

Subject	Capacity	z-score	p-value
1	Limited	-3.992	$p < .05$
2	Limited	-3.985	$p < .05$
3	Limited	-2.268	$p < .05$
4	Limited	-4.757	$p < .05$
5	Limited	-4.879	$p < .05$
6	Limited	-3.459	$p < .05$
7	Limited	-4.515	$p < .05$
8	Limited	-4.189	$p < .05$
9	Limited	-4.296	$p < .05$
10	Limited	-2.676	$p < .05$

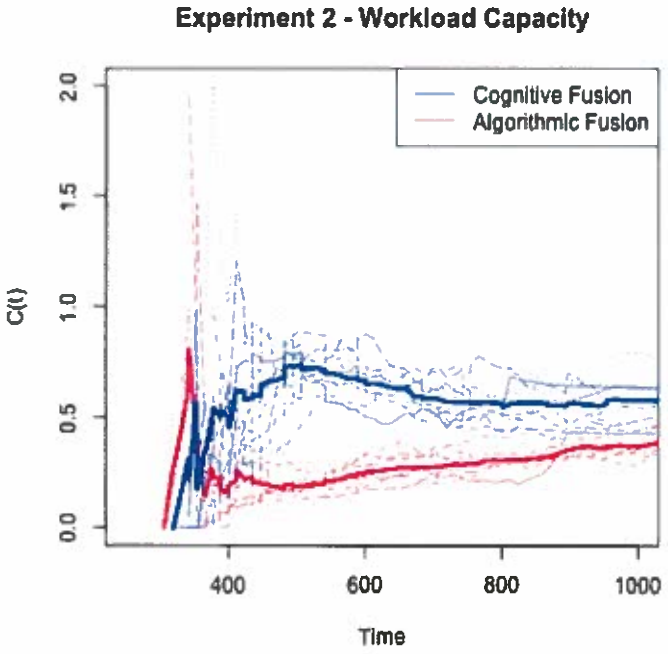

Figure 36. The capacity coefficient for both algorithmic and cognitive fusion in Experiment 1. The reference line is C(t) = 1 (unlimited capacity). The bold red line shows the group level for algorithmic fusion with red dashed lines showing each individual. The bold blue line shows the group level for cognitive fusion with the blue dashed lines showing each individual.

4.2.3 Blocking Effects. Identical to Experiment 1, most participants' performance exhibited no difference across sensor response time distributions when pulling each individual sensor trials intro a separate block of trials using a Bayesian t-test. However, some participants did show evidence for such effects. Table 29 and 30 list visible-only block effects with algorithmic and cognitive sensor presentation, respectively. Likewise, Table 31 and 32 list LWIR-only block effects with algorithmic and cognitive sensor presentation, respectively. Again, the direction was only reported for those participants with BF > 3.

4.2.3.1 Visible Images. . Participant 1 achieved low accuracy performance and was not used for analyses of blocking effects. For visible-only trials with algorithmic fusion presentation,

Participant 9 exhibited decisive evidence for effects ($M_{context}$ = 488.92ms, $M_{no\ context}$ = 566.08ms) while visible signal trials out of the presence of LWIR and multi-sensor images were slower than those in the block consisting all three trial types. Strong evidence for effects were found for Participant 10 ($M_{context}$ = 639.54ms, $M_{no\ context}$ = 571.57ms), while visible signals out of the presence of LWIR-only and multi-sensor imagery were faster than those in the mixed sensor block. There was a BF < .30 for 5 participants, which indicates evidence against a difference. The Bayes Factor with visible image effects with algorithmic fusion is listed for each participant in Table 29.

Table 29. Visible image blocking effects for the algorithmic fusion presentation in Experiment 2.

Subject	Bayes Factor	Direction
1	N/A	N/A
2	BF = 0.24	N/A
3	BF = 0.22	N/A
4	BF = 0.33	N/A
5	BF = 0.22	N/A
6	BF = 0.35	N/A
7	BF = 0.21	N/A
8	BF = 0.19	N/A
9	BF = 285.97	Negative
10	BF = 4.08	Positive

For visible-only trials with cognitive fusion display, decisive evidence for effects were found for Participant 3, 8, and 9 (Table 30). Participant 3 demonstrated a slower mean response time with the presence of LWIR-only and multi-sensor imagery ($M_{context}$ = 546.02ms, $M_{no\ context}$ = 498.96ms) while Participant 8 ($M_{context}$ = 612.31ms, $M_{no\ context}$ = 714.19ms) and Participant 9 ($M_{context}$ = 550.95ms, $M_{no\ context}$ = 599.88ms) exhibited faster response times with the presence of LWIR-only and multi-sensor trials as opposed to a block of trials with only visible images. There was evidence against a effect for 6 participants, BF < .30.

Table 30. Visible image blocking effects for the cognitive fusion presentation in Experiment 2.

Subject	Bayes Factor	Direction
1	BF = 0.85	N/A
2	BF = 0.16	N/A
3	BF = 10.51	Positive
4	BF = 0.15	N/A
5	BF = 0.30	N/A
6	BF = 0.25	N/A
7	BF = 0.17	N/A
8	BF = 56.74	Negative
9	BF = 9.96	Negative
10	BF = 0.20	N/A

4.2.3.2 LWIR Images. For LWIR-only trials with algorithmic fusion presentation, Participant 2 exhibited decisive evidence for blocking effects ($M_{context}$ = 515.77ms, $M_{no\ context}$ = 479.76ms) with LWIR signal trials out of the presence of visible and algorithmically fused images slower than than in the block consisting all three trial-types. Decisive evidence for effects were also found for Participant 3 ($M_{context}$ = 459.71ms, $M_{no\ context}$ = 427.71ms) with response times in the LWIR-only block faster than those in the block with visible and algorithmically fused images. There was BF < .30 for 4 participants, which indicates evidence against a difference in response times. The Bayes Factor with LWIR image blocking effects with algorithmic fusion is listed for each participant in Table 31.

Table 31. LWIR image blocking effects for the algorithmic fusion presentation in Experiment 2.

Subject	Bayes Factor	Direction
1	N/A	N/A
2	BF = 29.65	Positive
3	BF = 43.93	Positive
4	BF = 0.82	N/A
5	BF = 0.17	N/A
6	BF = 0.16	N/A
7	BF = 0.39	N/A
8	BF = 0.97	N/A
9	BF = 0.15	N/A
10	BF = 0.30	N/A

For cognitive fusion trials, substantial evidence for blocking effects were found for Participant 6 ($M_{context}$ = 525.38ms, $M_{no\ context}$ = 561.90ms) with LWIR signal trials out of the presence of visible and algorithmically fused images slower than those in the multi-sensor block. BF < .30 was found for 7 participants, indication for evidence against an effect. The Bayes Factor with LWIR image blocking effects with cognitive fusion is listed for each participant in Table 32.

Table 32. LWIR image blocking effects for the cognitive combined, multi-image display.

Subject	Bayes Factor	Direction
1	BF = 0.15	N/A
2	BF = 0.14	N/A
3	BF = 0.17	N/A
4	BF = 0.47	N/A
5	BF = 0.15	N/A
6	BF = 2.04	Negative
7	BF = 0.16	N/A
8	BF = 0.14	N/A
9	BF = 0.15	N/A
10	BF = 0.77	N/A

4.2.4 Survivor Interaction Contrast. Identical to Experiment 1 with algorithmically fused images, no participant's data satisfied the assumptions of selective influence thereby precluding the use of the SIC for model classification (Table 33). If selective influence held across the group, all assumptions listed in Table 33 would show significance at p < .05. Individual participant's ordering of survivor functions and corresponding SIC (uninterruptable) are shown in Figure 37 – 46.

Table 33. Distribution comparison K-S tests by participant for algorithmically fused images.

Subject	D_{HH-HL}	D_{HL-LL}	D_{HH-LH}	D_{LH-LL}
1	0.098	0.062	0.093	0.094
2	0.108	0.068	0.069	0.076
3	0.102	0.108	0.047	0.113
4	0.108	0.056	0.080	0.061
5	0.116	0.036	0.114	0.021
6	0.067	0.056	0.048	0.059
7	0.036	0.024	0.054	0.036
8	0.013	0.074	0.036	0.079
9	0.119	0.000	0.115	0.041
10	0.157	0.018	0.047	0.068

Note: ~* p <.10, * p < .05, ** p < .01, *** p < .001.

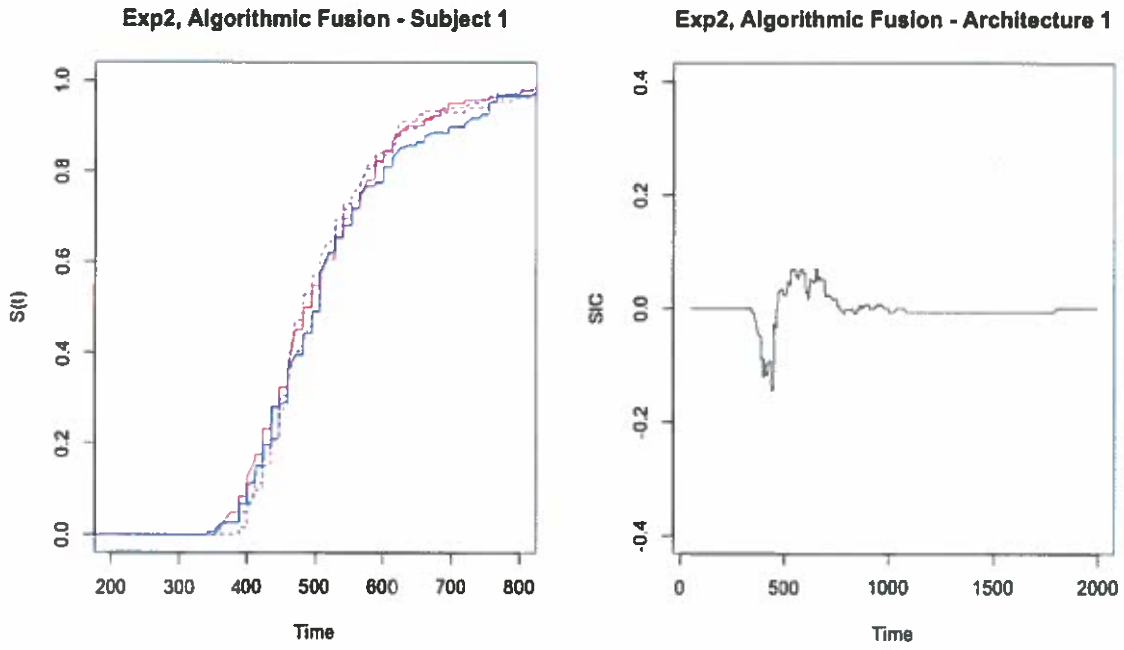

Figure 37. SIC analyses of selective influence and architecture for Participant 1 in the Experiment 2, algorithmic fusion block. The plot to the left shows the ordering of survivor functions. If the red line is fastest (furthest to the left) and the blue line is the slowest (furthest to the right), selective influence holds. If selective influence holds, the SIC function (plot to the right) is tested for positive and negative deviations from zero. If selective influence does not hold, SIC results are uninterruptable.

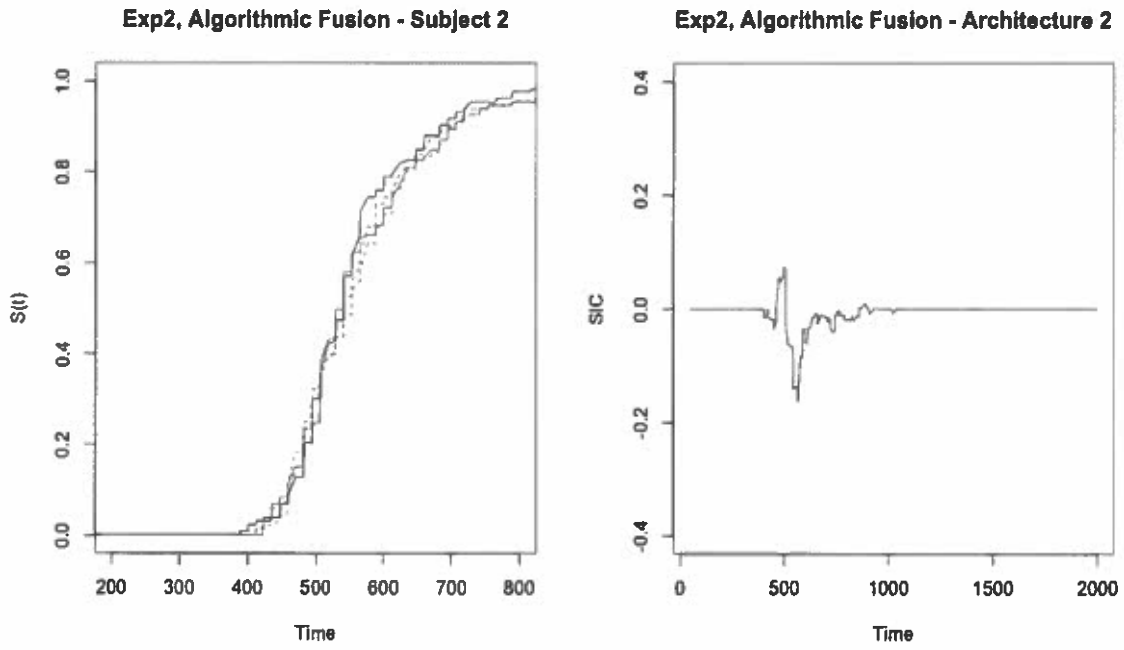

Figure 38. SIC analyses of selective influence and architecture for Participant 2 in the Experiment 2, algorithmic fusion block.

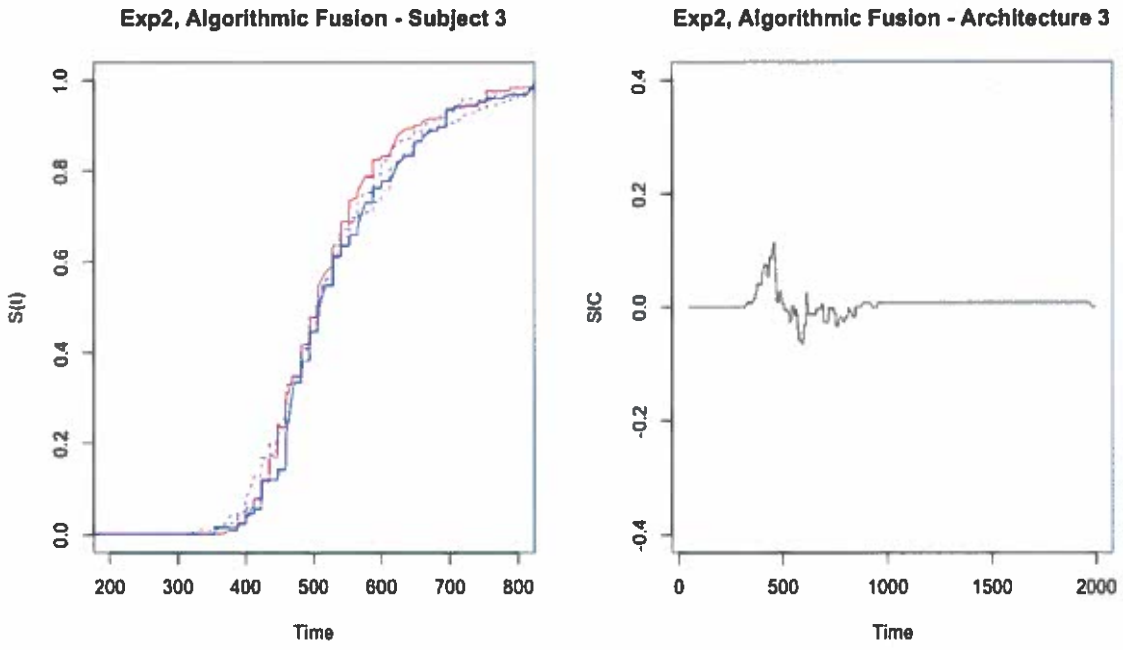

Figure 39. SIC analyses of selective influence and architecture for Participant 3 in the Experiment 2, algorithmic fusion block.

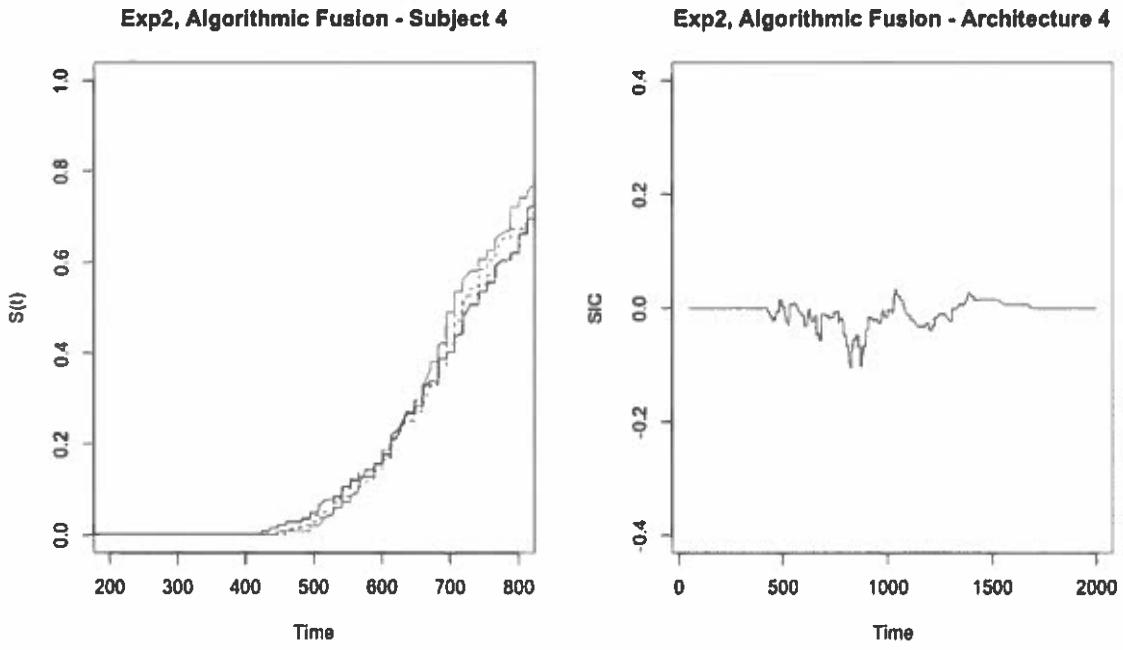

Figure 40. SIC analyses of selective influence and architecture for Participant 4 in the Experiment 2, algorithmic fusion block.

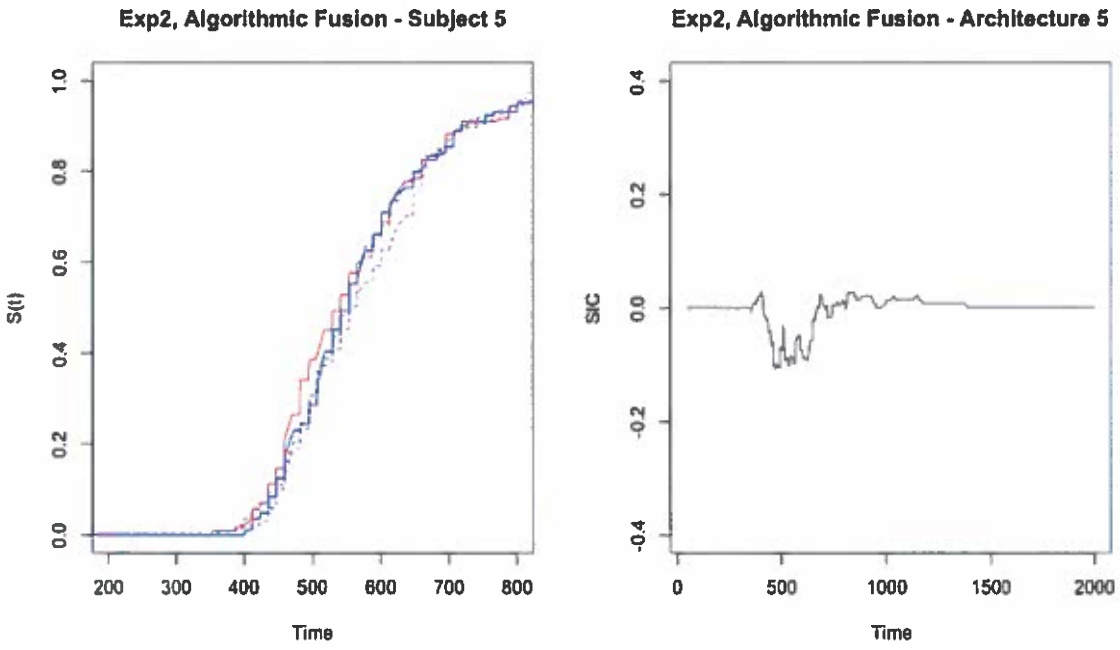

Figure 41. SIC analyses of selective influence and architecture for Participant 5 in the Experiment 2, algorithmic fusion block.

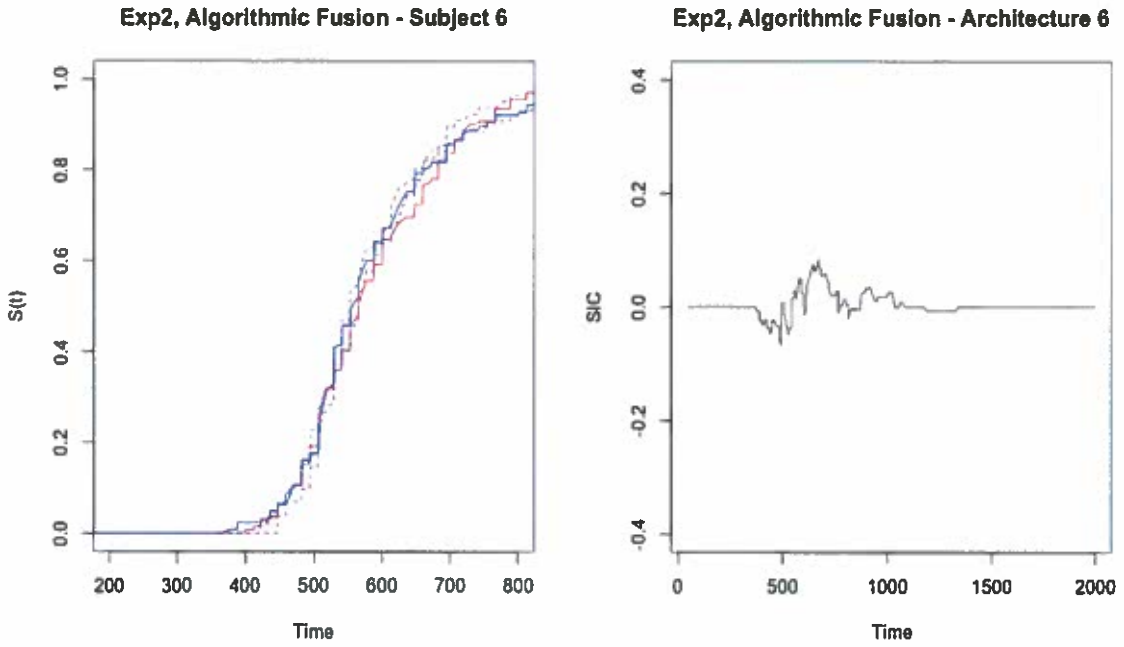

Figure 42. SIC analyses of selective influence and architecture for Participant 6 in the Experiment 2, algorithmic fusion block.

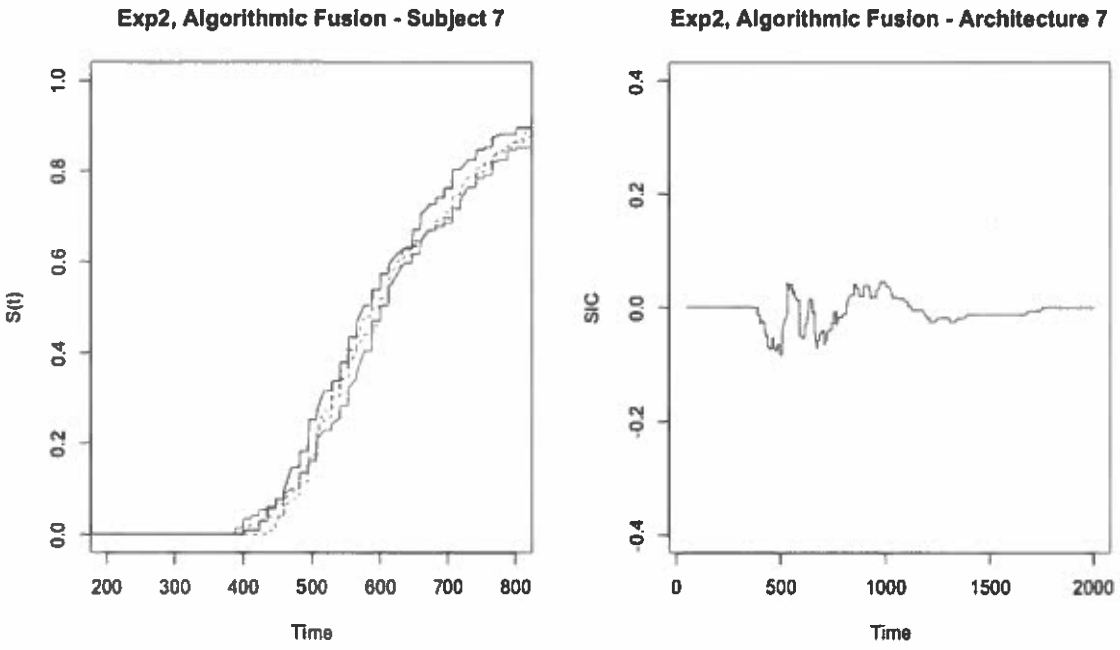

Figure 43. SIC analyses of selective influence and architecture for Participant 7 in the Experiment 2, algorithmic fusion block.

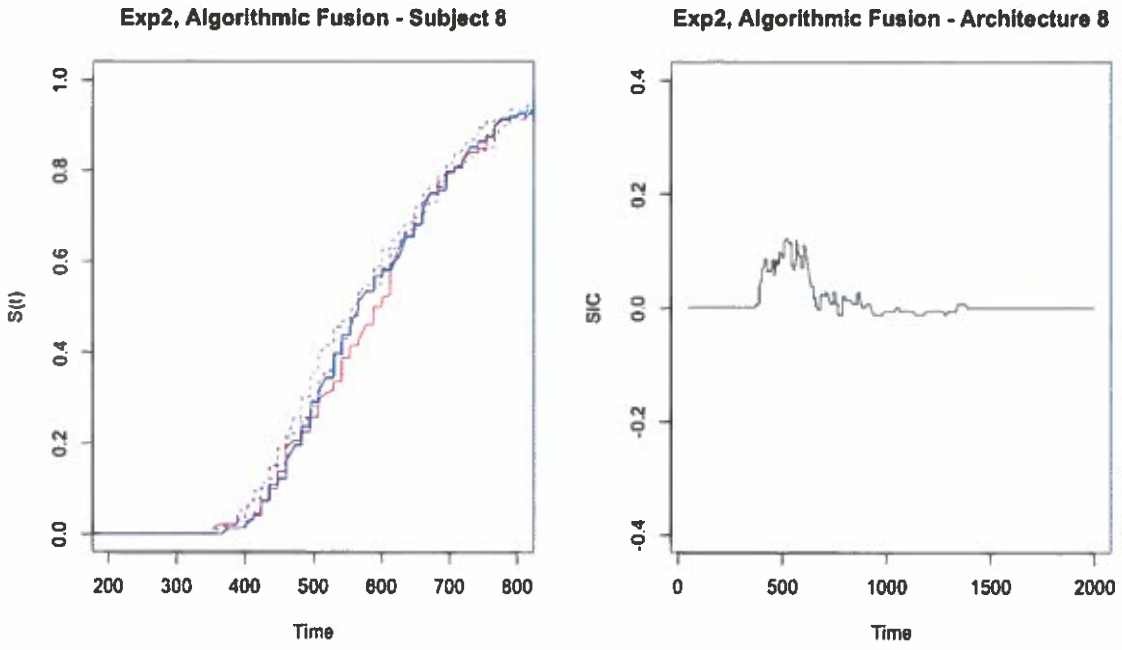

Figure 44. SIC analyses of selective influence and architecture for Participant 8 in the Experiment 2, algorithmic fusion block.

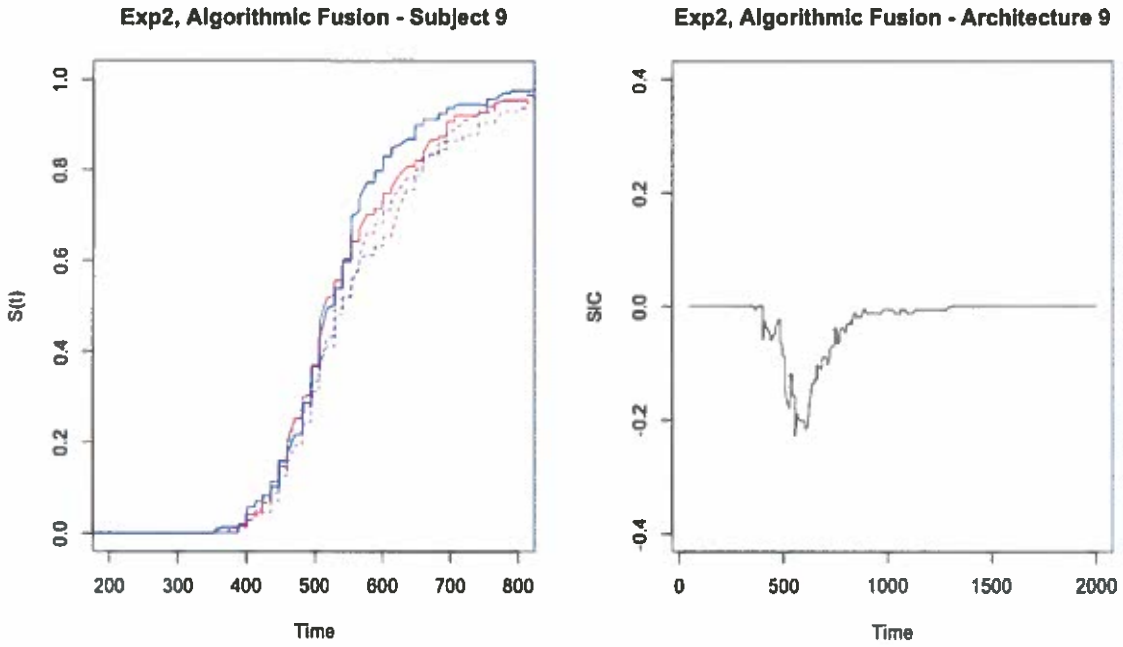

Figure 45. SIC analyses of selective influence and architecture for Participant 9 in the Experiment 2, algorithmic fusion block.

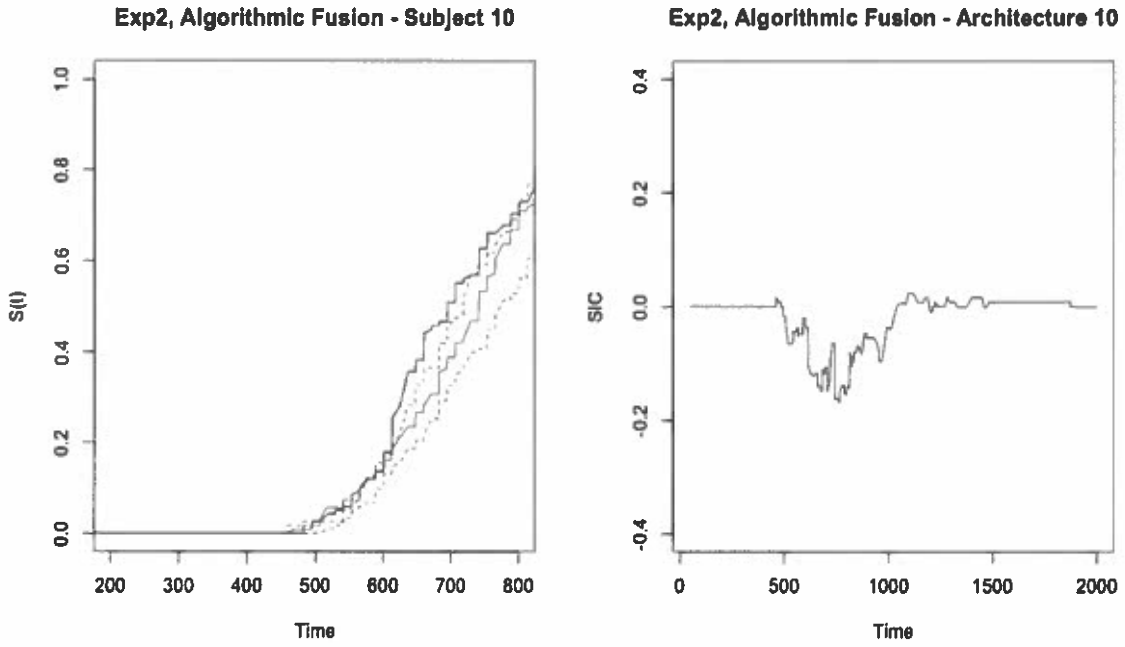

Figure 46. SIC analyses of selective influence and architecture for Participant 10 in the Experiment 2, algorithmic fusion block.

For cognitive fusion SIC analyses, selective influence was satisfied for 3 participants. The Houpt-Townsend SIC statistic (Houpt & Townsend, 2010) indicated 1 participant had a significantly ($p < .33$) positive SIC (parallel-OR) and 2 participants with a significantly ($p < .33$) negative SIC (parallel–AND). The remaining 3 participants failed tests of selective influence leading to ambiguous SIC interpretations. Table 33 lists each participants Houpt-Townsend SIC statistic for both positive and negative deviations from zero and corresponding K-S statistics with the amount of significance. Individual figures of ordering of survivor functions and corresponding SIC are listed below in Figure 47 – 56.

Table 34. Cognitive fusion results including: Houpt-Townsend statistic (D+, D-) and tests of selective influence (D) for each participant in Experiment 2. Bold D+ and D- statistics indicate a significant Houpt-Townsend statistic at $p < 0.33$.

Subject	D+	D-	$D_{HH\text{-}HL}$	$D_{HL\text{-}LL}$	$D_{HH\text{-}LH}$	$D_{LH\text{-}LL}$
1	N/A	N/A	0.136*	0.054	0.185*	0.031
2	N/A	N/A	0.080	0.227***	0.242***	0.043
3	N/A	N/A	0.097	0.150*	0.299***	0.036
4	N/A	N/A	0.065	0.107	0.158*	0.036
5	0.013	**0.156**	0.124~*	0.129~*	0.240***	0.018
6	0.063	**0.152**	0.126~*	0.134~*	0.192**	0.069
7	N/A	N/A	0.094	0.091	0.113	0.051
8	**0.136**	0.076	0.087	0.251***	0.175***	0.125~*
9	N/A	N/A	0.082	0.239***	0.336***	0.064
10	N/A	N/A	0.071	0.207**	0.159*	0.094

Note: **H-T statistic** = $p < 0.33$, ~* = $p < .10$, * = $p < .05$, ** = $p < .01$, *** = $p < .001$.

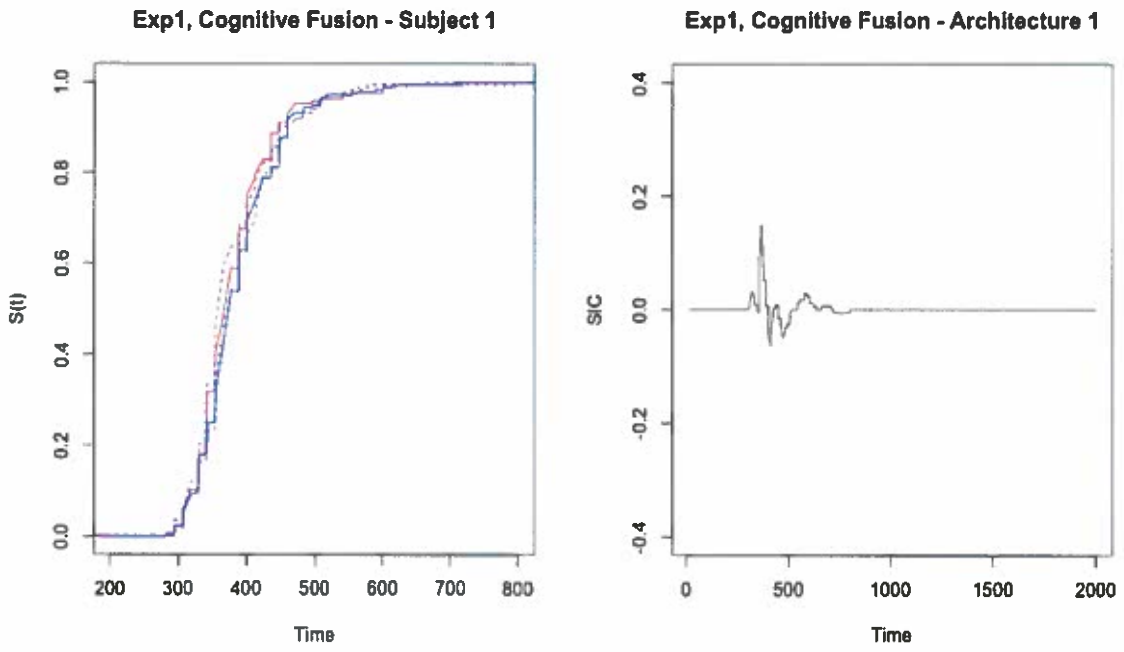

Figure 47. SIC analyses of selective influence and architecture for Participant 1 in the Experiment 2, cognitive fusion block. The plot to the left shows the ordering of survivor functions. If the red line is fastest (furthest to the left) and the blue line is the slowest (furthest to the right) then selective influence holds. If selective influence holds, the SIC function (plot to the right) is tested for positive and negative deviations from zero. If selective influence does not hold, SIC results are uninterruptable.

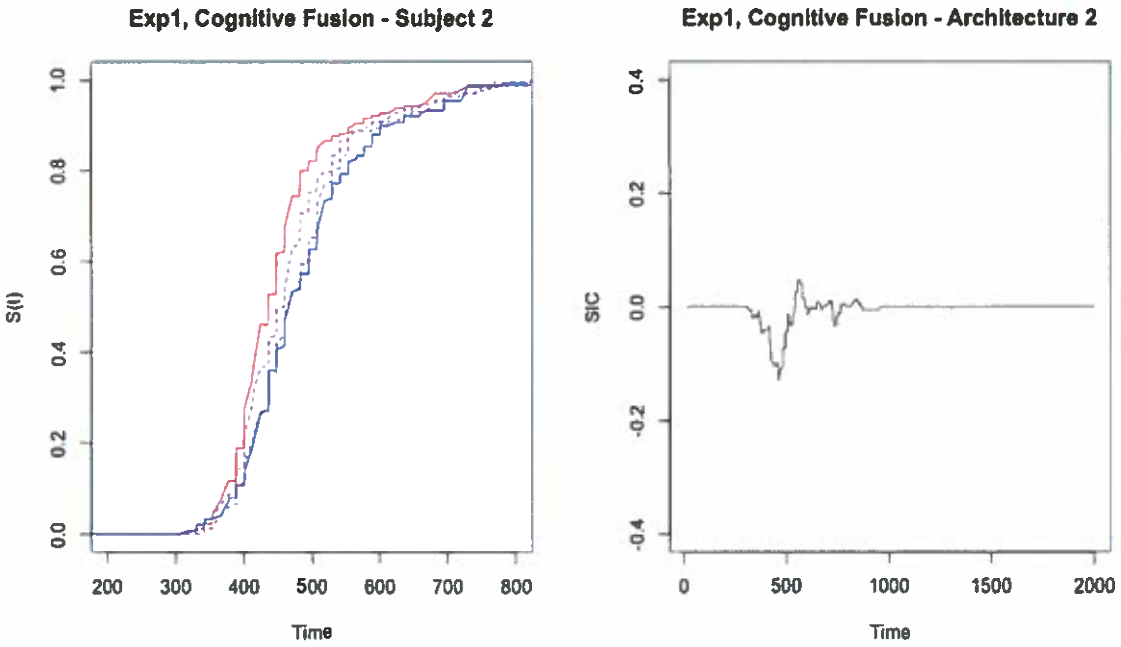

Figure 48. SIC analyses of selective influence and architecture for Participant 2 in the Experiment 2, cognitive fusion block.

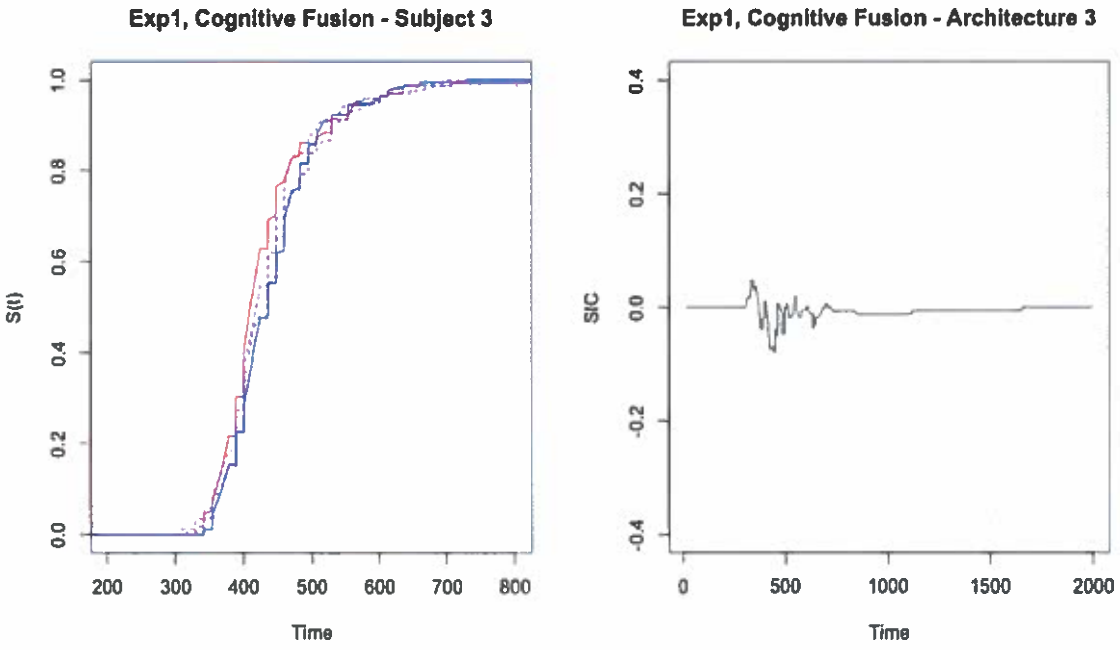

Figure 49. SIC analyses of selective influence and architecture for Participant 3 in the Experiment 2, cognitive fusion block.

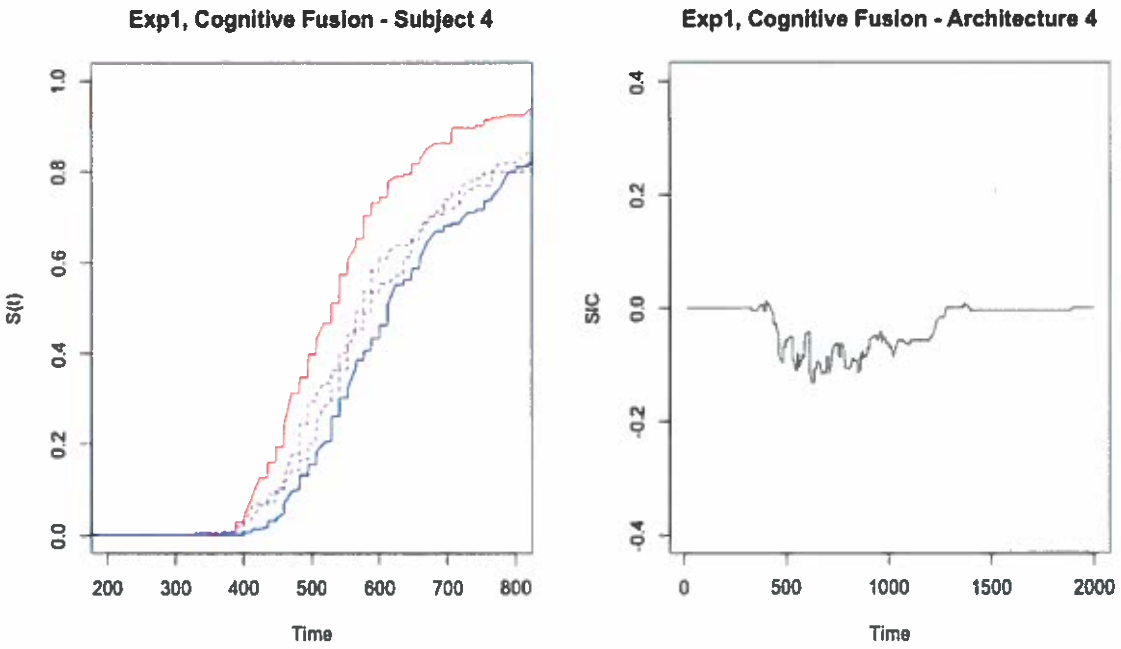

Figure 50. SIC analyses of selective influence and architecture for Participant 4 in the Experiment 2, cognitive fusion block.

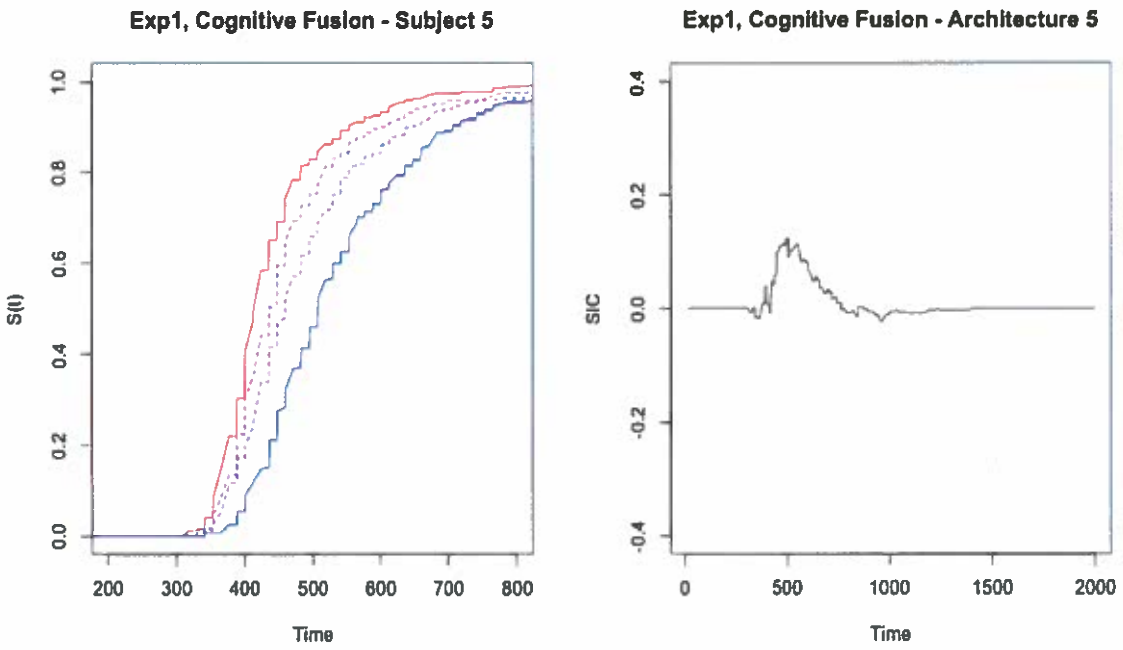

Figure 51. SIC analyses of selective influence and architecture for Participant 5 in the Experiment 2, cognitive fusion block.

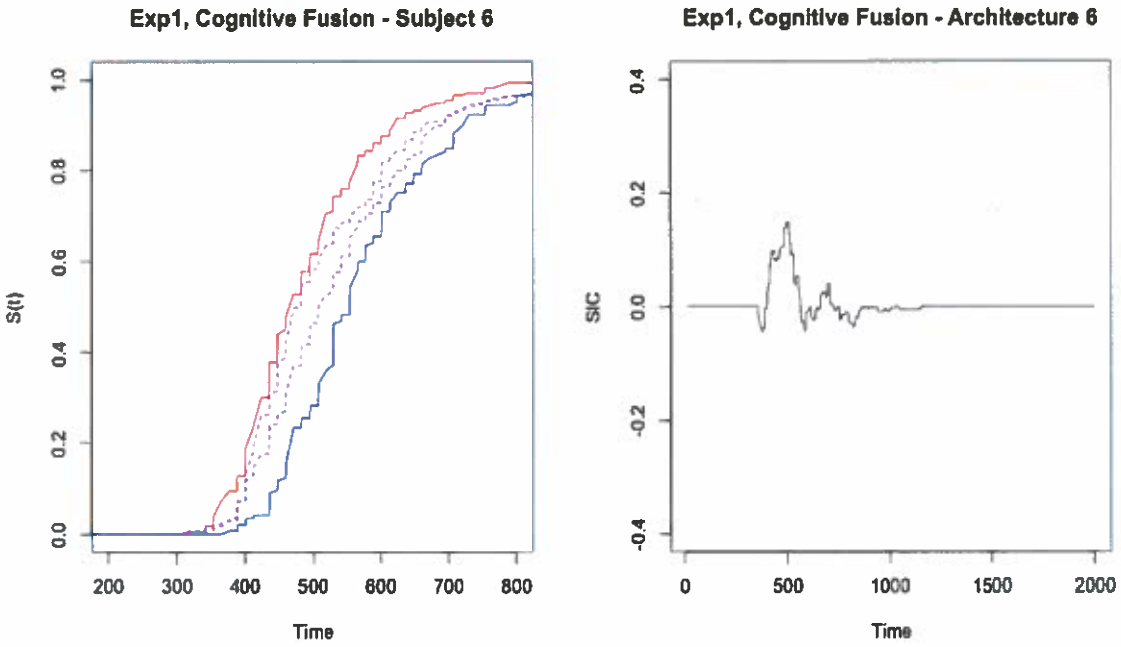

Figure 52. SIC analyses of selective influence and architecture for Participant 6 in the Experiment 2, cognitive fusion block.

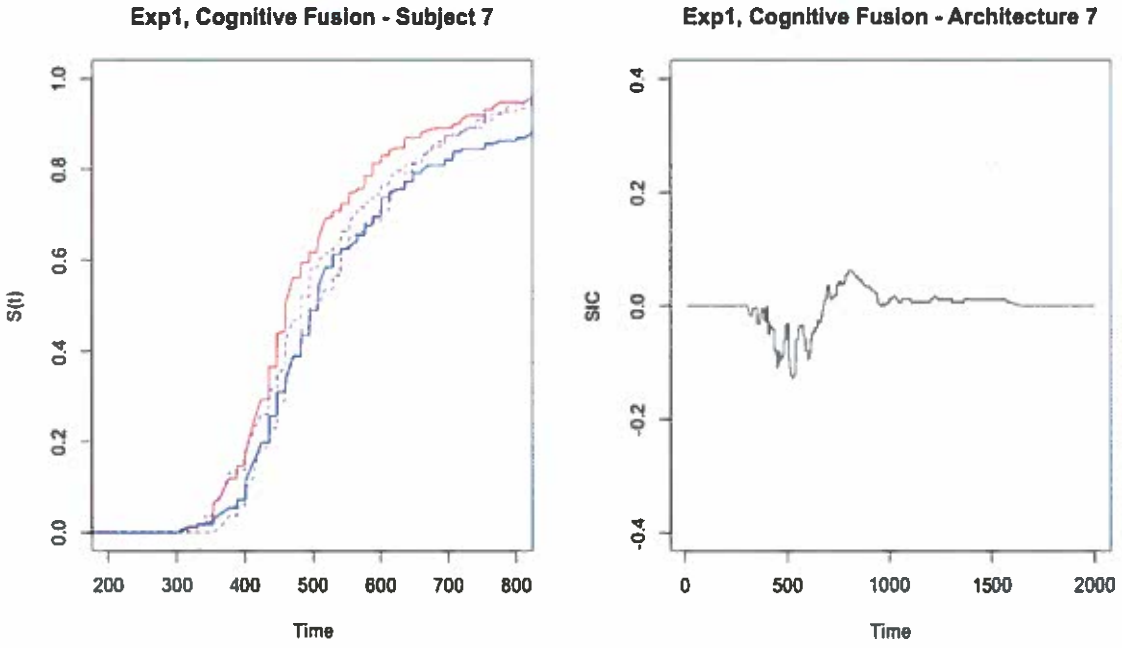

Figure 53. SIC analyses of selective influence and architecture for Participant 7 in the Experiment 2, cognitive fusion block.

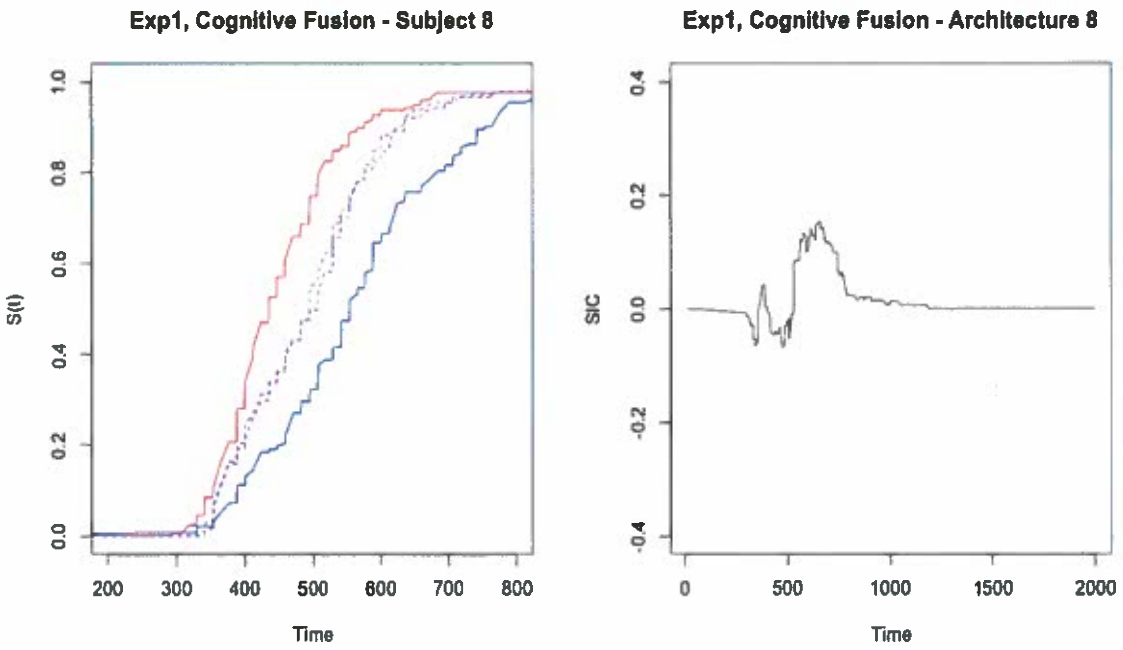

Figure 54. SIC analyses of selective influence and architecture for Participant 8 in the Experiment 2, cognitive fusion block.

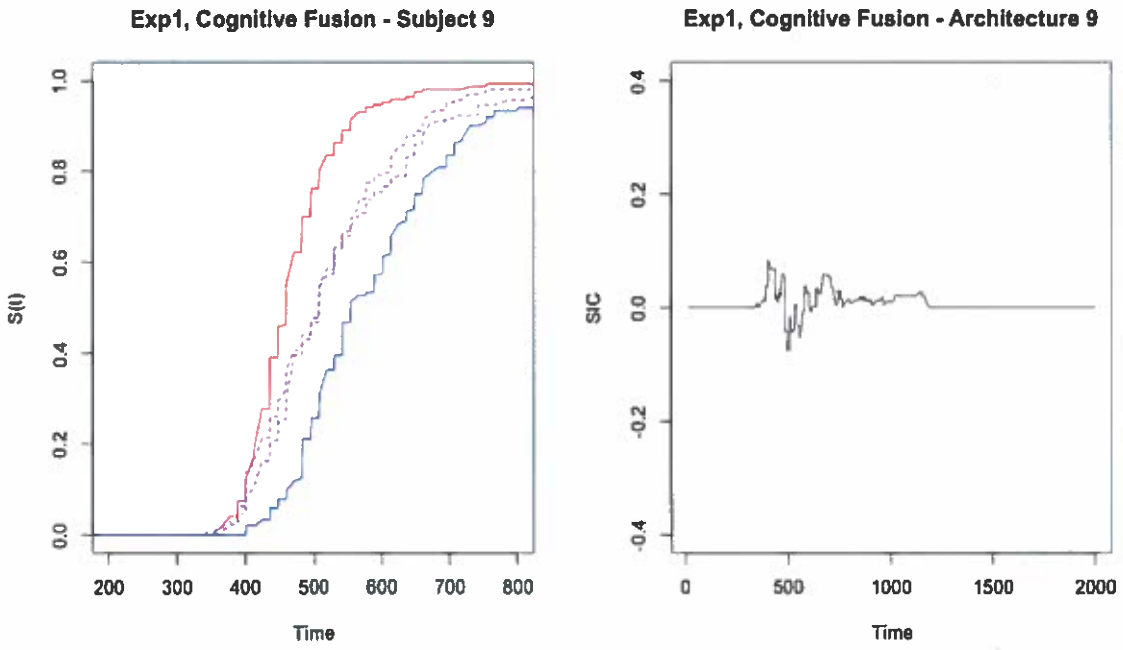

Figure 55. SIC analyses of selective influence and architecture for Participant 9 in the Experiment 2, cognitive fusion block.

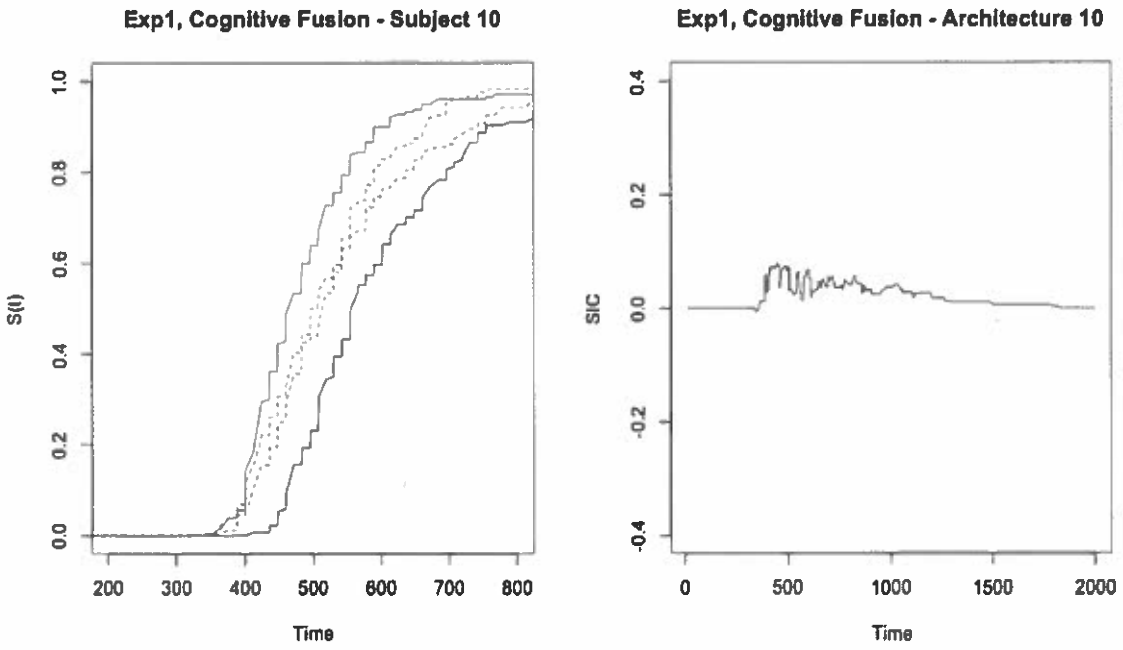

Figure 56. SIC analyses of selective influence and architecture for Participant 10 in the Experiment 2, cognitive fusion block.

Subsequent MIC analyses using a hierarchical Bayesian model indicate posterior probability distributions with MIC = 0 (45.5%) and MIC > 0 (43.3%) about equally likely, and MIC > 0 (11.2%) a less likely model. I used the Gelman-Rubin statistic to test the convergence of MCMC sampling chains factor for each participant. Factors ranged from $\hat{r}$ = 1.10 – 1.90 with 20,000 burn-in samples. Further individual level MIC analyses indicated evidence for 3 participants with a negative MIC (parallel - exhaustive processing) and 2 participants with a negative SIC (parallel-AND processing).

Table 35. Summary table of capacity and SIC analyses across algorithmic and cognitive fusion in Experiment 2 for each participant.

	Experiment 2			
	Algorithmic		*Cognitive*	
Participant	**Capacity**	**SIC**	**Capacity**	**SIC**
1	Limited	N/A	Limited	N/A
2	Limited	N/A	Limited	N/A
3	Limited	N/A	Limited	N/A
4	Limited	N/A	Limited	N/A
5	Limited	N/A	Limited	Parallel-AND
6	Limited	N/A	Limited	Parallel-AND
7	Limited	N/A	Limited	N/A
8	Limited	N/A	Limited	Parallel-OR
9	Limited	N/A	Limited	N/A
10	Limited	N/A	Limited	N/A

4.3 Discussion

All participants' performance with algorithmically and cognitive fused multi-sensor information resulted in limited workload capacity. In Experiment 2 individual sensor performance for both LWIR and visible imagery was just as good if not better than multi-sensor performance across both fusion techniques. The algorithmic and cognitive fusion did not aid in performance above that of individual sensors for the left/right discrimination task with spatial uncertainty of the target. In line with previous research, I predicted more efficient use of multi-sensor information in a more difficult task (Krebs et al., 2002). The results shown here indicate that the task in Experiment 2 did just the opposite; all participants' performance indicated less efficient processing of multi-sensor information than what was predicted given their performance with each individual sensor alone (UCIP model). However, this effect may result from introducing more uncertainty in the position of the target and less salient body features indicating whether the person is facing left or right rather than a change in task difficulty. The performance with algorithmically fused images indicated that the algorithmic fusion of images provided no benefit above that of an individual sensor image for any participant. A few participants

performance indicated a parallel architecture with the presentation of multi-sensor, cognitive fusion information. Perhaps training may be needed so people can better utilize multi-sensor information (Shiffrin & Schnieder, 1977).

5. GENERAL DISCUSSION

Participant response times varied across the chosen sets of images in most conditions of Experiment 1 and all conditions in Experiment 2. The images within each Experiment were chosen to represent a variety of spatial locations and target sizes. However, because these images were taken from a natural scene, other variables such as lighting conditions and body temperature could change due to the target location and/or identity. Such changes could make the task easier or more difficult for a particular subset of images within each sensor type; for example, participants self-reported that the "taller man" was easier than the "shorter man" across both Experiment 1 and Experiment 2. Looking at the images post hoc it seems as if the taller man is easier to detect with the LWIR images, indicating higher levels of body temperature than the shorter man. In the current study I focused on gathering a variety of each type of image to generalize across several image types and targets. However, it may be worthwhile in future studies to systematically vary target temperature and illumination to measure the effects of more specific environmental manipulations on response times with LWIR and visible images.

5.1 Algorithmic Fusion

I found a limited workload capacity across both levels of difficulty for algorithmically combined images. These results indicate that participants may need to explore all of the available data rather than making decisions based on algorithmic interpretations of important features. "Combining data together can reduce information overload but poses challenges if the human cannot determine why and how the algorithms are doing what they are doing" (Klein, Moon, & Hoffman, 2006A). The results reported here are consistent with the past literature. Previous research indicated that at best, algorithmic fusion performed just as well an individual sensor performance across several tasks, sensor types, and algorithms (Essock, Sinai, DeFord,

Hansen, Srinivasan, 2004; Steele & Perconti, 1997; Krebs & Sinai, 2002). Contradictory to the findings reported here, Toet et al. (1997) found performance improvements with algorithmically fused LWIR and visible images. The task in this study was tailored to specifically utilize both visible and LWIR information. The participants were asked to determine the position of a person relative to an environmental object (fence, walkway, tree). Therefore, to correctly identify the spatial location the participant *must* take advantage of unique information from each sensor. In the present study information was, for the most part, redundant across the two sensors. Image fusion may have the best results when each sensor alone does not supply redundant information; rather, only the combination of the individual sensor information allows for correct decision-making. Follow up studies should consider performance comparisons across multi-sensor information presented with algorithmic and cognitive fusion when the individual sensors each supply unique, useful information.

Complementary to the research reported here, Bittner et. al. (Bittner, Schill, Blaha & Houpt, 2014) is using ideal observer analysis (e.g., Geisler, 1989) with multi-sensor imagery of the Landolt C used in my pilot studies. Ideal observer analysis is a framework used to estimate human information efficiencies by comparing human performance to a Bayesian ideal observer. Also, Bittner's current work uses response classification (e.g., Ahumada, 2002; Ahumada & Lovell, 1971). Response classification uses noise masking to identify the important information in each single-sensor and multi-sensor image for an observer to make a decision. Clusters of pixels can determine what unique features of each image carry task relevant details. Utilizing this method tangential to SFT can ensure observers use different information from each single-sensor for decision-making rather than redundant information across the single-sensor images.

McCarley and Krebs (2006) found observers perceptually failed to separate contrast information for each sensor in an algorithmically fused image. Similarly, I found failures of selective influence when attempting to manipulate the processing speed of each individual sensor when adding random Gaussian noise. The Gaussian noise was individualized using an adaptive psychophysical method (QUEST) and added to each sensor image based on a threshold indicative of slower processing rates. While the effects of selective influence were consistently found with cognitive fusion, the manipulation of processing rate vanished when the images were algorithmically combined. This effect is suggestive of nonseperability of noise information for each individual sensor.

5.2 Cognitive Fusion

Cognitive fusion has not been researched with multi-sensor information in the past. In the current study participants were, at best, performing just as well as predicted by a UCIP model with cognitive fusion presentation of multi-sensor information with the left/right discrimination task (Experiment 1) and worse than predicted with left/right discrimination task with spatial uncertainty of the target (Experiment 2). Although cognitive fusion did not provide clear performance benefits above that of algorithmic fusion in these findings it is worthwhile to invest further efforts to understand the benefits it may have with additional training and individual sensor image enhancement techniques such as contrast manipulation (Smeelen, Schwering, Toet, & Loog, 2014).

Additional training can use strategic methods for observers to learn the unique strengths each single-sensor may possess. Observers can more efficiently utilize single-sensor information after becoming familiar with how each sensor processes and displays environmental information (e.g., LWIR images can display hottest elements as white and coolest elements as black). With

practice, knowledge of single-sensor benefits could produce unlimited or super workload capacity and parallel processing with cognitive fusion display of multi-sensor information. Another display type of interest is the option for observers to quickly flip between the single-sensor images within the same visual field. For instance, the interface could display a LWIR by default but with a press of a button it switches to visible, or vice versa. Allowing the observer to switch between the two as quickly as desired can mimic an image fusion like process. This display method satisfies one substantial benefit of algorithmic fusion by restricting the amount of visual information at a given instant; also, it satisfies a benefit of cognitive fusion by giving the observer all of the available information to explore. Perhaps future research should investigate alternative methods of displaying multi-sensor information above just that of algorithmic and cognitive fusion.

The role of task, sensor, fusion algorithm, and quality of individual image information has shown to change the benefits of algorithmic image fusion over an individual sensor image in previous research. In the current study, I've shown evidence that while keeping overall task, sensor, and fusion algorithm consistent the change of original image information can alter performance with multi-sensor information presented with cognitive fusion. I was not able to give substantial evidence to determine whether the method of presentation changes observer performance but have shown that other methods of presentation must be considered as an alternative to algorithmic fusion.

Furthermore, people may benefit from guidance of important information in each individual sensor without the system altering the original information altogether. Training that is aimed at strengthening the relationship between automated image enhancement and human

capabilities can better utilize the strengths of both human and machine to maximize overall performance across task types (Klein, Moon, & Hoffman, 2006B).

6. CONCLUSIONS

Using a theoretically driven, cognitive framework I developed an understanding for which underlying processes are involved in closely controlled experimental manipulations of stimulus information and multi-sensor fusion techniques. This thesis was a necessary step to gain traction for how (if at all) multi-sensor displays provide benefits above individual sensor displays. Displays using data fusion often times debate the benefits of algorithmically combining information or displaying all available information to the observer. Until the current study, no research has investigated the debate surrounding data fusion with multi-sensor information. Future research with multi-sensor displays should not disregard the potential benefits that displaying all of the available information may have over the algorithmic interpretations of important information.

7. REFERNCES

Ahumada, A. J. (2002). Classification image weights and internal noise level estimation. *Journal of Vision, 2*(1), 121-131.

Ahumada, A., & Krebs, W. (2000). Signal detection in fixed pattern chromatic noise. *Investigative Ophthalmology and Visual Science, 41*, 3796-3804.

Ahumada, A. J.Jr. Lovell, J. (1971). Stimulus features in signal detection. *Journal of the Acoustical Society of America, 49*, 1751–1756.

Bittner, J., Schill, T., Blaha, L., & Houpt, J. (2014). Ideal Observer Analysis of Fused Multispectral Imagery. *Journal of Vision, 14(10)*, 1359. doi: 10.1167/14.10.1359.

Blasch, E., & Plano, S. (2005). Proactive decision fusion for site security. *Information Fusion, 2005 8th International Conference, 2*, 1-8.

Blum, R. (2006). *Multi-sensor image fusion and its applications.* Boca Raton, FL: Taylor & Francis.

Chavez, P., Sides, S., & Anderson, J. (1991). Comparison of three different methods to merge multiresolution and multispectral data: TM & SPOT pan. *Photogrammetric Engineering and Remote Sensing, 57*, 295-303.

Dong, J., Zhuang, D., Huang, Y., & Fu, J. (2009). Advances in multi-senor data fusion: Algorithms and applications. *Sensors, 9*, 7771-7784.

Duncan, J. (1980). The locus of interference in the perception of simultaneous stimuli. *Psychological Review, 87*, 272-300.

Essock, E., Sinai, M., McCarley, J., Krebs, W., & DeFord, J. (1999). Perceptual ability with real-world nighttime scenes: image-intensified, infrared, and fused-color imagery. *Human Factors: The Journal of the Human Factors and Ergonomics Society, 41*, 438-452.

Geisler, W. S. (1989). Sequential ideal-observer analysis of visual discriminations. *Psychological review*, *96*, 267-314.

Gelman, A., & Rubin, D.B. (1992). Inference from iterative simulation using multiple sequences, *Statistical Science*, *7*, 457-511.

Houpt, J.W. (2014). A comparison of statistical analyses for the survivor interaction contrast. Talk presented at the 55th Annual Meeting of the Psychonomic Society; Long Beach, CA.

Houpt, J. W., Blaha, L. M., McIntire, J. P., Havig, P. R., & Townsend, J. T. (2014). Systems Factorial Technology with R. *Behavior Research Methods, 46,* 307-330.

Houpt, J. W. & Fifić, M. (2013). A hierarchical Bayesian approach to distinguishing serial and parallel processing. *Psychonomicss Society Annual Meeting; Toronto, ON.* Poster.

Houpt, J., Heathcote, A., Eidels, A., Medeiros-Ward, N., Watson, J., & Strayer, D. (2012). Capacity coefficient variations. *Psychonomics Society Annual Meeting.* Poster.

Houpt, J.W. & Townsend, J.T. (2010). The statistical properties of the survivor interaction contrast. *Journal of Mathematical Psychology, 54*, 446-453.

Houpt, J.W. & Townsend, J.T. (2012). Statistical measures for workload capacity analysis. *Journal of Mathematical Psychology, 56*, 341-355.

Kahneman, D. (1973). *Attention and effort.* Englewood Cliffs, NJ: Prentice-Hall.

Klein, G., Moon, B. M., & Hoffman, R. R. (2006). Making sense of sensemaking 1: Alternative perspectives. *IEEE intelligent systems*, *21*, 70-73.

Klein, G., Moon, B., & Hoffman, R. R. (2006). Making sense of sensemaking 2: A macrocognitive model. *Intelligent Systems, IEEE*, *21*, 88-92.

Krebs, W. K., Xing, J., & Ahumada, A. J. (2002). A simple tool for predicting the readability of a monitor. *Proceedings of the Human Factors and Ergonomics Society Annual Meeting, 46,* 1659-1663.

Krebs, W. K., & Sinai, M. J. (2002). Psychophysical assessments of image-sensor fused imagery. *Human Factors: The Journal of the Human Factors and Ergonomics Society, 44,* 257-271.

Krishnamoorthy, S., & Soman, K. P. (2010). Implementation and comparative study of image fusion algorithms. *International Journal of Computer Applications, 9(2),* 25-35.

McCarley, J., & Krebs, W. (2000). Visibility of road hazards in thermal, visible, and sensor-fused nighttime imagery. *Applied Ergonomics, 31,* 523-530.

McCarley, J., & Krebs, W. (2006). The psychophysics of sensor fusion: A multidimensional signal detection analysis. *Proceedings of the Human Factors and Ergonomics Society Annual Meeting, 50,* 2094-2098.

O'Kane, B. L., Crenshaw, M. D., D'Agostino, J., & Tomkinson, D. (1993). Human target detection using thermal systems. In J. S. Accetta & M.J. Cantella (Eds.), *Proceedings of SPIE Aerospace/Defense Sensing, Simulation and Controls, 2075,* 75-88.

Peirce, J.W., (2009) Generating stimuli for neuroscience using PsychoPy. Front. Neuroinform. 2:10. doi:10.3389/neuro.11.010.2008

Petrović, V. (2001). *Multisensor pixel-level image fusion.* Unpublished master's thesis, University of Manchester.

Petrović, V. (2007). Subjective tests for image fusion evaluation and objective metric validation. *Information Fusion, 8,* 208-216.

Petrović, V., & Xydeas, C. (2004). Evaluation of image fusion performance with visible differences. *Computer Vision-ECCV,* 380-391.

Piella, G., & Heijmans, H. (2003). A new quality metric for image fusion. Proceedings of *Image Processing International Conference, 3,* 111-173.

Qu, G., Zhang, D., & Yan, P. (2002). Information measure for performance of image fusion. *Electronics Letters, 38,* 313-315.

Ryan, D. M., & Tinkler, R. D. (1995). Night pilotage assessment of image fusion. *SPIE Symposium on OE/Aerospace Sensing and Dual Use Photonics at International Society for Optics and Photonics,* 50-67.

Schistad-Solberg, A., Jain, A., & Taxt, T. (1994). Multisource classification of remotely sensed data: Fusion of Landsat TM and SAR images. *I.E.E.E. Transactions on Geoscience and Remote Sensing, 32,* 768-778.

Shiffrin, R. M., & Schneider, W. (1977). Controlled and automatic human information processing: II. Perceptual learning, automatic attending and a general theory. *Psychological review, 84,* 127-187.

Sims, S. R. F., & Phillips, M. A. (1997). Target signature consistency of image data fusion alternatives. *Optical Engineering, 36,* 743-754.

Sinai, M. J., McCarley, J. S., & Krebs, W. K. (1999). Scene recognition with infrared, low-light, and sensor-fused imagery. *In Preceedings of the Infrared Information Symposia (IRIS) Specialty Groups on Passive Sensors Infrared Information Analysis (IRIA),* Ann Arbor, MI, 1-9.

Sinai, M. J., McCarley, J., Krebs, W. K., & Essock, E. A. (1999). Psychophysical comparisons of single-and dual-band fused imagery. *AeroSense 1999,* 176-183. International Society for Optics and Photonics.

Smeelen, M. A., Schwering, P. B., Toet, A., & Loog, M. (2014). Semi-hidden target recognition in gated viewer images fused with thermal IR images. *Information Fusion, 18,* 131-147.

Steele, P., & Perconti, P. (1997). Part-task investigation of multispectral image fusion using gray scale and synthetic color night vision sensor imagery for helicopter pilotage. In W. R.Watkins & D. Clement (Eds.), *Proceedings of the SPIE -Aerospace/Defense Sensing, Simulation and Controls, 3062,* 88-100. Bellingham, WA: SPIE – International Society for Optical Engineering.

Strobl, D., Raggam, J., & Buchroithner, M. (1990). Terrain correction geocoding of a multi-sensor image data set. *Proceedings 10th EARSeL Symposium.* Toulouse, France, 98-107.

Suits, G., Malila, W., & Weller, T. (1988). Procedures for using signals from one sensor as substitutes for signals of another. *Remote Sensing of Environment, 25,* 395-408.

Toet A. (2013). Registration of a dynamic multimodal target image test set for the evaluation of image fusion techniques. Final report in support of The Air Force Office of Scientific Research (AFOSR) and European Office of Aerospace Research and Development (EOARD). Grant No.: FA8655-11-1-3015. Soesterberg, The Netherlands.

Toet, A., & Franken, E. M. (2003). Perceptual evaluation of different image fusion schemes, *Displays, 24,* 25-37.

Toet, A., Ijspeert, I., Waxman, A., & Aguilar, M. (1997). Fusion of visible and thermal imagery improves situational awareness. In J. G. Verly (Ed.), *Proceedings of the SPIE - Enhanced and Synthetic Vision, 3088,* 177-188. Bellingham, WA: SPIE - International Society for

Optical Engineering.

Toet, A., de Jong, M. J., Hogervorst, M. A., & Hooge, I. T. (2014). Perceptual evaluation of colorized nighttime imagery. *IS&T/SPIE Electronic Imaging, 9014(12),* 1-14. International Society for Optics and Photonics.

Toet, A., Hogervorst, M. A. (2009). TRICLOBS portable triband color lowlight observation system. In *SPIE Defense, Security, and Sensing, 7345(03),* 1-11. International Society for Optics and Photonics.

Toet, A., Hogervorst, M. A., Nikolov, S. G., Lewis, J. J., Dixon, T. D., Bull, D. R., & Canagarajah, C. N. (2010). Towards cognitive image fusion. *Information fusion, 11,* 95-113.

Townsend, J. T. (1990). Serial vs. parallel processing: Sometimes they look like Tweedledum and Tweedledee but they can (and should) be distinguished. *Psychological Science, 1,* 46-54.

Townsend, J., & Nozawa, G. (1995). Spatio-temporal properties of elementary perception: An investigation of parallel, serial, and coactive theories. *Journal of Mathematical Psychology, 39,* 321-359.

Townsend, J., & Wenger, M. (2004). A theory of interactive parallel processing: new capacity measures and predictions for a response time inequality series. *Psychological Review, 111,* 1003-1035.

Üner, M. K., Ramac, L. C., Varshney, P. K., & Alford, M. G. (1997). Concealed weapon detection: An image fusion approach. *Enabling Technologies for Law Enforcement and Security.* 123-132. Interaction Society for Optics and Photonics.

Wald, L., Ranchin, T., & Mangolini, M. (1997). Fusion of satellite images of different spatial resolutions: Assessing the quality of resulting images. *Photogrammetric Engineering and Remote Sensing, 63,* 691-699.

Watson, A. & Pelli, D. (1983). QUEST: A Bayesian adaptive psychometric method. *Perception & Psychophysics, 33,* 113-120.

Xydeas, C. S., & Petrović, V. S. (2000). Objective pixel-level image fusion performance measure. *AeroSense,* 89-98. International Society for Optics and Photonics.